Title
Synthesis and Reactivity of Boron-Functionalized Carborane-Based Chalcogenides

Author
Alsarhan, Fadi

Publication Date
2021

Peer reviewed|Thesis/dissertation

UNIVERSITY OF CALIFORNIA

Los Angeles

Synthesis and Reactivity of Boron-Functionalized Carborane-Based Chalcogenides

A thesis submitted in partial satisfaction of the requirements for the degree of Master of Science in Chemistry

by

Fadi Alsarhan

2021

ABSTRACT OF THE THESIS

Synthesis and Reactivity of Boron-Functionalized Carborane-Based Chalcogenides

by

Fadi Alsarhan

Master of Science in Chemistry

University of California, Los Angeles, 2021

Professor Alexander Michael Spokoyny, Chair

Organochalcogen chemistry is a well-established field: organosulfur compounds find a wide variety of uses in synthetic chemistry; organoselenium and organotellurium compounds, despite being less prevalent than organosulfur compounds, have established niche uses in synthetic chemistry and are attracting a lot of research interest. Carboranes are three-dimensional boron-rich clusters with delocalized bonding analogous to the aromaticity of benzene and a steric profile similar to adamantane. These unique properties, along with their electronic tunability based on the chosen vertex of functionalization, give carboranes a variety of applications in fields such as medicinal chemistry and materials science. *Ortho*- and *meta*-Carborane clusters functionalized with chalcogen atoms at the electron rich B(9) position are relatively unexplored; there has been reports in the 1970's-1980's of the synthesis and basic reactivity of these clusters, as well as reports of some applications (Self-Assembled Monolayers, Boron Neutron Capture

Therapy) for the sulfur-functionalized clusters, but that is all. In this thesis, the field of B(9)-functionalized carborane chalcogenides has been expanded in two ways: 1) new B(9)-S functionalized reagents have been synthesized and tested for their propensity to undergo B-S bond cleavage, a completely unexplored field in carboranes, and 2) the synthesis and reactivity of a variety of new B(9)-Se and B(9)-Te compounds has been discussed.

The thesis of Fadi Alsarhan is approved.

Paula Loredana Diaconescu

Chong Liu

Alexander Michael Spokoyny, Committee Chair

University of California, Los Angeles

2021

TABLE OF CONTENTS

ABSTRACT OF THE THESIS ii

COMMITTEE PAGE iv

TABLE OF CONTENTS v

LIST OF FIGURES viii

LIST OF TABLES xiii

LIST OF ACRONYMS xiv

ACKNOWLEDGMENTS xvi

Chapter 1: Synthesis and Reactivity of Sulfur-Functionalized Carborane Reagents at the B(9) Position 1

1.1. Introduction 1

1.2. Discussion 3

1.2.1. Synthesis of Carboranyl Sulfonium Reagent 3

1.2.2. Synthesis and Reactivity Studies of Zinc Bis(carboranyl sulfinates) 3

1.3. Results 8

1.3.1. Carboranyl Sulfonium Reagent 8

1.3.2. Zinc Bis(carboranyl sulfinates) 13

1.4. Conclusion and Future Steps 29

1.5. Methods 30

1.5.1. General Considerations 30

1.5.2. Instrumentation 30

1.5.3. Carboranyl Sulfonium Reagent 31

1.5.3.1. Synthesis of **compound 1b** 31

1.5.3.2. Synthesis of **compound 1c** 31
1.5.4. Zinc Bis(carboranyl sulfinates) 31
1.5.4.1. Synthesis of **compound 2b** 31
1.5.4.2. Synthesis of **compound 2c** 32
1.5.4.3. Synthesis of **compound 3b** 32
1.5.4.4. Synthesis of **compound 3c** 32
1.5.4.5. Synthesis of **compound 3d** 33
1.6. References 34
Chapter 2: Synthesis and Reactivity of Selenium- and Tellurium- Functionalized Carborane Reagents at the B(9) Position 39
2.1. Introduction 39
2.2. Discussion 40
2.2.1. General Considerations 40
2.2.2. Target Compounds 40
2.2.3. Nucleophilic Chemistry of Selenium-Based Carboranyl Compounds 41
2.2.4. Electrophilic Chemistry of Selenium-Based Carboranyl Compounds 42
2.2.5. Nucleophilic Chemistry of Tellurium-Based Carboranyl Compounds 43
2.2.6. Electrophilic Chemistry of Tellurium-Based Carboranyl Compounds 46
2.3. Results 49
2.3.1. Nucleophilic Chemistry of Selenium-Based Carboranyl Compounds 49
2.3.2. Electrophilic Chemistry of Selenium-Based Carboranyl Compounds 60
2.3.3. Nucleophilic Chemistry of Tellurium-Based Carboranyl Compounds 63
2.3.4. Electrophilic Chemistry of Tellurium-Based Carboranyl Compounds 97

2.4. Conclusion and Future Steps 114
2.5. Methods 115
2.5.1. General Considerations 115
2.5.2. Instrumentation 115
2.5.3. Nucleophilic Chemistry of Selenium-Based Carboranyl Compounds 116
2.5.3.1. Synthesis of **compound 4b** 116
2.5.3.2. Synthesis of **compound 5b** 116
2.5.4. Electrophilic Chemistry of Selenium-Based Carboranyl Compounds 117
2.5.4.1. General considerations for synthesis of **compounds 6a, 6b** 117
2.5.5. Nucleophilic Chemistry of Tellurium-Based Carboranyl Compounds 117
2.5.5.1. Synthesis of **compound 7a** 117
2.5.5.2. Synthesis of **compound 7b** 118
2.5.5.3. Synthesis of **compound 7c** 118
2.5.5.4. Synthesis of **compound 7d** 119
2.5.5.5. Synthesis of **compound 8b** 119
2.5.6. Electrophilic Chemistry of Tellurium-Based Carboranyl Compounds 120
2.5.6.1. Synthesis of **compound 9b** 120
2.5.6.2. General considerations for synthesis of **compound 9c** 120
2.5.6.3. Synthesis of **compound 10a** 120
2.5.6.4. Synthesis of **compound 10b** 121
2.5.6.5. Synthesis of **compounds 11a and 11b** 121
2.5.6.6. Synthesis of **compounds 12a and 12b** 121
2.6. References 122

LIST OF FIGURES

Figure 1-1 Numbering, naming, and labeling conventions for the different icosahedral carborane isomers 2

Figure 1-2 Synthetic scheme for the 9-*ortho*-carboranyl dimethyl sulfonium triflate 3

Figure 1-3 Synthetic scheme for the zinc bis(9-*ortho*-carboranyl sulfinate) 4

Figure 1-4 Synthetic scheme for the zinc bis(9-*meta*-carboranyl sulfinate), including the synthesis of the 9-*meta*-carboranyl sulfonamide 5

Figure 1-5 General scheme depicting the oxidative generation of a B-centered on a carborane cluster 6

Figure 1-6 ^{1}H NMR spectrum of **compound 1b** in $CDCl_3$ 8

Figure 1-7 ^{11}B NMR spectrum of **compound 1b** in $CDCl_3$ 9

Figure 1-8 ^{11}B NMR spectrum of **compound 1b** in $CDCl_3$ 10

Figure 1-9 GCMS spectrum of **compound 1b** 11

Figure 1-10 ^{11}B NMR spectrum of **compound 1c** in CD_3CN 12

Figure 1-11 ^{11}B NMR spectrum of **compound 2b** in non-deuterated CH_3CN 14

Figure 1-12 $^{11}B\{^{1}H\}$ NMR spectrum of **compound 2b** in non-deuterated CH_3CN 15

Figure 1-13 ^{11}B NMR spectrum of **compound 2c** in CD_3CN 16

Figure 1-14 $^{11}B\{^{1}H\}$ NMR spectrum of **compound 2c** in CD_3CN 17

Figure 1-15 ^{1}H NMR spectrum of **compound 3b** in CD_3CN 18

Figure 1-16 ^{11}B NMR spectrum of **compound 3b** in CH_2Cl_2 19

Figure 1-17 $^{11}B\{^{1}H\}$ NMR spectrum of **compound 3b** in CH_2Cl_2 20

Figure 1-18 ^{1}H NMR spectrum of **compound 3c** (H_2O batch) in D_2O 21

Figure 1-19 ^{11}B NMR spectrum of **compound 3c** (H_2O batch) in D_2O 22

Figure 1-20 $^{11}B\{^{1}H\}$ NMR spectrum of **compound 3c** (H_2O batch) in D_2O 23

Figure 1-21 Cyclic Voltammogram of **compound 3c** (H_2O batch)..... 24

Figure 1-22 ^{11}B NMR spectrum of **compound 3c** (THF batch) in non-deuterated THF 25

Figure 1-23 $^{11}B\{^{1}H\}$ NMR spectrum of **compound 3c** (THF batch) in nondeuterated THF . 26

Figure 1-24 Cyclic Voltammogram of **compound 3c** (THF batch) 27

Figure 1-25 $^{11}B\{^{1}H\}$ NMR spectrum of **compound 3b** in CH_2Cl_2 28

Figure 2-1 Synthetic scheme for the generation of bis(*ortho*-carboranyl) dichalcogenides ... 41

Figure 2-2 Synthetic scheme for the generation of carboranyl chalcogenolates and chalcogen halides 41

Figure 2-3 Reaction scheme for the synthesis of the *ortho*-carboranyl selenol 42

Figure 2-4 Reaction scheme for the synthesis of a *meta*-carboranyl selenoether..... 42

Figure 2-5 Synthetic scheme for the reactivity of carboranyl chalcogen halides..... 43

Figure 2-6 Synthetic scheme for the nucleophilic reactivity of the *orhto*-carboranyl tellurolate anion..... 44

Figure 2-7 Reaction scheme for the synthesis of a *meta*-carboranyl telluroether..... 46

Figure 2-8 Reaction scheme for probing the Li-Te exchange properties of the *meta*-carboranyl tellurides..... 47

Figure 2-9 Reaction scheme for the synthesis attempts of various *meta*-carboranyl tellurium trihalides 48

Figure 2-10 Reaction scheme for reactivity of the *meta*-carboranyl tellurinyl (IV) trichloride..... 48

Figure 2-11 ^{1}H NMR spectrum of **compound 4b** in CD_2Cl_2..... 50

Figure 2-12 ^{11}B NMR spectrum of **compound 4b** in CD_2Cl_2..... 51

Figure 2-13 ^{1}H NMR spectrum of **compound 5b** in $CDCl_3$ 52

Figure 2-14 Zoomed-in ^{1}H NMR spectrum of **compound 5b** in $CDCl_3$ 53

Figure 2-15 ^{13}C NMR spectrum of **compound 5b** in $CDCl_3$ 54

Figure 2-16 Zoomed-in ^{13}C NMR spectrum of **compound 5b** in $CDCl_3$ 55

Figure 2-17 ^{11}B NMR spectrum of **compound 5b** in $CDCl_3$ 56

Figure 2-18 ^{11}B{^{1}H} NMR spectrum of **compound 5b** in $CDCl_3$ 57

Figure 2-19 ^{125}Te NMR spectrum of **compound 5b** in $CDCl_3$ 58

Figure 2-20 ^{1}H-^{1}H COSY NMR spectrum of **compound 5b** in $CDCl_3$..... 59

Figure 2-21 GCMS spectra of **compound 6b** 61

Figure 2-22 GCMS spectra of **compound 6c**..... 62

Figure 2-23 ^{1}H NMR spectrum of **compound 7a** in THF-d8 64

Figure 2-24 ^{13}C NMR spectrum of **compound 7a** in THF-d8 65

Figure 2-25 ^{11}B NMR spectrum of **compound 7a** in THF-d8 66

Figure 2-26 ^{11}B{^{1}H} NMR spectrum of **compound 7a** in THF-d8 67

Figure 2-27 ^{125}Te NMR spectrum of **compound 7a** in THF-d8 68

Figure 2-28 ^{1}H NMR spectrum of **compound 7a** in C_6D_6..... 69

Figure 2-29 ^{11}B NMR spectrum of **compound 7a** in C_6D_6..... 70

Figure 2-30 ^{11}B{^{1}H} NMR spectrum of **compound 7a** in C_6D_6..... 71

Figure 2-31 ^{1}H NMR spectrum of **compound 7b** in THF-d8 72

Figure 2-32 ^{1}H NMR spectra comparison of **compound 7b** in $CDCl_3$ and THF-d8..... 73

Figure 2-33 ^{13}C NMR spectrum of **compound 7b** in THF-d8 74

Figure 2-34 ^{11}B NMR spectrum of **compound 7b** in THF-d8 75

Figure 2-35 ^{11}B{^{1}H} NMR spectrum of **compound 7b** in THF-d8 76

Figure 2-36 ^{125}Te NMR spectrum of **compound 7b** in THF-d8 77

Figure 2-37 ^{1}H NMR spectrum stability study of **compound 7b** in THF-d8 78

Figure 2-38 ^{11}B{^{1}H} NMR spectrum stability study of **compound 7b** in THF-d8..... 79

Figure 2-39 GCMS spectrum of **compound 7b** 80

Figure 2-40 ^{1}H NMR spectrum of **compound 7c** in $CDCl_3$..... 81

Figure 2-41 ^{11}B NMR spectrum of **compound 7c** in $CDCl_3$ 82

Figure 2-42 ^{11}B{^{1}H} NMR spectrum of **compound 7c** in $CDCl_3$..... 83

Figure 2-43 ^{1}H NMR spectrum of **compound 7d** (with expansion) in THF-d8 84

Figure 2-44 ^{13}C NMR spectrum of **compound 7d** in THF-d8..... 85

Figure 2-45 ^{11}B NMR spectrum of **compound 7d** in THF-d8..... 86

Figure 2-46 ^{11}B{^{1}H} NMR spectrum of **compound 7d** in THF-d8 87

Figure 2-47 ^{125}Te NMR spectrum of **compound 7d** in THF-d8 88

Figure 2-48 ^{1}H NMR spectrum of **compound 8b** in $CDCl_3$ 89

Figure 2-49 Zoomed-in 1H NMR spectrum of **compound 8b** in $CDCl_3$ 90

Figure 2-50 ^{13}C NMR spectrum of **compound 8b** in $CDCl_3$..... 91

Figure 2-51 Zoomed-in ^{13}C NMR spectrum of **compound 8b** in $CDCl_3$..... 92

Figure 2-52 ^{11}B NMR spectrum of **compound 8b** in $CDCl_3$..... 93

Figure 2-53 ^{11}B{^{1}H} NMR spectrum of **compound 8b** in $CDCl_3$ 94

Figure 2-54 ^{125}Te NMR spectrum of **compound 8b** in $CDCl_3$ 95

Figure 2-55 ^{1}H-^{1}H COSY NMR spectrum of **compound 8b** in $CDCl_3$..... 96

Figure 2-56 GCMS spectrum of **compound 9c** from lithiation of **compound 9a** 98

Figure 2-57 GCMS spectrum of **compound 9c** from lithiation of **compound 9b**..... 99

Figure 2-58 ^{1}H NMR spectrum of **compound 10a** in THF-d8 100

Figure 2-59 ^{13}C NMR spectrum of **compound 10a** in THF-d8 101

Figure 2-60 ^{11}B NMR spectrum of **compound 10a** in THF-d8 102

Figure 2-61 ^{11}B{^{1}H} NMR spectrum of **compound 10a** in THF-d8 103

Figure 2-62 ^{125}Te NMR spectrum of **compound 10a** in THF-d8 104

Figure 2-63 ^{1}H NMR spectrum of **compound 10b** in THF-d8 105

Figure 2-64 ^{13}C NMR spectrum of **compound 10b** in THF-d81 106

Figure 2-65 ^{11}B NMR spectrum of **compound 10b** in THF-d8 107

Figure 2-66 ^{11}B{^{1}H} NMR spectrum of **compound 10b** in THF-d8 108

Figure 2-67 ^{125}Te NMR spectrum of **compound 10b** in THF-d8 109

Figure 2-68 ^{125}Te NMR spectrum of **compound 11a** in $CDCl_3$..... 110

Figure 2-69 ^{125}Te NMR spectrum of **compound 11b** in $CDCl_3$ 111

Figure 2-70 ^{125}Te NMR spectrum of **compound 12a** in $CDCl_3$..... 112

Figure 2-71 ^{125}Te NMR spectrum of **compound 12b** in $CDCl_3$ 113

LIST OF TABLES

Table 1-1 Reaction conditions for B-S bond activation 7

Table 2-1 Reactivity of **compound 6a** with several alkenes and a ketone 43

Table 2-2 Reaction conditions for attempted generation of aryl tellurides through S_NAr and oxidative coupling..... 45

LIST OF ACRONYMS

AcOH	Acetic Acid
BNCT	Boron Neutron Capture Therapy
CAN	Ceric Ammonium Nitric
COSY	Correlation Spectroscopy
DCM	Dichloromethane
DMF	Dimethylformamide
DMSO	Dimethyl Sulfoxide
DTBP	Di-*tert*-butylperoxide
Et_2O	Diethyl Ether
Et_3N	Triethylamine
EtOAc	Ethyl Acetate
EtOH	Ethanol
Fc/Fc^+	Ferrocene/Ferrocenium Redox Couple
GCMS	Gas Chromatography – Mass Spectrometry
MeCN	Acetonitrile
MeI	Methyl Iodide
MeOTf	Methyl Triflate
nBuLi	*n*-Butyllithium
NCS	N-chlorosuccinimide
NMR	Nuclear Magnetic Resonance
Ph	Phenyl
rt	Room Temperature

SAM	Self-Assembled Monolayer
TBA	Tetra-*n*-butylammonium
TBHP	*Tert*-butyl Hydroperoxide
TBP	4-*tert*-butylpyridine
TEMPO	(2,2,6,6-Tetramethylpiperidin-1-yl)oxyl
THF	Tetrahydrofuran
THF-d8	Deuterated Tetrahydrofuran
TLC	Thin Layer Chromatography

ACKNOWLEDGMENTS

I would like to wholeheartedly thank Professor Alexander Spokoyny for being an outstanding advisor and giving me the opportunity to explore the exciting world of boron cluster chemistry for the past few years. I am also especially grateful to Harrison Mills for his continuous mentorship, training, and endless support. Furthermore, I would like to thank the entirety of the Spokoyny group for being welcoming and playing an essential role in helping me mature as a scientist. Finally, I would like to thank my family, friends, loved ones, and everyone I crossed paths with during my time at UCLA for their continuous love and support; I am especially grateful to my parents for their massive sacrifices in hope of providing me with a better future.

Chapter 1 includes contributions from Harrison Mills; he synthesized and characterized **compounds 1a and 3a**, and performed B-S bond cleavage studies on *meta*-carboranyl sulfonium analogues of **compound 1c** (not included in this thesis)

Chapter 2 includes contributions from Harrison Mills; he synthesized and characterized **compounds 4a, 5a, 6a, 8a, and 9a** and carried out major work studying the nucleophilic and electrophilic reactivity of *meta*-carboranyl selenides and tellurides (partly included in the thesis).

To gain a complete understanding of the scope of this work and for additional experiments, please also refer to the dissertation of Harrison Mills as well as a manuscript in preparation detailing the synthesis and reactivity studies of carboranes functionalized with Se and Te at the B(9) position. Support for the work in this thesis was provided by the Arthur Furst as well as the Raymond and Dorothy Wilson Endowment Summer Undergraduate Research Fellowships.

Chapter 1: Synthesis and Reactivity of Sulfur-Functionalized Carborane Reagents at the B(9) Position

1.1. Introduction

Organosulfur compounds play a prominent role in synthetic organic chemistry, as highlighted by their wide range of synthetic transformations and their omnipresence in the agrochemical and pharmaceutical industries[1-6]. One notable mode of reactivity of organosulfur compounds is C-S cleavage chemistry, which allows for the construction of new C-C bonds from common sulfur-based functional groups. While the traditional method for C-S bond cleavage involves transition metal catalysis[7-9], there has been significant recent interest in achieving C-S bond modification through alternative methods such as photoredox catalysis or the utilization of chemical oxidants[10-11]. One notable recent example is the development and utilization of zinc sulfinate reagents by the Baran group to functionalize heterocycles[12-14].

Icosahedral carboranes ($C_2B_{10}H_{12}$) are boron-rich three-dimensional clusters that exist as *ortho*-, *meta*-, and *para*- isomers based on the relative position of the two carbon vertices on the cage (**Figure 1-1**). They exhibit three-dimensional electron delocalization analogous to aromaticity in benzene[15], while possessing a steric profile similar to that of adamantane[16]. Additionally, they offer electronic tunability based on the chosen vertex for functionalization: the carbon vertices are typically electron deficient while the boron vertices farthest away from carbon are typically electron rich[16]. As a result of their unique properties, carborane clusters find applications in a wide variety of fields ranging from materials to medicinal chemistry[17,18].

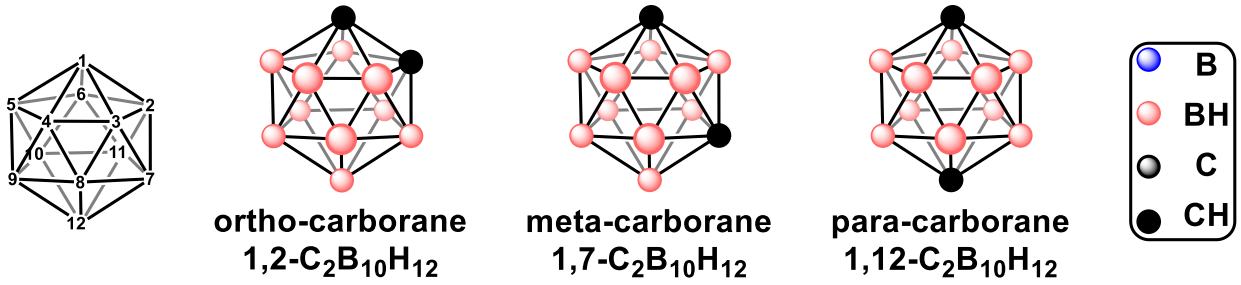

Figure 1-1. Numbering, naming, and labeling conventions for the different icosahedral carborane isomers

Carboranes with a B-S bond at the electron-rich B(9) vertex were first reported in the late 1970s.[19-22] Since then, these compounds have found uses in a variety of areas such as self-assembled monolayers (SAMs), Boron-Neutron Capture Therapy (BNCT), and as ligands for metal surfaces and transition metal ions[23-28]. Thus far, much of the research in the field has been focused on the process of B-S bond formation as well as applications of carboranes containing the B-S moiety; several common sulfur-based functional groups—such as thioethers, sulfonyl chlorides, and sulfonamides—have been constructed from the 9-SH functionalized carborane. There have been no studies exploring the B-S bond-breaking process, however.

In this thesis, I will describe the synthesis of two classes of S-functionalized carborane derivatives that are candidates for B-S bond cleavage—carboranyl dimethyl sulfoniums and zinc bis(carboranyl sulfinates). Furthermore, I will survey a series of reaction conditions that I employed to screen the reactivity of the zinc bis(*meta*-carboranyl sulfinate) reagent towards B-S bond cleavage.

1.2. Discussion

1.2.1. Synthesis of Carboranyl Sulfonium Reagent

Sulfoniums have a general formula of $[R_3S]^+X^-$. The synthetic scheme for the target sulfonium salt, [9-(Me_2S)-*ortho*-$C_2B_{10}H_{11}$]OTf (**compound 1c**), is depicted below in **Figure 1-2**.

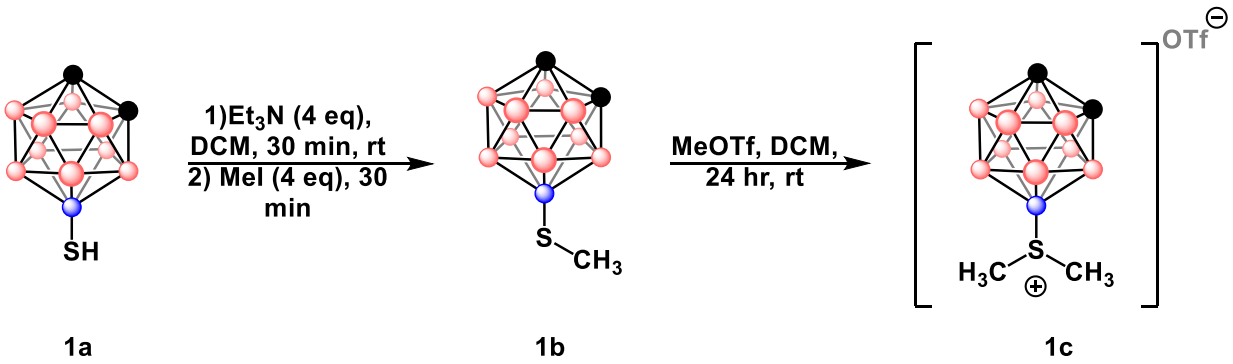

Figure 1-2. Synthetic scheme for the 9-*ortho*-carboranyl dimethyl sulfonium triflate

Compound 1a was synthesized according to procedures reported by Plešek et al. and Zakharkin et al[19-22] and matches reported characterization. Attempting to oxidize **compound 1b** to a sulfoxide by reacting it with hydrogen peroxide resulted in decomposition of the cage as determined by ^{11}B NMR resonances corresponding to a *nido*-carborane[29]. Note that **compound 1c** was synthesized differently from previous reports[19-22] by utilizing a different electrophilic methylating agent.

1.2.2. Synthesis and Reactivity Studies of Zinc Bis(carboranyl sulfinates)

Zinc bis(alkylsulfinates) were previously shown to be competent reagents in the functionalization of nitrogen-rich heterocycles by the Baran group[12]. The synthetic scheme for the zinc bis(*ortho*-carboranyl sulfinate) is shown in **Figure 1-3**. Compound 2b was synthesized under much milder conditions than the original reports from Zakharkin et al. and Plešek et al.[19-22]

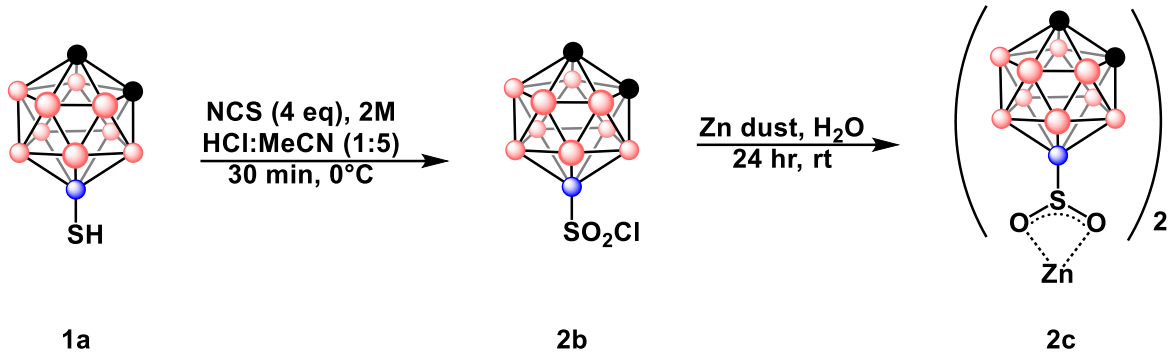

Figure 1-3. Synthetic scheme for the zinc bis(9-*ortho*-carboranyl sulfinate)

by adapting a procedure from Nishiguchi et al.[30] **Compound 2c** was synthesized according to a procedure adapted from Fujiwara et al. and O'Hara et al.[12,13] See methods section for full experimental details. To confirm the formation of a sulfonyl chloride, **compound 2b** was reacted with a variety amines to form a sulfonamide, but it was observed that **compound 2b** undergoes deboronation similarly to **compound 1b**. These observations are consistent with the general trend that the *ortho*- isomer of carborane is less stable than the *meta*- isomer towards certain oxidizing and basic conditions[16]. This led to the decision to work with the *meta*- isomer instead. The synthetic scheme for zinc bis(*meta*-carboranyl sulfinate) is shown in **Figure 1-4** and is similar to the scheme for the *ortho*- isomer. Likewise, **compound 3a** was synthesized according to procedures reported by Plešek et al. and Zakharkin et al[19-22] and matches reported characterization.

Unlike **compound 2b**, **compound 3b** rapidly and cleanly reacts with benzylamine to afford the corresponding sulfonamide (**compound 3d**) as can be seen in **Figure 1-4**. **Compound 3c** was also synthesized using THF as the solvent instead of H_2O, affording a similar-looking compound that had slight differences in the NMR resonances. This, combined with the

observation that product made in THF was insoluble in H_2O while the product made in H_2O was insoluble in THF, suggested that there is some sort of solvent adduct formation. Despite the solubility differences, both compounds displayed similar reactivity towards the oxidative conditions used to attempt to activate the B-S bond. **Figure 1-5** shows the general reaction scheme for the attempts at oxidative B-S bond cleavage. **Table 1-1** summarizes the reaction conditions employed in an attempt to activate the B-S bond on **compound 3c** (as can be seen in the scheme of **Figure 1-5**). Ultimately, two reagents (di-tert-butylperoxide and the pyrylium-based photocatalyst) were both able to activate the B-S bond. However, trapping the intermediate radical state was unsuccessful. These results are nevertheless promising, showing that the generated **compound 3c** can be a competent source for B-S bond cleavage under the appropriate conditions.

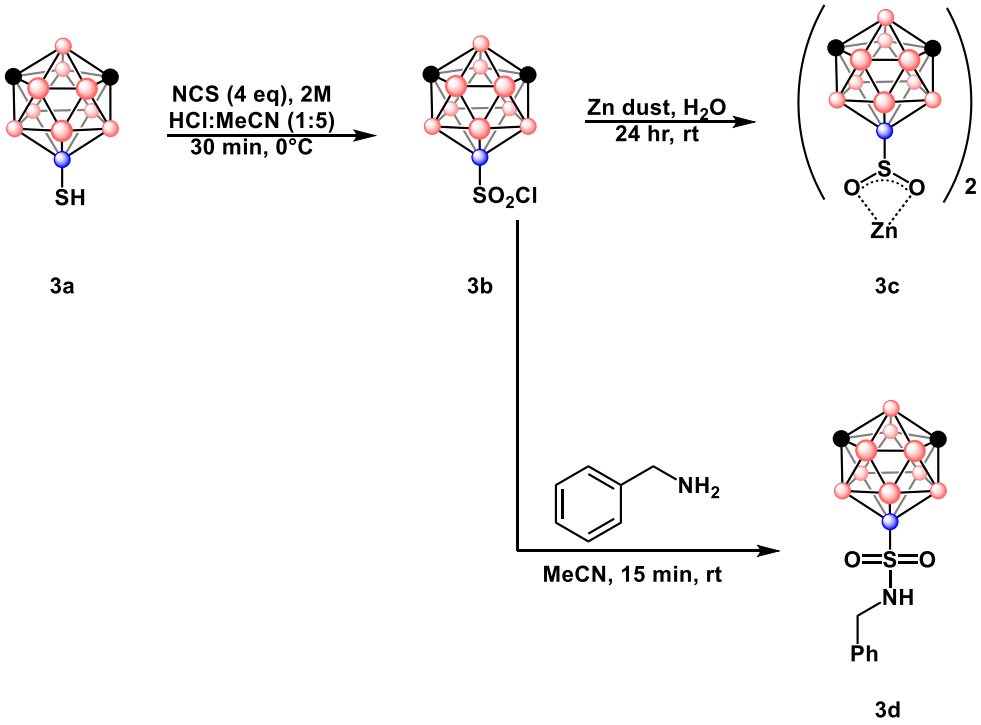

Figure 1-4. Synthetic scheme for the zinc bis(9-*meta*-carboranyl sulfinate), including the synthesis of the 9-*meta*-carboranyl sulfonamide

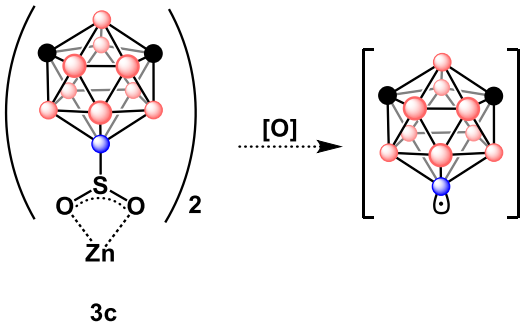

Figure 1-5. General scheme depicting the oxidative generation of a B-centered on carborane

Finally, cyclic voltammetry was used to probe the oxidation potential of **compound 3c** (both the batch synthesized in H_2O as well as in THF). The obtained voltammograms had high levels of noise, but some crude results can be extracted from them showing that the oxidation potential of **compound 3c**—with very little variation due to what solvent it adducts with—is around 1.0 V with respect to the Fc/Fc^+ redox couple.

Entry	Oxidant (equivalents)	Trap/Substrate (equivalents)	Solvent	Temperature	Time	Result
1	DTBP (3)	TBP (0.5)	H_2O	Room temp.	24 hr	A
2	$Mn(OAc)_3 \cdot 2H_2O$ (4)	TEMPO (2)	AcOH	60 ˚C	16 hr	B
3	Photocatalyst (0.2)	TEMPO (2)	MeCN	Room temp.	16 hr	A
4	Photocatalyst (0.1)	Benzyl Bromide (2)	MeCN	Room temp.	1.5 hr	A
5	Photocatalyst (0.05)	None (control)	MeCN	Room temp.	1 hr	A
6	CAN (2.5)	TEMPO (2)	H_2O:MeCN (1:1)	Room temp.	16 hr	C
7	CAN (3) + NaI (4)	TEMPO (3)	H_2O:MeCN (1:2)	40 ˚C	16 hr	C
8	CAN (0.5) + H_2O_2 (6)	TEMPO (3)	H_2O:MeCN (1:2)	50 ˚C	16 hr	C
9	TBHP (3)	TEMPO (0.5)	DMSO	50 ˚C	48 hr	C
10	TBHP (3)	TBP (0.5)	DMSO	50 ˚C	48 hr	C
11	TBHP (6)	TEMPO (0.5)	DMSO	Room temp.	24 hr	C
12	TBHP (4) + I_2 (0.5) + $FeSO_4 \cdot 7H_2O$ (3)	TEMPO (3)	THF	50 ˚C	16 hr	C

Table 1-1. Reaction conditions for B-S bond activation. Reactions run on a 0.05 mmol scale with respect to sulfinate. DTBP: di-tert-butyl peroxide; TBP: 4-tert-butyl pyridine; CAN: ceric ammonium nitrate; TEMPO: (2,2,6,6-Tetramethylpiperidin-1-yl)oxyl; TBHP: tert-butyl hydroperoxide; Photocatalyst: 2,4,6-tri(p-tolyl)pyrylium tetrafluoroborate with blue LED irradiation; **Results: A (recover unfunctionalized *meta*-carborane); B (deboronation); C (no reaction)**

1.3. Results

1.3.1. Carboranyl Sulfonium Reagent

The 9-*ortho*-carboranyl methyl sulfide (**compound 1b**) was characterized by ^{1}H (**Figure 1-6**), ^{11}B (**Figure 1-7**), and $^{11}B\{^{1}H\}$ (**Figure 1-8**) NMR spectroscopy as well as by GCMS (**Figure 1-9**). The 9-*ortho*-carboranyl dimethyl sulfonium (**compound 1c**) was characterized by 11B (**Figure 1-10**) NMR spectroscopy.

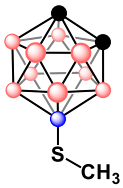

1b

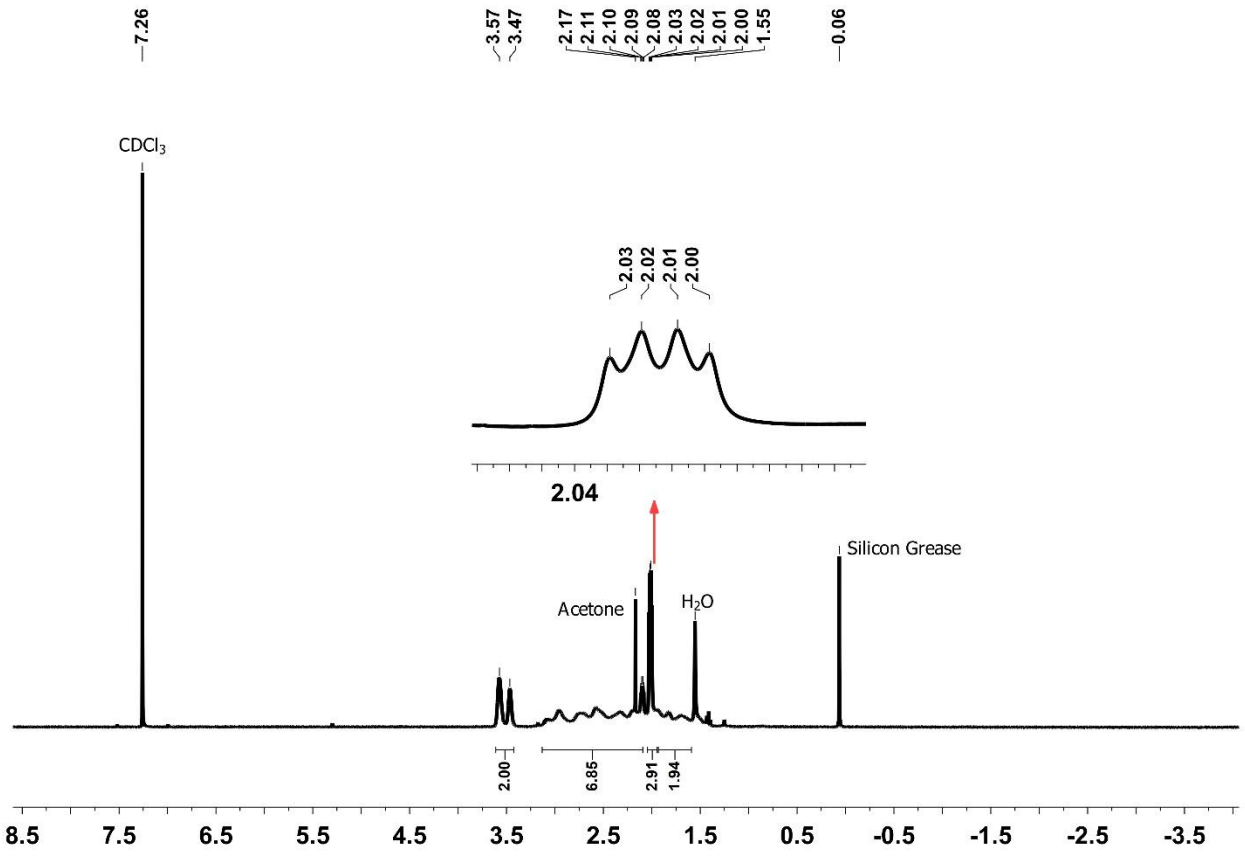

Figure 1-6. ^{1}H NMR spectrum of **compound 1b** in $CDCl_3$

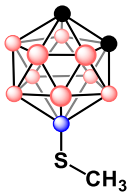

1b

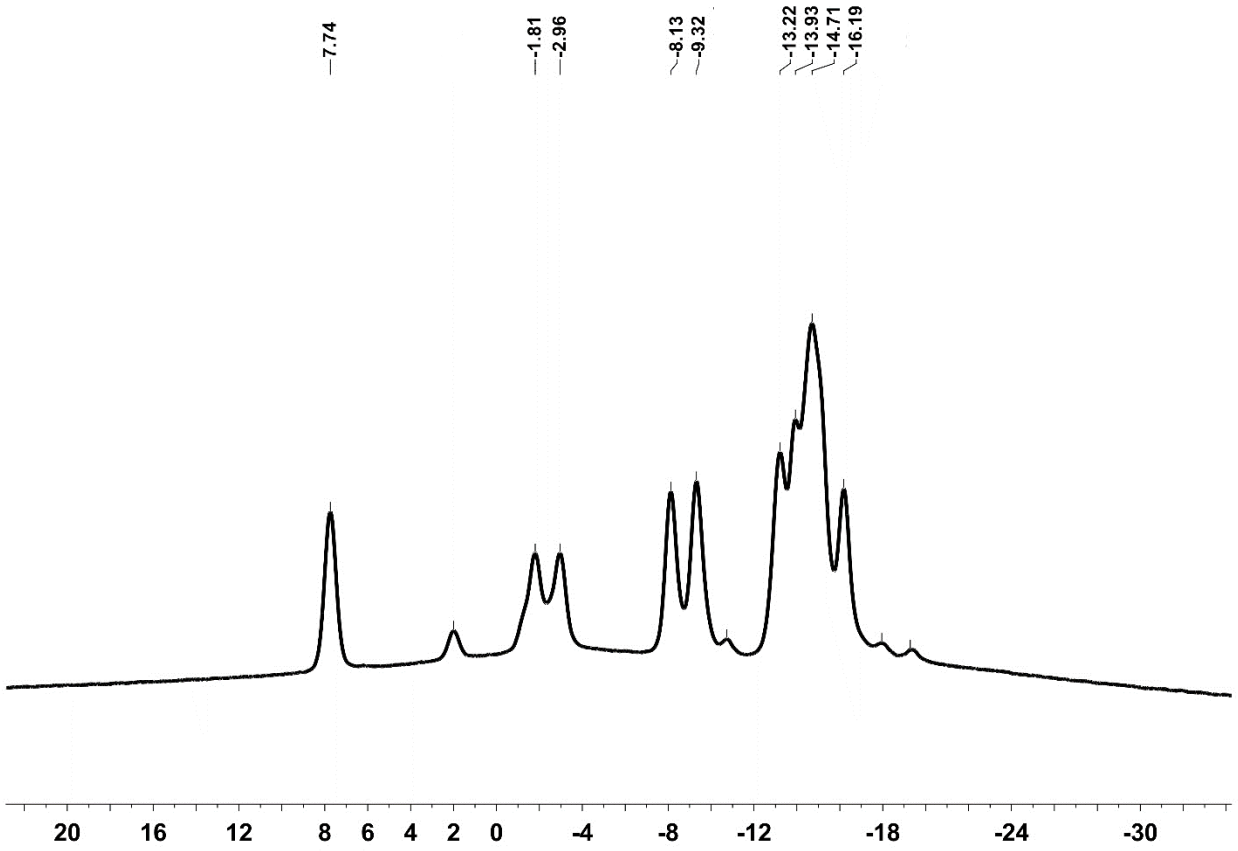

Figure 1-7. ^{11}B NMR spectrum of **compound 1b** in $CDCl_3$

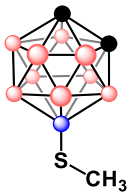

1b

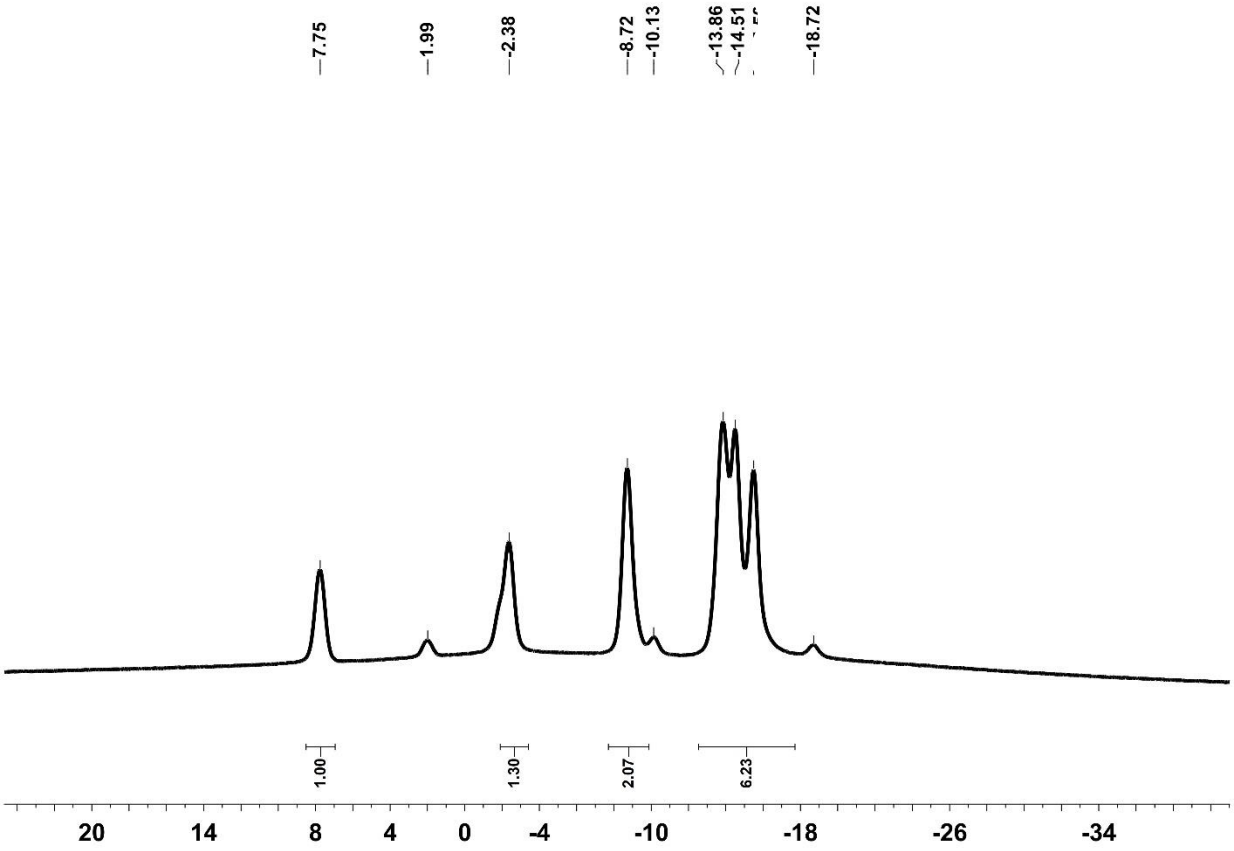

Figure 1-8. ^{11}B NMR spectrum of **compound 1b** in $CDCl_3$

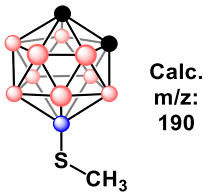

Calc. m/z: 190

1b

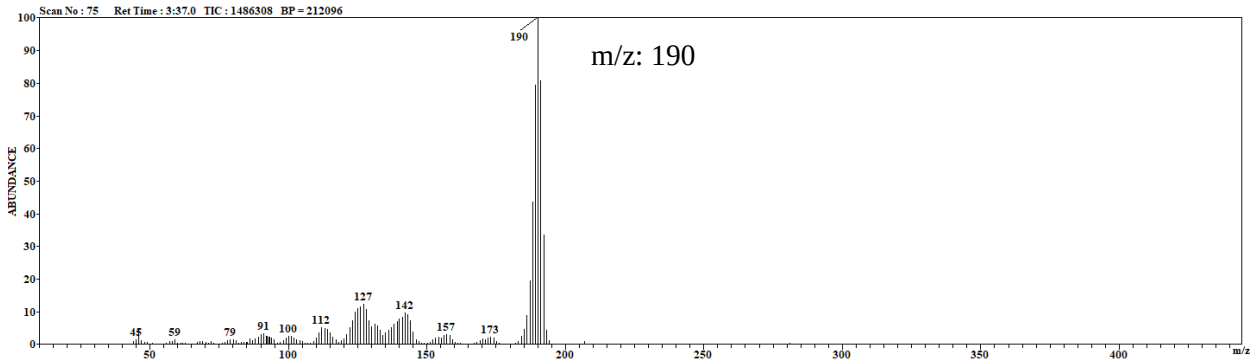

Figure 1-9. GCMS spectrum of **compound 1b**

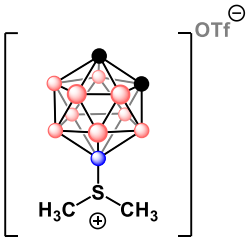

1c

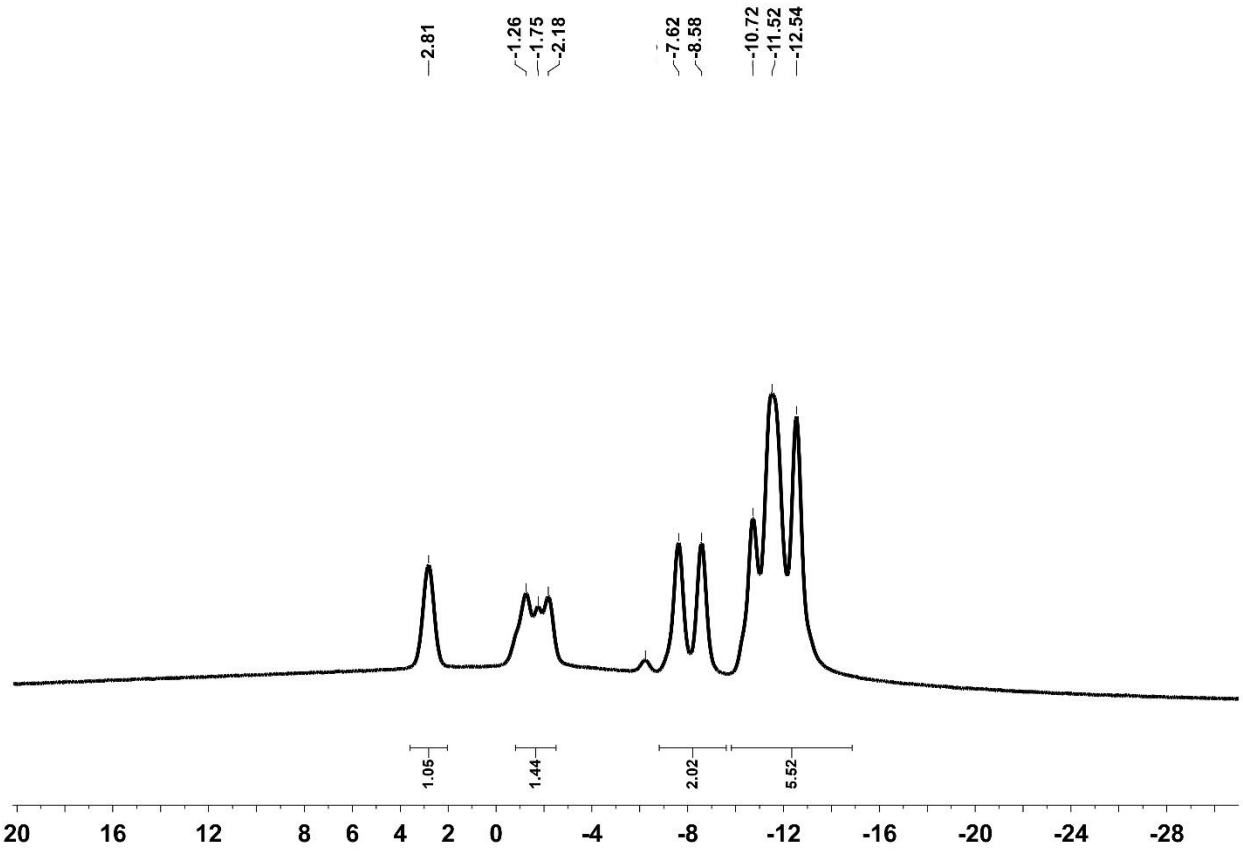

Figure 1-10. ^{11}B NMR spectrum of **compound 1c** in CD_3CN

1.3.2. Zinc Bis(carboranyl sulfinates)

The 9-*ortho*-carboranyl sulfonyl chloride (**compound 2b**) was characterized by ^{11}B (**Figure 1-11**) and $^{11}B\{^{1}H\}$ (**Figure 1-12**) NMR spectroscopy. The zinc bis(9-*ortho*-carboranyl sulfinate) (**compound 2c**) was characterized by ^{11}B (**Figure 1-13**) and $^{11}B\{^{1}H\}$ (**Figure 1-14**) NMR spectroscopy. Similarly, the 9-*meta*-carboranyl sulfonyl chloride (**compound 3b**) was characterized by ^{1}H (**Figure 1-15**), ^{11}B (**Figure 1-16**) and $^{11}B\{^{1}H\}$ (**Figure 1-17**) NMR spectroscopy. The zinc bis(9-*meta*-carboranyl sulfinate) (**compound 3c**) was characterized by ^{1}H (**Figure 1-18**), ^{11}B (**Figure 1-19/22**), and $^{11}B\{^{1}H\}$ (**Figure 1-20/23**), as well as cyclic voltammetry (**Figure 1-21/24**). Finally, the N-benzyl (9-*meta*-carboranyl) sulfonamide (**compound 3d**) was characterized by ^{11}B (**Figure 1-25**) NMR spectroscopy.

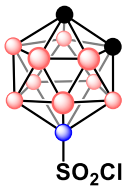

2b

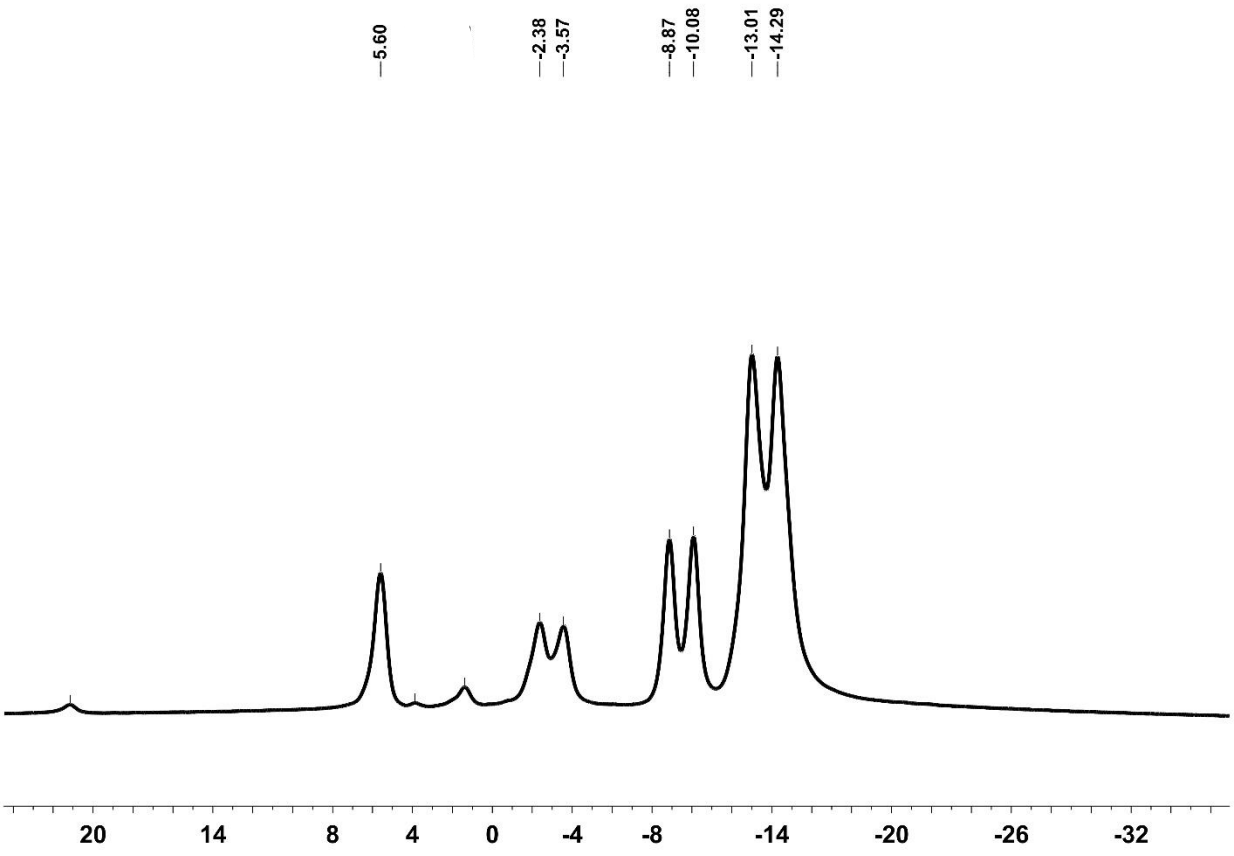

Figure 1-11. ^{11}B NMR spectrum of **compound 2b** in non-deuterated CH_3CN

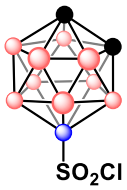

2b

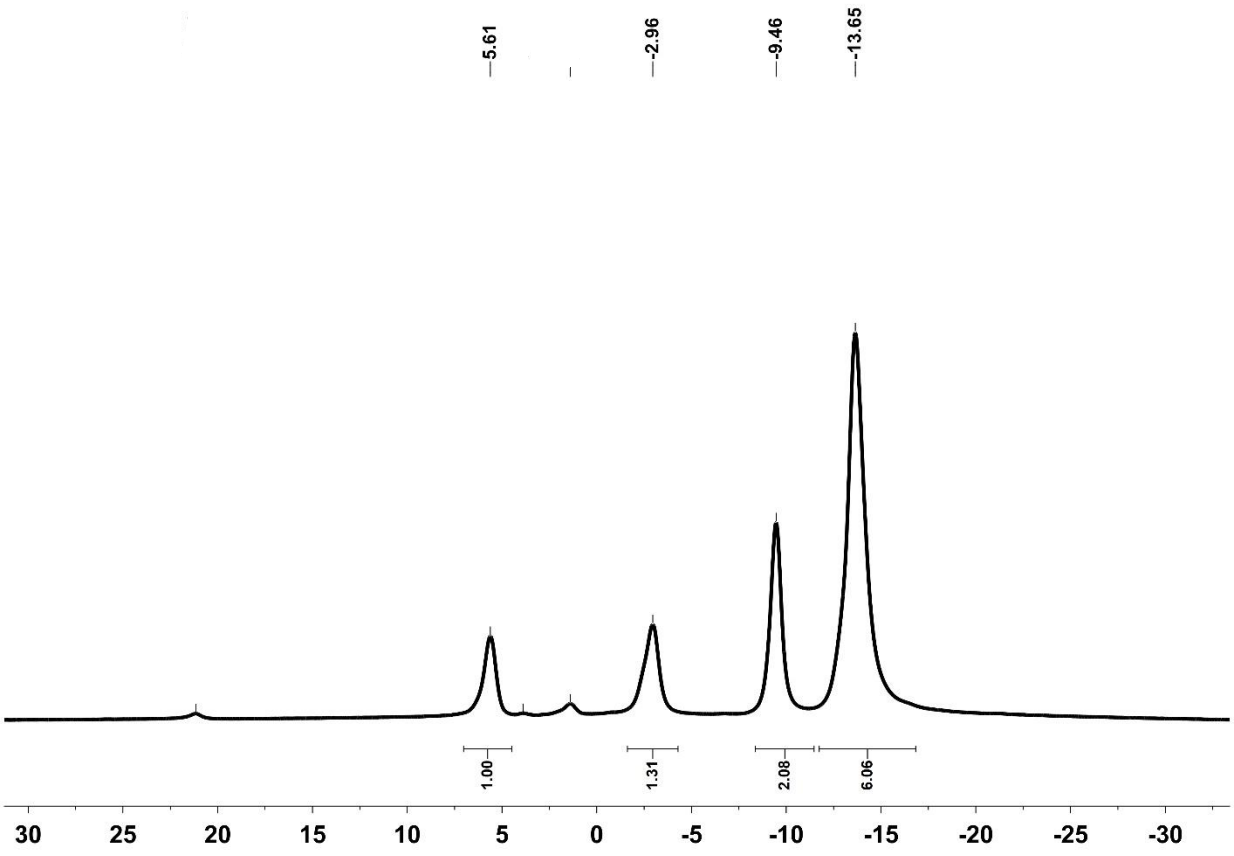

Figure 1-12. $^{11}B\{^{1}H\}$ NMR spectrum of **compound 2b** in non-deuterated CH_3CN

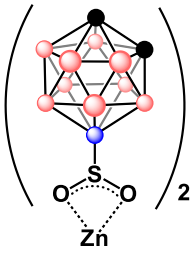

2c

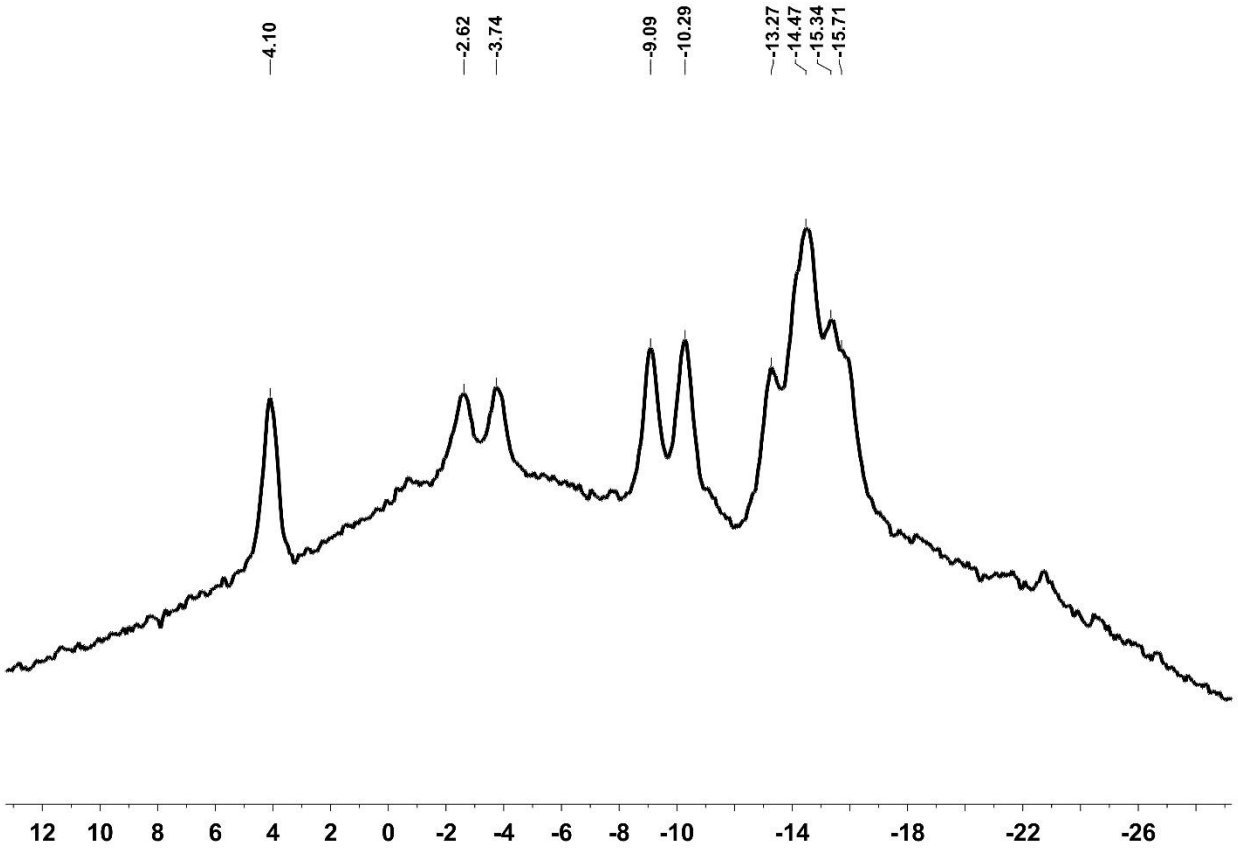

Figure 1-13. ^{11}B NMR spectrum of **compound 2c** in CD_3CN

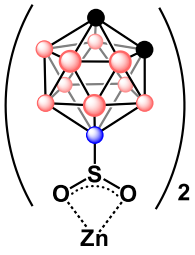

2c

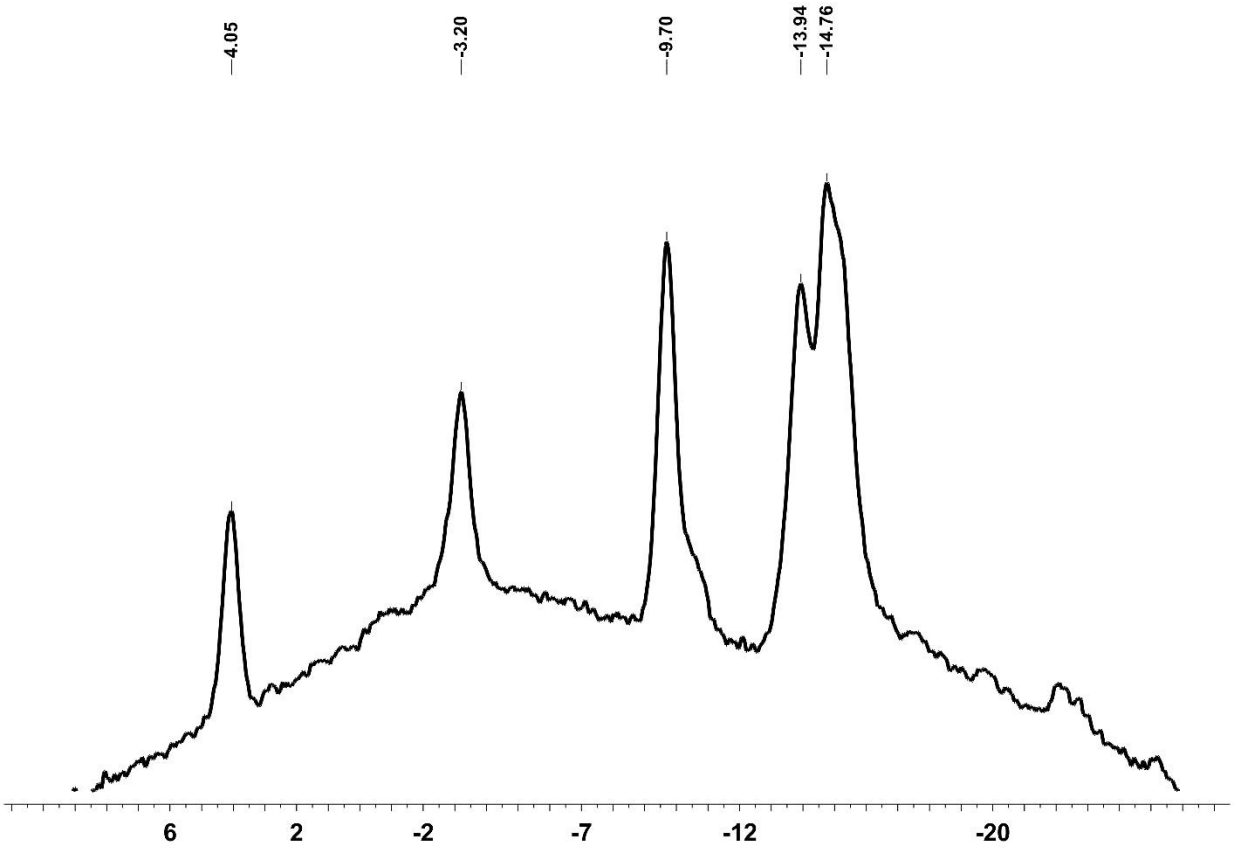

Figure 1-14. $^{11}B\{^{1}H\}$ NMR spectrum of **compound 2c** in CD_3CN

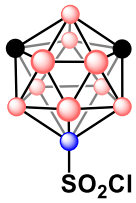

3b

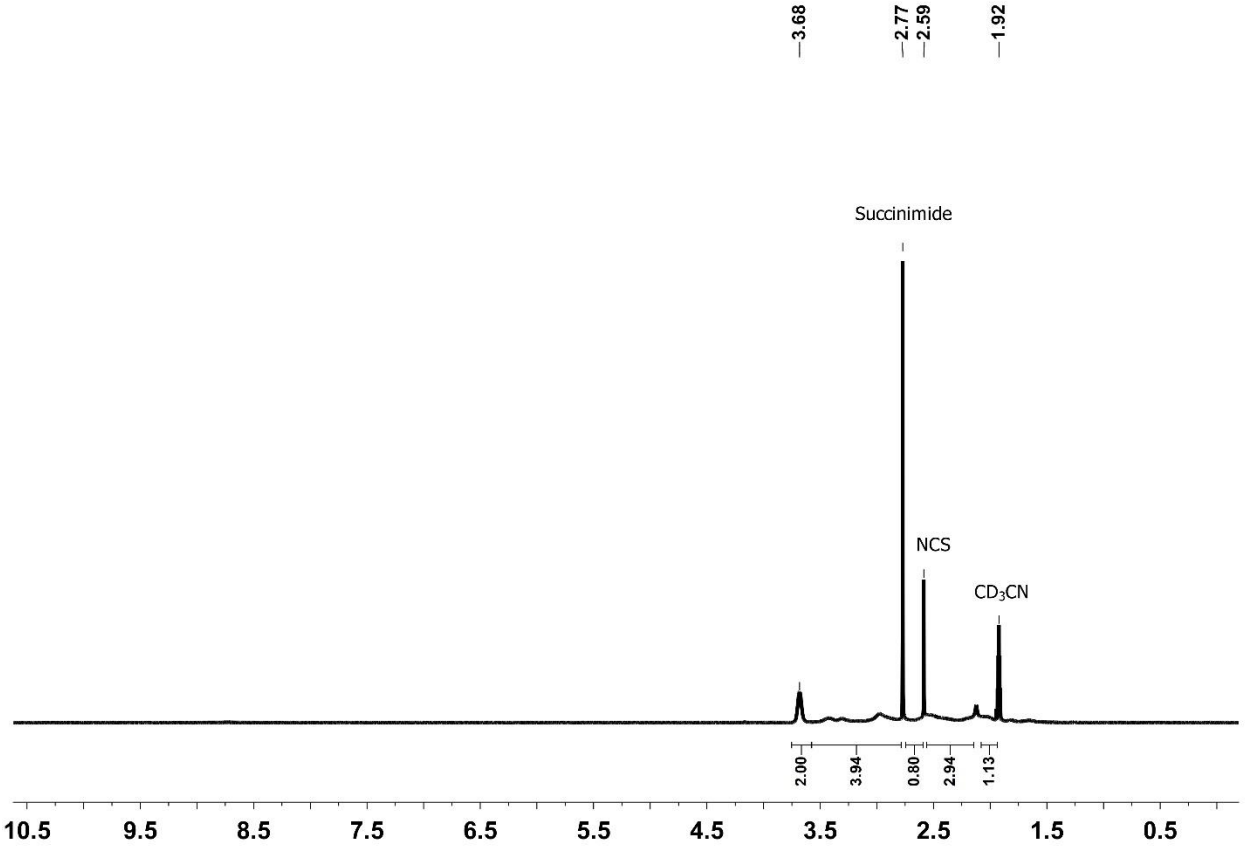

Figure 1-15. ^{1}H NMR spectrum of **compound 3b** in CD_3CN

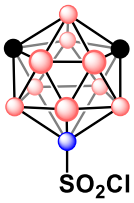

3b

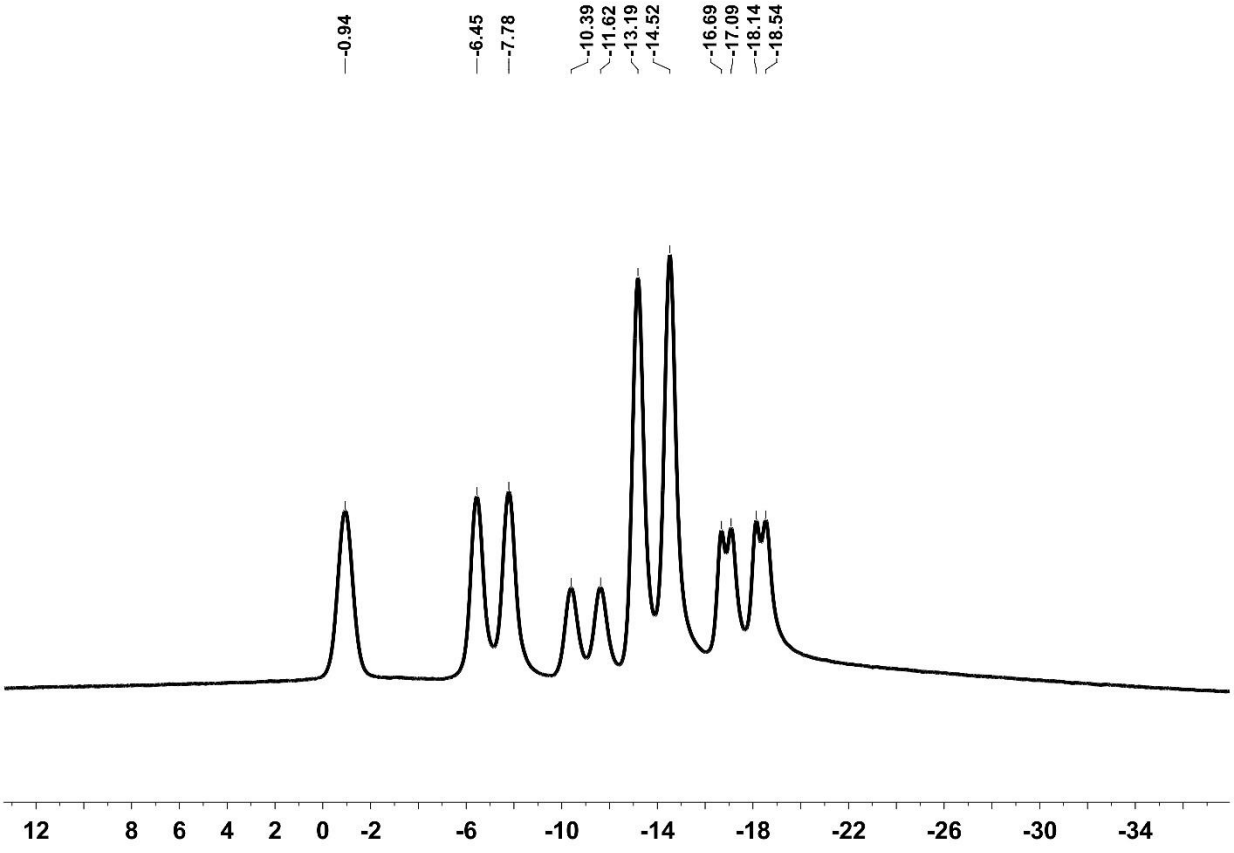

Figure 1-16. ^{11}B NMR spectrum of **compound 3b** in CH_2Cl_2

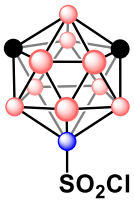

3b

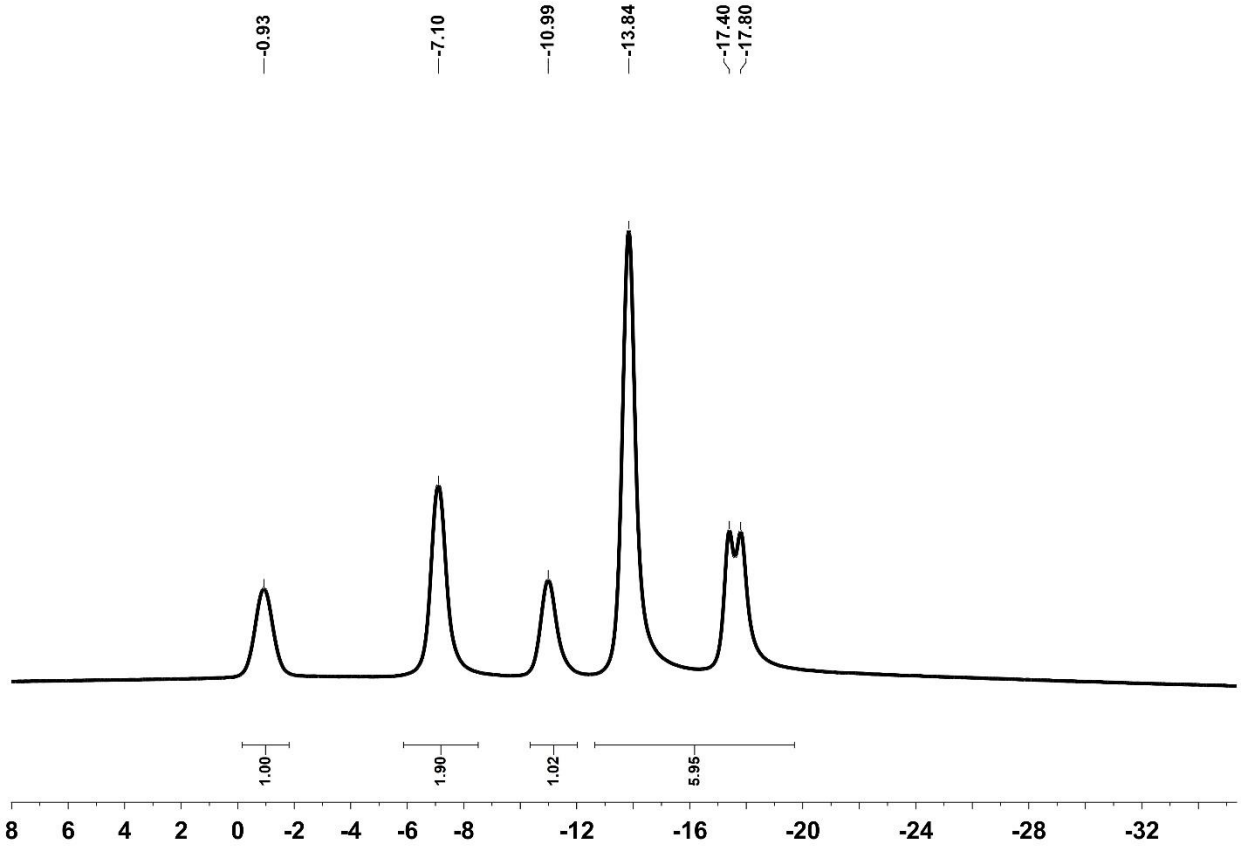

Figure 1-17. $^{11}B\{^{1}H\}$ NMR spectrum of **compound 3b** in CH_2Cl_2

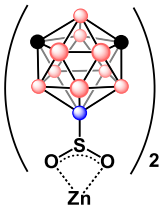

3c

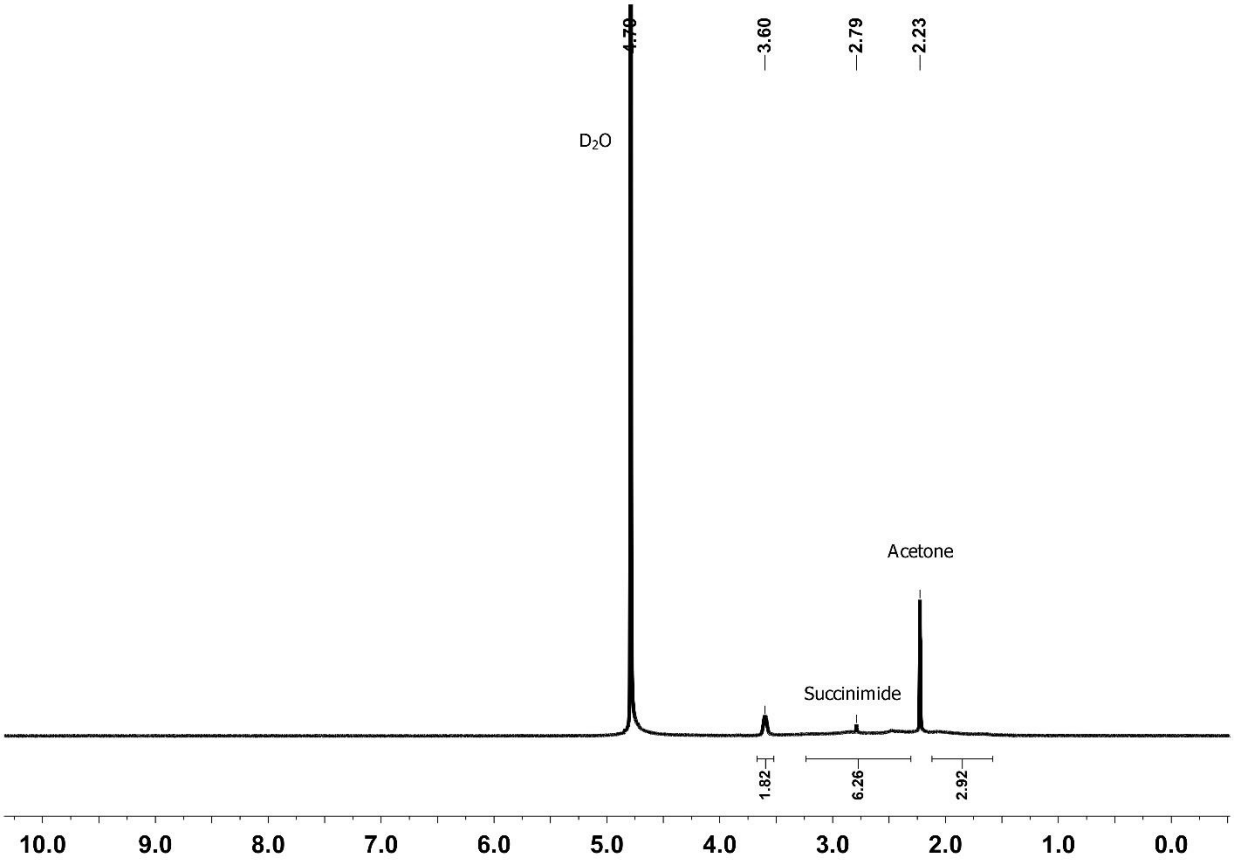

Figure 1-18. ^{1}H NMR spectrum of **compound 3c** (H_2O batch) in D_2O

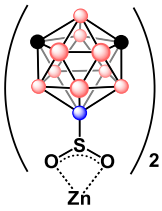

3c

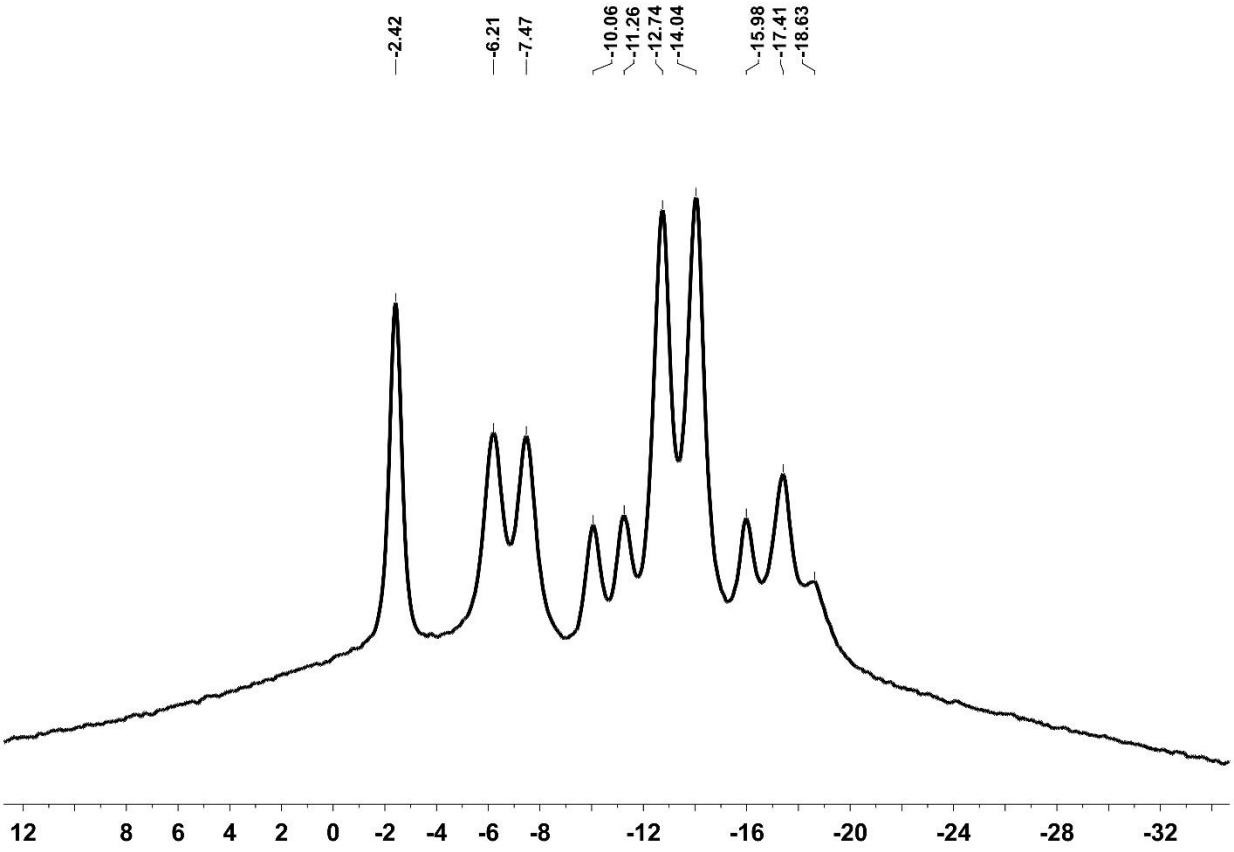

Figure 1-19. ^{11}B NMR spectrum of **compound 3c** (H_2O batch) in D_2O

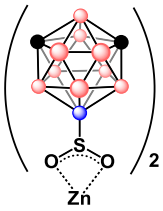

3c

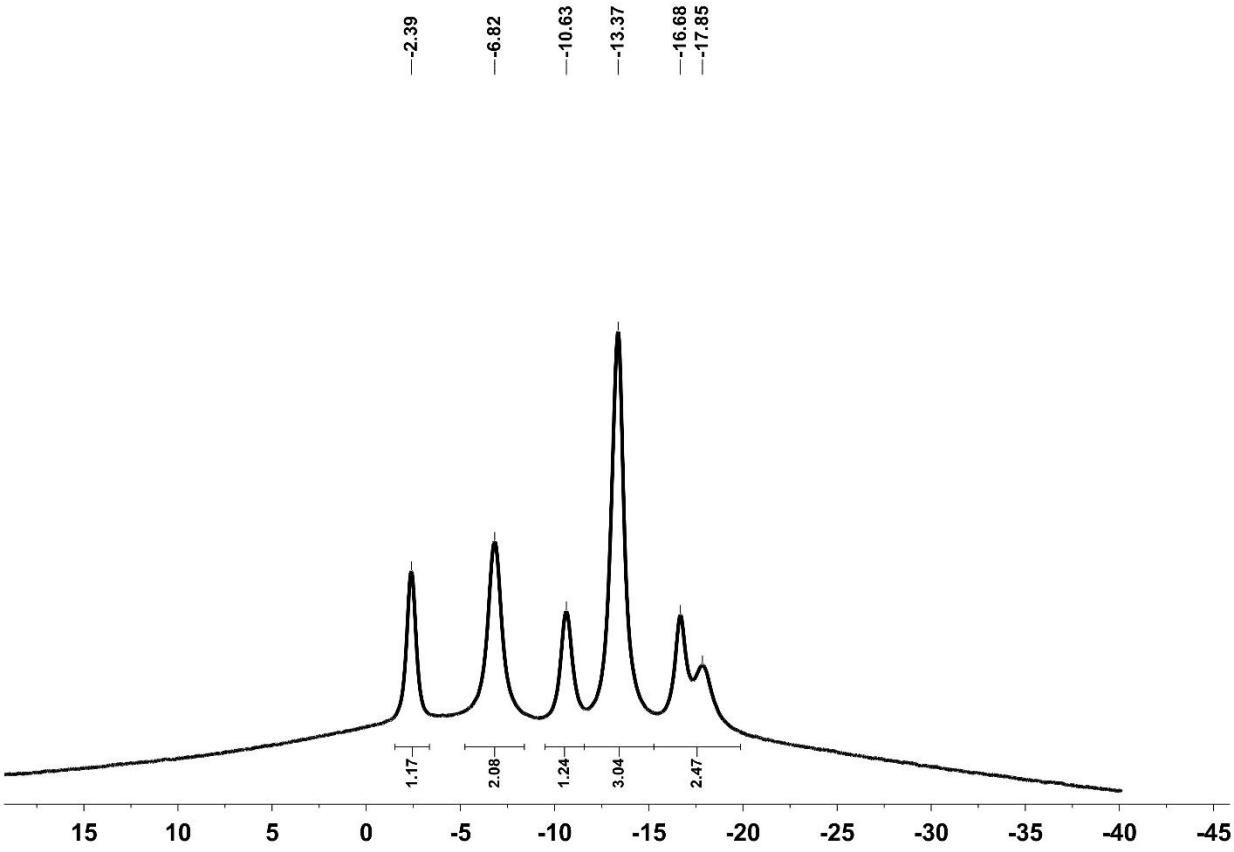

Figure 1-20. $^{11}B\{^{1}H\}$ NMR spectrum of **compound 3c** (H_2O batch) in D_2O

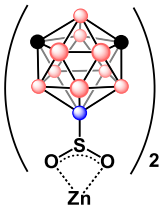

3c

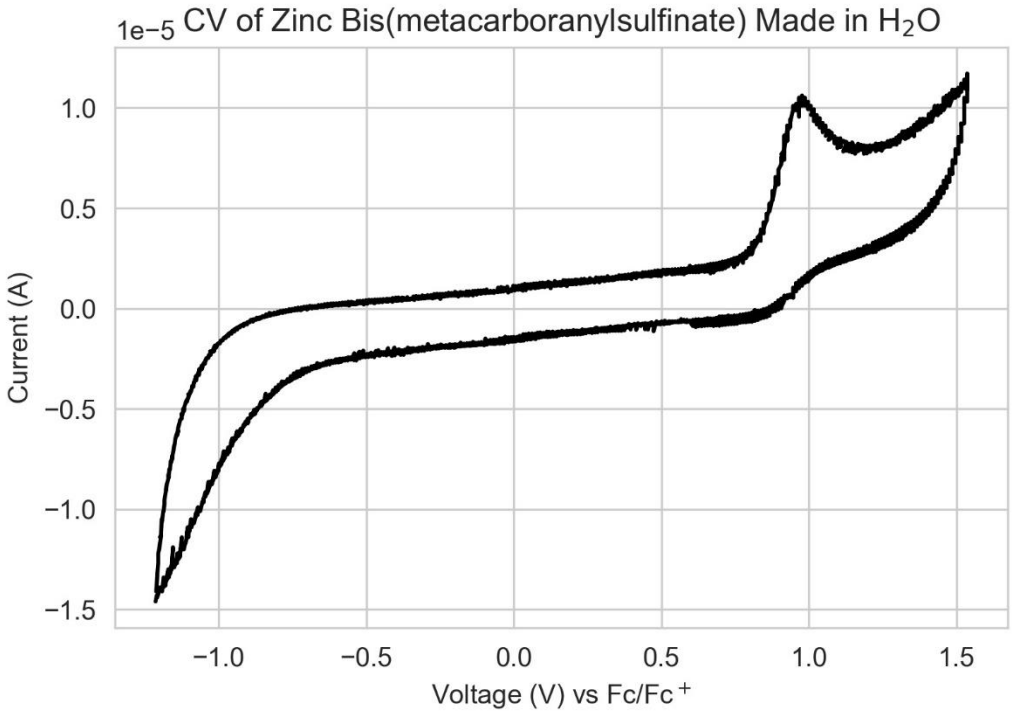

Figure 1-21. Cyclic Voltammogram of **compound 3c** (H_2O batch) measured at a scan rate of 100 mV/s using 0.1M of [TBA][PF_6] as supporting electrolyte. Referenced internally vs Fc/Fc^+. Used glassy carbon working electrode, platinum wire counter electrode and Ag wire pseudo-reference electrode. 3 mM concentration of analyte in CH_3CN at room temperature.

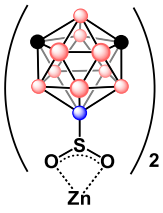

3c

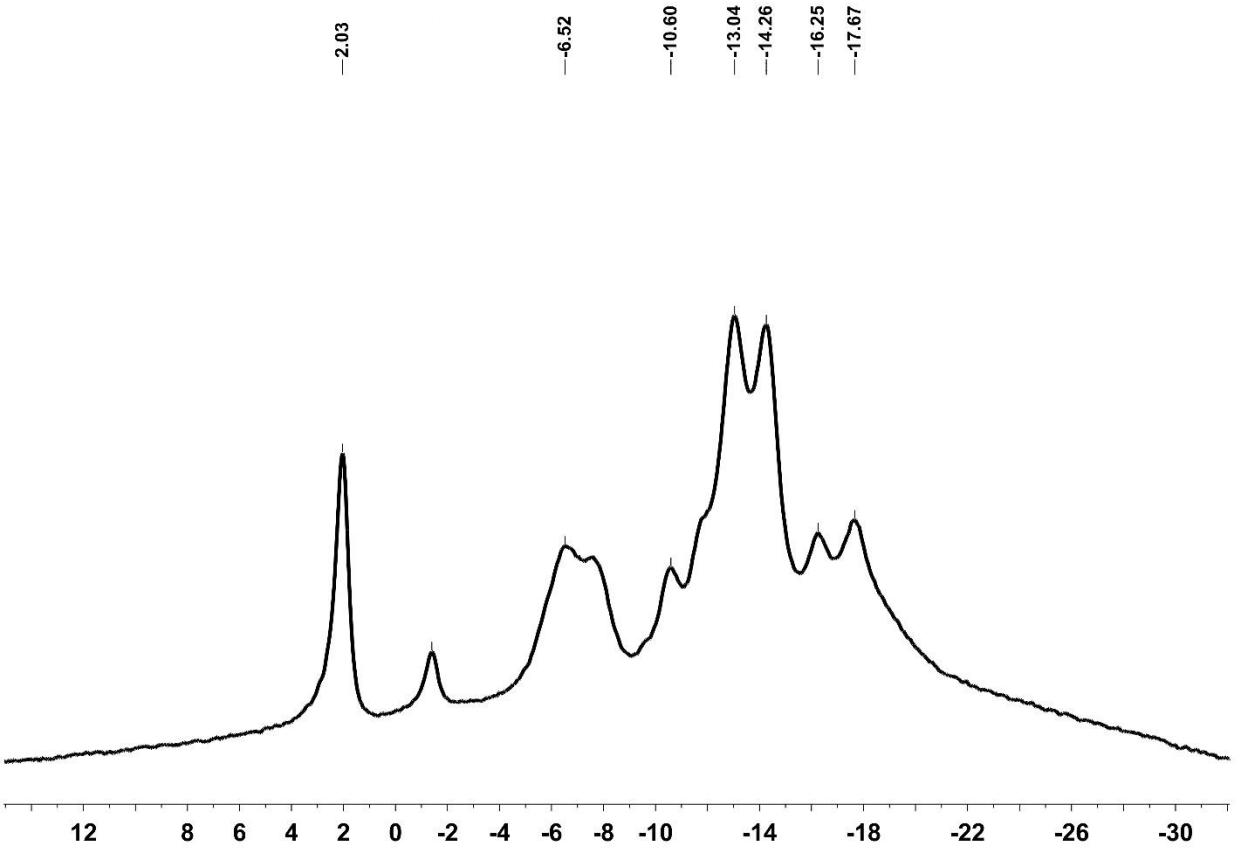

Figure 1-22. ^{11}B NMR spectrum of **compound 3c** (THF batch) in non-deuterated THF

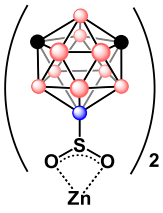

3c

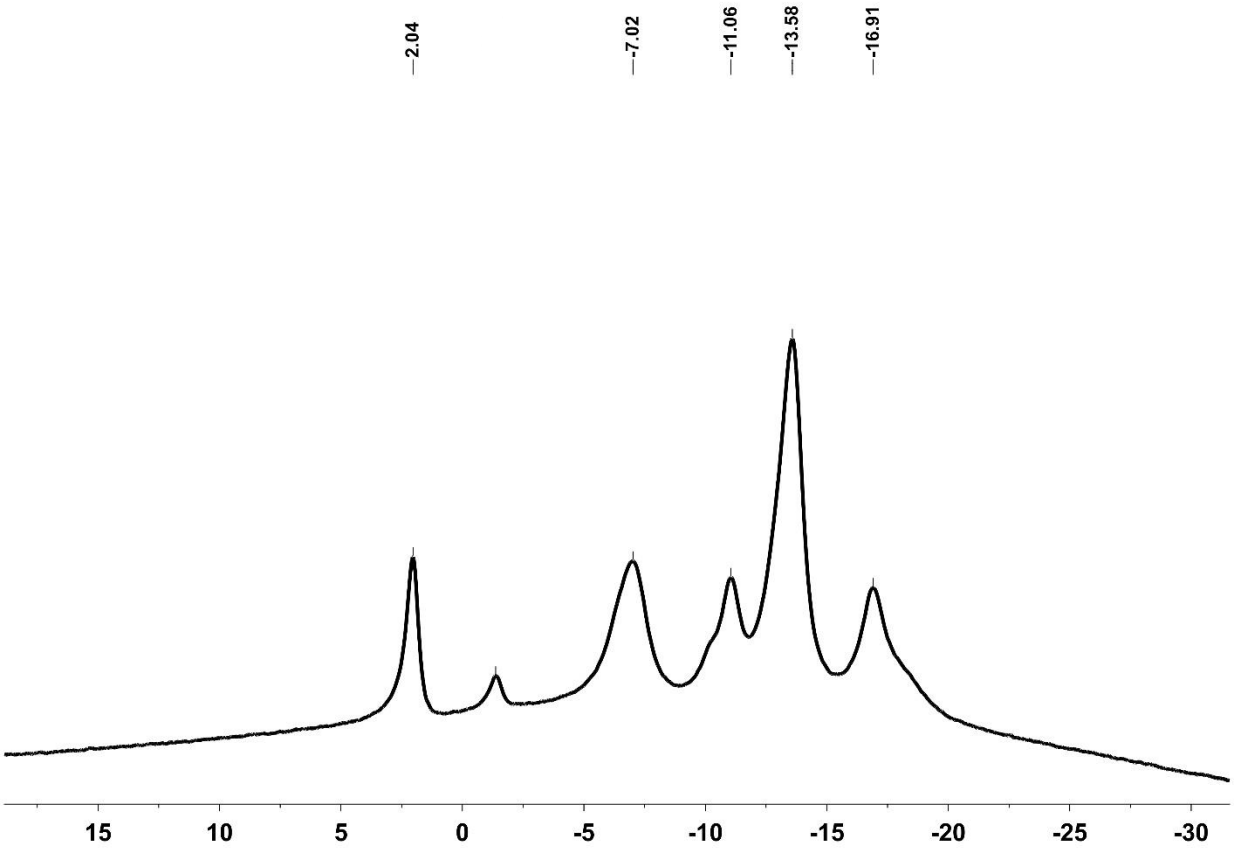

Figure 1-23. $^{11}B\{^{1}H\}$ NMR spectrum of **compound 3c** (THF batch) in non-deuterated THF

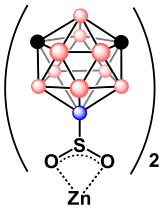

3c

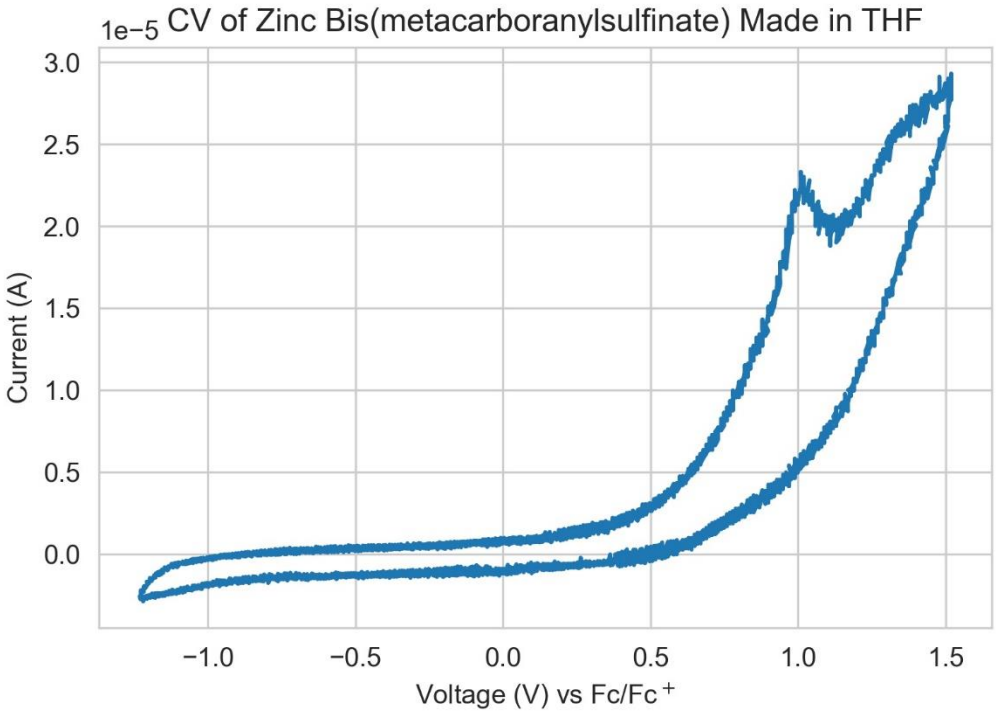

Figure 1-24. Cyclic Voltammogram of **compound 3c** (THF batch) measured at a scan rate of 100 mV/s using 0.1M of [TBA][PF_6] as supporting electrolyte. Referenced internally vs Fc/Fc^+. Used glassy carbon working electrode, platinum wire counter electrode and Ag wire pseudo-reference electrode. 3 mM concentration of analyte in CH_3CN at room temperature.

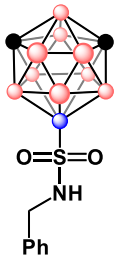

3d

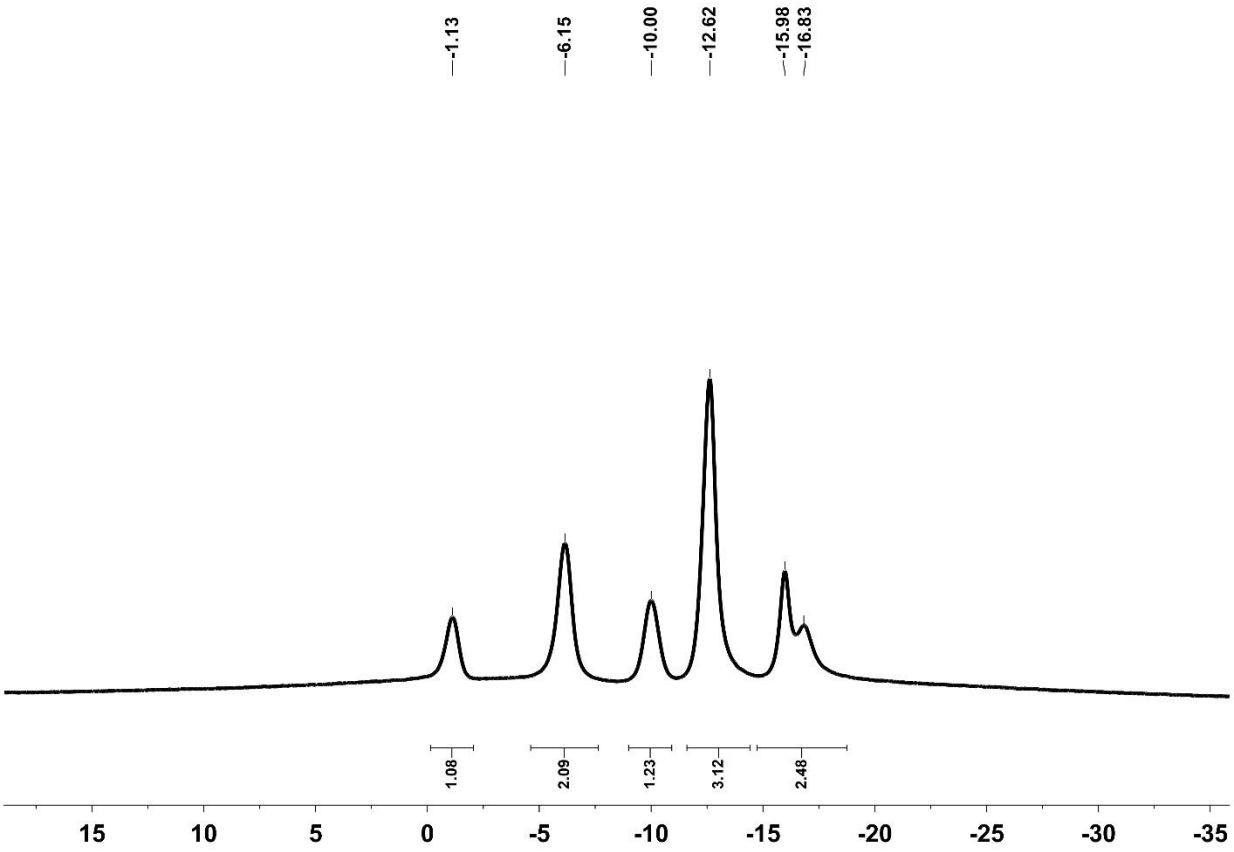

Figure 1-25. $^{11}B\{^{1}H\}$ NMR spectrum of **compound 3b** in CH_2Cl_2

1.4. Conclusion and Future Steps

In this chapter, two classes of S-functionalized icosahedral carboranes were synthesized and characterized. Additionally, preliminary reactivity and cyclic voltammetry studies were conducted on the zinc sulfinate class of reagents, and some chemical and photochemical oxidants were found to cleave the B-S bond.

Future work remains to be done in terms of developing conditions that allow for the trapping for the intermediate generated from the B-S cleavage. Using the data obtained from cyclic voltammetry, reaction conditions can be better designed to match the oxidation potential of the B-S bond. Additionally, more characterization remains to be done in terms of determining the structure of the zinc sulfinate reagent.

1.5. Methods

1.5.1. General Considerations

Meta- and *ortho*-$C_2B_{10}H_{12}$ (Katchem, Alfa Aesar) were used as is. Dry solvents were obtained from a Solvent Purification System (SPS). All reactions were carried out under ambient conditions (unless otherwise noted). Deuterated solvents were purchased from Cambridge Isotope Laboratories and used as is. All other reagents and solvent were purchased from commercial vendors and used as is. Plastic-backed Baker-flex Silica Gel IB2-F TLC plates were used for thin layer chromatography. SiliaFlash® G60 60-200 um (70-230 mesh) purchased from Silicycle was used for flash chromatography. TLC samples for carborane-containing compounds were stained with 1 wt. % $PdCl_2$ in 6M HCl and developed with heat. **Compounds 1a and 3a** were prepared by Harrison Mills according to reported procedures[19-22] (see acknowledgements section) and used as is.

1.5.2. Instrumentation

^1H, ^{13}C, ^{11}B, and $^{11}B\{^1H\}$ NMR spectra were recorded on a Bruker AV400 spectrometer. MestReNova software was used to process all NMR data. ^1H and ^{13}C spectra were referenced to residual solvent resonances in deuterated solvents and are reported relative to tetramethylsilane ($\delta = 0$ ppm). ^{11}B and $^{11}B\{^1H\}$ spectra were referenced to $BF_3{\cdot}Et_2O$ as an external standard ($\delta = 0$ ppm). Gas Chromatography Mass Spectrometry (GCMS) measurements were collected on an Agilent 6890-5975 GCMS. Cyclic voltammetry data was collected using a Gamry Instruments Interface 1010E potentiostat.

1.5.3. Carboranyl Sulfonium Reagent

1.5.3.1. Synthesis of compound 1b

Compound 1a (349 mg; 1.98 mmol) was dissolved in 10 mL of DCM in a scintillation vial, and then Et_3N (1.1 mL; 8 mmol) was added and the mixture was allowed to stir for 30 minutes at room temperature. MeI (0.5 mL; 8 mmol) was then added and the mixture was allowed to stir for 30 more minutes. The reaction progress was checked by TLC (35:65 DCM:Hexanes), and upon completion the mixture was washed twice with water to remove salts and then dried with $MgSO_4$. The solvent in the organic layer was removed *in vacuo* to yield 280 mg of crude **compound 1b** (75% yield) that was then used for the synthesis of **compound 1c** without any further purification.

1.5.3.2. Synthesis of compound 1c

Compound 1b (75 mg; 0.40 mmol) was dissolved in 2 mL of dry DCM in a scintillation vial, and then MeOTf (51 μL; 0.46 mmol) was added and the mixture was allowed to stir for 24 hr. The mixture was then triturated with pentane which resulted in 80 mg of crude product as an oil (~58% yield).

1.5.4. Zinc Bis(carboranyl sulfinates)

1.5.4.1. Synthesis of compound 2b

Following an adapted procedure[30], **compound 1a** (40 mg; 0.23 mmol) was dissolved in a 2 mL v/v solution of 1:5 HCl(2M):MeCN and stirred at 0 ˚C. Then N-chlorosuccinimide (NCS; 125 mg; 0.94 mmol) was added and the mixture was allowed to stir for 30 minutes. After confirming the completion of the reaction by TLC (35:65 DCM:Hexanes), the crude

product mixture was characterized by ^{11}B and $^{11}B\{^{1}H\}$ NMR spectroscopy and subsequently dried *in vacuo* and used to synthesize **compound 2c**.

1.5.4.2. Synthesis of compound 2c

Following a modified adapted procedure[12,13], **compound 2b** (used as is from the previous step) was dissolved in 1.5 mL of THF, and an excess of Zinc dust (160 mg; 2.46 mmol) was added to the mixture, which was then allowed to stir overnight. After 24 hr, the reaction mixture was filtered over a pad of celite and solvent was removed to yield a white powder that was subsequently dissolved in CD_3CN and characterized via ^{11}B and $^{11}B\{^{1}H\}$ NMR spectroscopy.

1.5.4.3. Synthesis of compound 3b

Following an adapted procedure[30], **compound 3a** (457 mg; 2.5 mmol) was dissolved in a 4 mL v/v solution of 1:5 HCl(2M):MeCN and stirred at 0 ˚C. Then N-chlorosuccinimide (1.335 g; 10 mmol) was added and the mixture was allowed to stir for 30 minutes. After confirming the completion of the reaction by TLC (35:65 DCM:Hexanes), the crude product mixture was diluted with 0.75 mL of Et_2O and washed with water (3 x 0.3 mL; last wash was with brine). The organic layer was then collected and the solvent removed *in vacuo* to yield 440 mg of **compound 3b** as a white powder (70% yield). Note: there is some NCS left in the product mixture, but it does not affect the syntheses of **compounds 3c and 3d**.

1.5.4.4. Synthesis of compound 3c

Following a modified adapted procedure[12,13], **compound 3b** (400 mg; 1.65 mmol) was dissolved in 3.5 mL of THF, and an excess of Zinc dust (1.51 g; 23.07 mmol) was added

to the mixture, which was then allowed to stir overnight. After 24 hr, the reaction mixture was filtered over a pad of celite and solvent was removed *in vacuo*. Finally, the resulting powder was put on a fritted funnel with a filter paper and washed 2x with 10 mL of a 1:1 solution of DCM:EtOAc, each time being allowed to sit for 45 seconds before applying vacuum. The product was obtained as a free-flowing white powder (167 mg; 42% yield). Note 1: this synthesis can also be done in water without changing the procedure. Note 2: the washing steps are in attempt to remove $ZnCl_2$ impurities that usually do not affect reactivity.

1.5.4.5. Synthesis of compound 3d

Compound 3a (40 mg; 0.16 mmol) was dissolved in a 1.5 mL v/v solution of 1:5 HCl(2M):MeCN and stirred at 0 ˚C. Then N-chlorosuccinimide (125 mg; 10 mmol) was added and the mixture was allowed to stir for around 30 minutes. Solvent was then removed *in vacuo* and the reaction mixture was resuspended in 1.5 mL of MeCN. After that, Benzylamine (50 μL; 0.46 mmol) was added and the reaction mixture was allowed to stir for 15 mins, after which solvent was removed *in vacuo* and the crude product was dissolved in DCM and characterized by ^{11}B NMR spectroscopy.

1.6. References

1. Cremlyn, R. J. W. *An Introduction to Organosulfur Chemistry*; Wiley: Chichester ; New York, 1996.
2. Otsuka, S.; Nogi, K.; Yorimitsu, H. C–S Bond Activation. *Top Curr Chem (Z)* **2018**, *376* (2), 13. https://doi.org/10.1007/s41061-018-0190-7.
3. *Handbook of Chalcogen Chemistry: New Perspectives in Sulfur, Selenium and Tellurium*, 2nd ed..; Devillanova, F. A., Du Mont, W.-W., Eds.; RSC Publishing: Cambridge, 2013.
4. Block, E. *Reactions of Organosulfur Compounds*; Organic chemistry : a series of monographs; Academic Press: New York, 1978.
5. Kazemi, M.; Sajjadifar, S.; Abdelkarim, A. Biological and Pharmaceutical Organosulfur Molecules. *J. Med. Chem. Sci.* **2018**, *1*, 1-4.
6. Lamberth, C.; Walter, H.; Kessabi, F. M.; Quaranta, L.; Beaudegnies, R.; Trah, S.; Jeanguenat, A.; Cederbaum, F. The Significance of Organosulfur Compounds in Crop Protection: Current Examples from Fungicide Research. *Phosphorus, Sulfur, Silicon Relat. Elem.* **2015**, *190* (8), 1225–1235. https://doi.org/10.1080/10426507.2014.984033.
7. Modha, S. G.; Mehta, V. P.; Eycken, E. V. V. der. Transition Metal-Catalyzed C–C Bond Formation via C–S Bond Cleavage: An Overview. *Chem. Soc. Rev.* **2013**, *42* (12), 5042–5055. https://doi.org/10.1039/C3CS60041F.
8. Wang, L.; He, W.; Yu, Z. Transition-Metal Mediated Carbon–Sulfur Bond Activation and Transformations. *Chem. Soc. Rev.* **2012**, *42* (2), 599–621. https://doi.org/10.1039/C2CS35323G.

9. Lou, J.; Wang, Q.; Wu, P.; Wang, H.; Zhou, Y.-G.; Yu, Z. Transition-Metal Mediated Carbon–Sulfur Bond Activation and Transformations: An Update. *Chem. Soc. Rev.* **2020**, *49* (13), 4307–4359. https://doi.org/10.1039/C9CS00837C.
10. Gao, J.; Feng, J.; Du, D. Shining Light on C−S Bonds: Recent Advances in C−C Bond Formation Reactions via C−S Bond Cleavage under Photoredox Catalysis. *Chem. Asian J.* **2020**, *15* (22), 3637–3659. https://doi.org/10.1002/asia.202000905.
11. Kaiser, D.; Klose, I.; Oost, R.; Neuhaus, J.; Maulide, N. Bond-Forming and -Breaking Reactions at Sulfur(IV): Sulfoxides, Sulfonium Salts, Sulfur Ylides, and Sulfinate Salts. *Chem. Rev.* **2019**, *119* (14), 8701–8780. https://doi.org/10.1021/acs.chemrev.9b00111.
12. Fujiwara, Y.; Dixon, J. A.; O'Hara, F.; Funder, E. D.; Dixon, D. D.; Rodriguez, R. A.; Baxter, R. D.; Herlé, B.; Sach, N.; Collins, M. R.; Ishihara, Y.; Baran, P. S. Practical and Innate Carbon–Hydrogen Functionalization of Heterocycles. *Nature* **2012**, 492 (7427), 95–99. https://doi.org/10.1038/nature11680.
13. O'Hara, F.; Baxter, R. D.; O'Brien, A. G.; Collins, M. R.; Dixon, J. A.; Fujiwara, Y.; Ishihara, Y.; Baran, P. S. Preparation and Purification of Zinc Sulfinate Reagents for Drug Discovery. *Nat. Protoc.* **2013**, 8 (6), 1042–1047. https://doi.org/10.1038/nprot.2013.059.
14. Gianatassio, R.; Kawamura, S.; Eprile, C. L.; Foo, K.; Ge, J.; Burns, A. C.; Collins, M. R.; Baran, P. S. Simple Sulfinate Synthesis Enables C-H Trifluoromethylcyclopropanation. *Angew. Chem. Int. Ed.* **2014**, 53 (37), 9851–9855. https://doi.org/10.1002/anie.201406622.

15. Schleyer, P. von R.; Najafian, K. Stability and Three-Dimensional Aromaticity of Closo-Monocarbaborane Anions, CBn-1Hn-, and Closo-Dicarboranes, C2Bn-2Hn. *Inorg. Chem.* **1998**, 37 (14), 3454–3470. https://doi.org/10.1021/ic980110v.

16. Scholz, M.; Hey-Hawkins, E. Carbaboranes as Pharmacophores: Properties, Synthesis, and Application Strategies. *Chem. Rev.* **2011**, 111 (11), 7035–7062. https://doi.org/10.1021/cr200038x.

17. Grimes, R. N. *Carboranes*, 3rd ed..; Elsevier/AP: Amsterdam ; Boston, 2016.

18. Plešek, J. Potential Applications of the Boron Cluster Compounds. *Chem. Rev.* **1992**, 92 (2), 269–278. https://doi.org/10.1021/cr00010a005.

19. Plešek J; Hermanek S. Sulphydrylation of Icosahedral Carboranes. *Chem. Ind. (London)* **1977,** *9* 360.

20. Plešek, J.; Janoušek, Z.; Heřmánek, S. Chemistry of 9-Mercapto-1,7-Dicarba-Closo-Dodecaborane. *Collect. Czech. Chem. Commun.* **1978**, 43 (5), 1332–1338. https://doi.org/10.1135/cccc19781332.

21. Zakharkin, L. I.; Pisareva, I. V.; Agakhanova, T. B. Synthesis of Some B-Sulfur Derivatives of o- and m-Carboranes. *Russ. Chem. Bull*. **1978**, 27 (12), 2529–2531. https://doi.org/10.1007/BF00941121.

22. Zakharkin, L. I.; Pisareva, I. V. A New Simple Method for the Production and Some Conversions of B-S Bond Containing o- and m- Carboranyl. *Phosphorus Sulfur Rel. Elem.* **1984**, 20 (3), 357–370. https://doi.org/10.1080/03086648408077645.

23. Hohman, J. N.; Zhang, P.; Morin, E. I.; Han, P.; Kim, M.; Kurland, A. R.; McClanahan, P. D.; Balema, V. P.; Weiss, P. S. Self-Assembly of Carboranethiol Isomers on Au{111}:

Intermolecular Interactions Determined by Molecular Dipole Orientations. *ACS Nano* **2009**, 3 (3), 527–536. https://doi.org/10.1021/nn800673d.

24. Serino, A. C.; Anderson, M. E.; Saleh, L. M. A.; Dziedzic, R. M.; Mills, H.; Heidenreich, L. K.; Spokoyny, A. M.; Weiss, P. S. Work Function Control of Germanium through Carborane-Carboxylic Acid Surface Passivation. *ACS Appl. Mater. Interfaces* **2017**, 9 (40), 34592–34596. https://doi.org/10.1021/acsami.7b10596.
25. Ahrens, V. M.; Frank, R.; Boehnke, S.; Schütz, C. L.; Hampel, G.; Iffland, D. S.; Bings, N. H.; Hey-Hawkins, E.; Beck-Sickinger, A. G. Receptor-Mediated Uptake of Boron-Rich Neuropeptide Y Analogues for Boron Neutron Capture Therapy. *ChemMedChem* **2015**, 10 (1), 164–172. https://doi.org/10.1002/cmdc.201402368.
26. Ol'shevskaya, V. A.; Zaitsev, A. V.; Kalinin, V. N.; Shtil, A. A. Synthesis and Antitumor Activity of Novel Tetrakis[4-(Closo-Carboranylthio)Tetrafluorophenyl]Porphyrins. *Russ Chem Bull* **2014**, 63 (10), 2383–2387. https://doi.org/10.1007/s11172-014-0751-z.
27. Spokoyny, A. M.; Machan, C. W.; Clingerman, D. J.; Rosen, M. S.; Wiester, M. J.; Kennedy, R. D.; Stern, C. L.; Sarjeant, A. A.; Mirkin, C. A. A Coordination Chemistry Dichotomy for Icosahedral Carborane-Based Ligands. *Nat. Chem.* **2011**, 3 (8), 590–596. https://doi.org/10.1038/nchem.1088.
28. Lyubimov, S. E.; Davankov, V. A.; Petrovskii, P. V.; Hey-Hawkins, E.; Tyutyunov, A. A.; Rys, E. G.; Kalinin, V. N. Chiral Carborane-Derived Thiophosphites: A New Generation of Ligands for Rh-Catalyzed Asymmetric Hydrogenation. *J. Organomet. Chem.* **2008**, 693 (25), 3689–3691. https://doi.org/10.1016/j.jorganchem.2008.09.032.

29. Fox, M. A.; Wade, K. Deboronation of 9-Substituted-Ortho- and -Meta-Carboranes. *J. Organomet. Chem.* **1999**, 573 (1), 279–291. https://doi.org/10.1016/S0022-328X(98)00881-X.

30. Nishiguchi, A.; Maeda, K.; Miki, S. Sulfonyl Chloride Formation from Thiol Derivatives by N-Chlorosuccinimide Mediated Oxidation. *Synthesis* **2006** (24), 4131–4134. https://doi.org/10.1055/s-2006-950353.

Chapter 2: Synthesis and Reactivity of Selenium- and Tellurium-Functionalized Carborane Reagents at the B(9) Position

2.1. Introduction

Despite not being as prevalent as organosulfur compounds, organoselenium compounds have a fairly well-established chemistry and have found some niche roles in synthetic organic chemistry[1-5]. Organotellurium chemistry, on the other hand, is much less well-developed than both organoselenium and organosulfur chemistry[4-7]. This is due to several reasons, most notably the general instability of organotellurium compounds, their foul odor, and their relatively high toxicity[8].

Shortly after the reports of the synthesis of carboranes with exopolyhedral B(9)-S bonds, there were reports of the selenium and tellurium analogues of these carborane chalcogenides[9-15]. There has been very little study of these compounds since their initial reports, however. Additionally, the initial reports contain very little characterization of the electrophilic and nucleophilic properties of these compounds beyond simple S_N2 reactions and the synthesis of some potential electrophilic reagents. The characterization that has been performed on these compounds is also very limited—consisting mainly of melting points and elemental analyses, with scarce NMR analysis performed on the dichalcogenides.

In this chapter, I will describe the synthesis of a variety of B(9) selenium- and tellurium-functionalized carboranes. I will then explore the nucleophilic and electrophilic reactivities of several of the synthesized reagents.

2.2. Discussion

2.2.1. General Considerations

This chapter will cover a few specific sections of a broader work, and as a result is not all-inclusive. The complement to this work can be found in another dissertation and in a manuscript in preparation (see acknowledgements section). The parent compound for the majority of the reagents are the carboranyl dichalcogenides, whose general synthetic scheme can be seen in **Figure 2-1**.

2.2.2. Target Compounds

Throughout this chapter, there will be references to nucleophilic and electrophilic reagents. The nucleophilic reagents are those where the Selenium or Tellurium atom bears a negative charge, and those species can be either generated *in situ* by reducing the corresponding dichalcogenide using $NaBH_4$ to the corresponding chalcogenolate as can be seen below in **Figure 2-2**, or by deprotonating the corresponding chalcogenol. On the other hand, the electrophilic reagents are those where the Selenium or Tellurium atoms are bonded to one or more electronegative elements—halogens for the purpose of this thesis—and thus bear a positive charge. Those reagents are generated by the treatment of the corresponding dichalcogenide with an elemental halogen source—as can be seen in **Figure 2-2**. Note that sulfuryl chloride (SO_2Cl_2) was used as a source of Cl_2 due to ease of handling compared to chlorine gas.

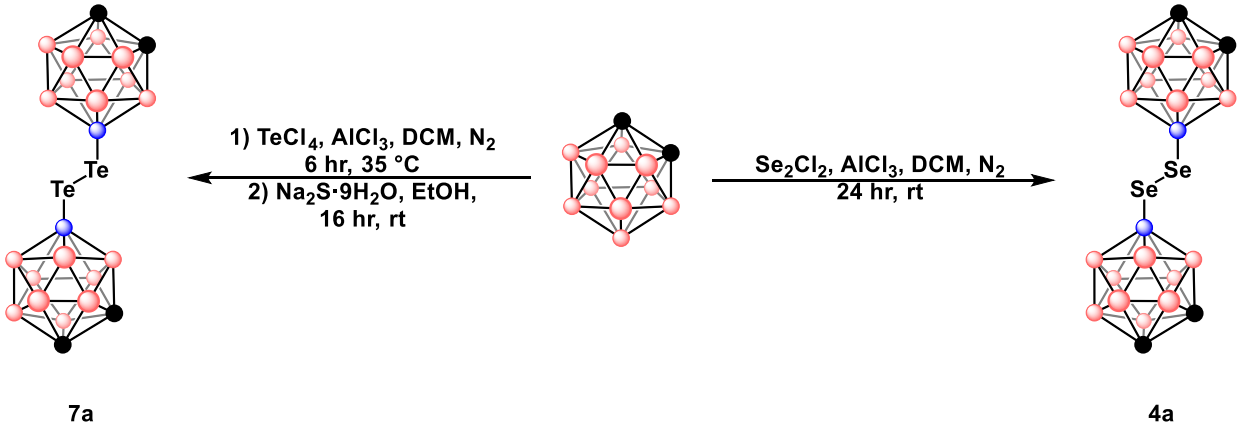

Figure 2-1. Synthetic scheme for the generation of bis(*ortho*-carboranyl) dichalcogenides

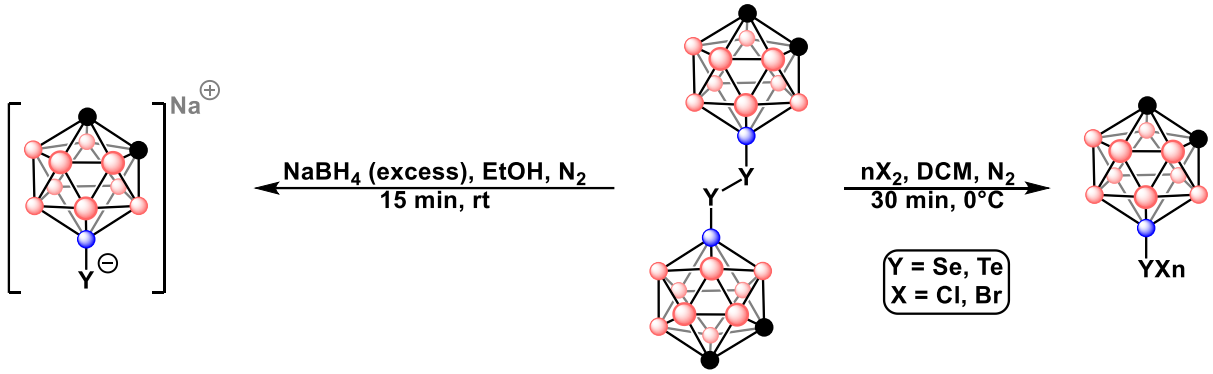

Figure 2-2. Synthetic scheme for the generation of carboranyl chalcogenolates and chalcogen halides

2.2.3. Nucleophilic Chemistry of Selenium-Based Carboranyl Compounds

This section will describe the reactivity of the carboranyl selenolate anion. **Figure 2-3** shows the synthetic scheme for the synthesis of an *ortho*-carboranyl selenol resulting from the acidification of the selenolate generated *in situ* from the corresponding diselenide (**compound 4a**; see **Figure 2-1** for scheme). **Figure 2-4** shows the reactivity of the *meta*-carboranyl selenolate anion in an S_N2-type epoxide ring-opening reaction with propylene oxide. **Compounds 4a, 4b, and 5a** were all synthesized according to previous reported procedures[11] with minor modifications.

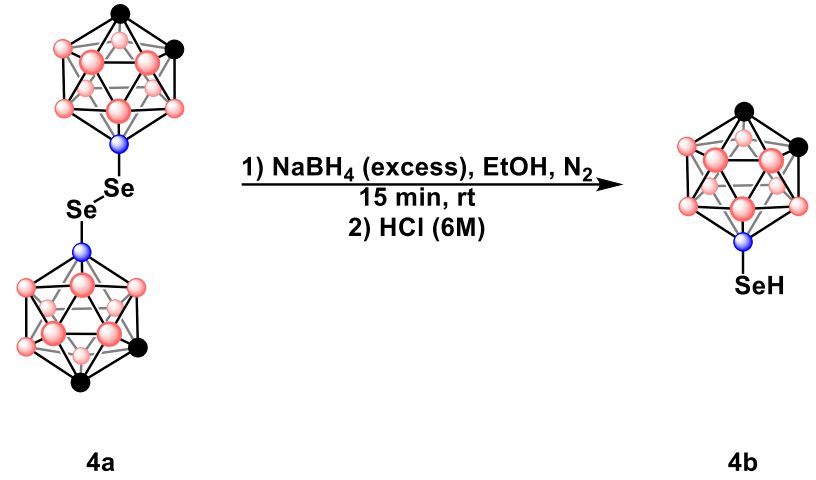

Figure 2-3. Reaction scheme for the synthesis of the *ortho*-carboranyl selenol

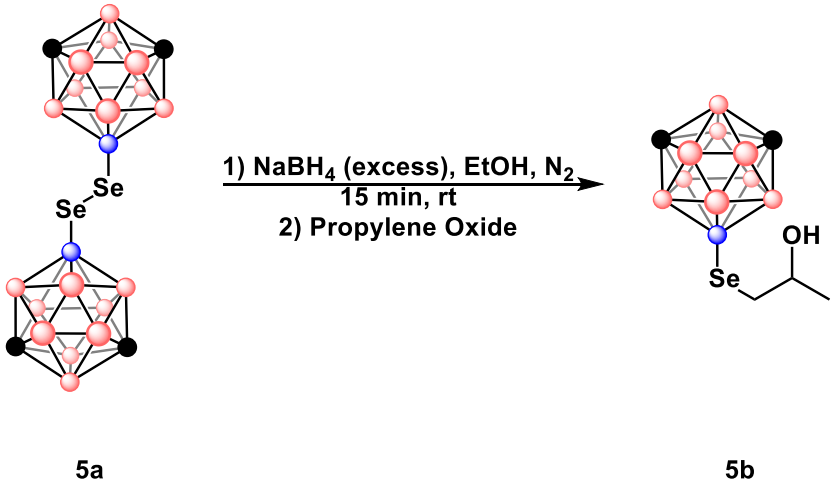

Figure 2-4. Reaction scheme for the synthesis of a *meta*-carboranyl selenoether

2.2.4. Electrophilic Chemistry of Selenium-Based Carboranyl Compounds

This section will describe the electrophilic reactivity of 9-*meta*-carboranyl selenyl (II) chloride (**compound 6a**), as can be seen in **Table 2-1**. The general synthetic scheme is shown in **Figure 2-5**. The synthesis and purification of **compound 6a** will be described in a different dissertation as well as a manuscript in preparation (see acknowledgements).

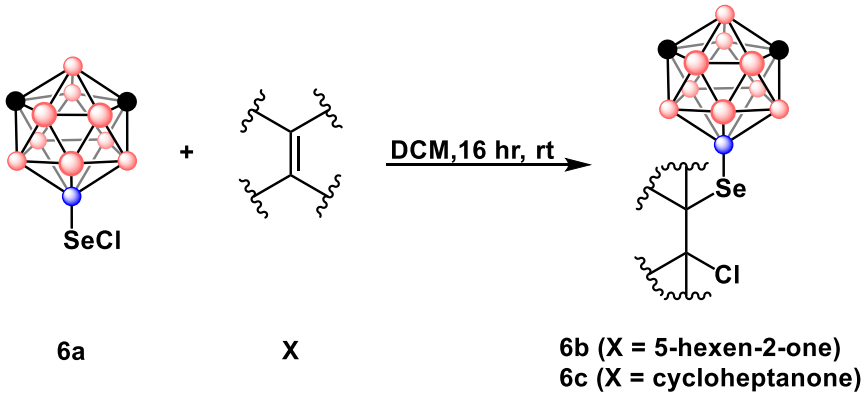

Figure 2-5. Synthetic scheme for the reactivity of carboranyl chalcogen halides

Entry	X	Result
1	*trans*-Chalcone	No reaction
2	Cholesterol	No reaction
3	5-hexen-2-one	Product observed via GCMS (-Cl)
4	N-vinyl Pyrrolidone	Color change; reverts back to **compound 4a** overnight
5	Cycloheptanone	Product observed via GCMS (-Cl)

Table 2-1. Reactivity of **compound 6a** with several alkenes and a ketone (see results section for more details)

2.2.5. Nucleophilic Chemistry of Tellurium-Based Carboranyl Compounds

This section details the nucleophilic reactivity of the tellurium-based carboranyl reagents. The general synthetic scheme follows **Figure 2-2**, where a tellurolate anion is generated by the *in situ* reduction of the 9.9'-bis-*ortho*-carboranyl ditelluride (**compound 7a**; see **Figure 2-1** for scheme). The anion is then either subjected to an acidic workup to produce the tellurol or reacted with different alkyl halides (such as methyl iodide and benzyl bromide) to produce the corresponding alkyl telluroether. **Figure 2-6** outlines these reactions. Based on surveyed literature reports, **compounds 7a-d** as well as **8a-b** have the most upfield or near the most upfield ^{125}Te chemical shifts reported[4-8]. **Compound 7b** has been reported before[11] but has not

been characterized via NMR spectroscopy. Additionally, its stability was studied with respect to decomposition in solvent over time. **Compound 7d** was exceptionally unstable, starting to decompose in a J-Young NMR tube throughout the course of characterization, leading to the hypothesis that it is light sensitive. Additionally, **compound 7d** decomposed in the glovebox freezer over time at -30 ˚C, showing that it is likely also thermally unstable. The instability of the *ortho*-carboranyl tellurol is already expected because tellurols are generally unstable to begin with and an *ortho*-carboranyl substitutent at the B(9) position is a highly electron rich substituent. Interestingly, attempts to generate an aryl telluroether through S_NAr-type reactions or through oxidative radical coupling reactions of the ditelluride (dotted arrows in **Figure 2-6**) were largely unsuccessful. The details are summarized in **Table 2-2**.

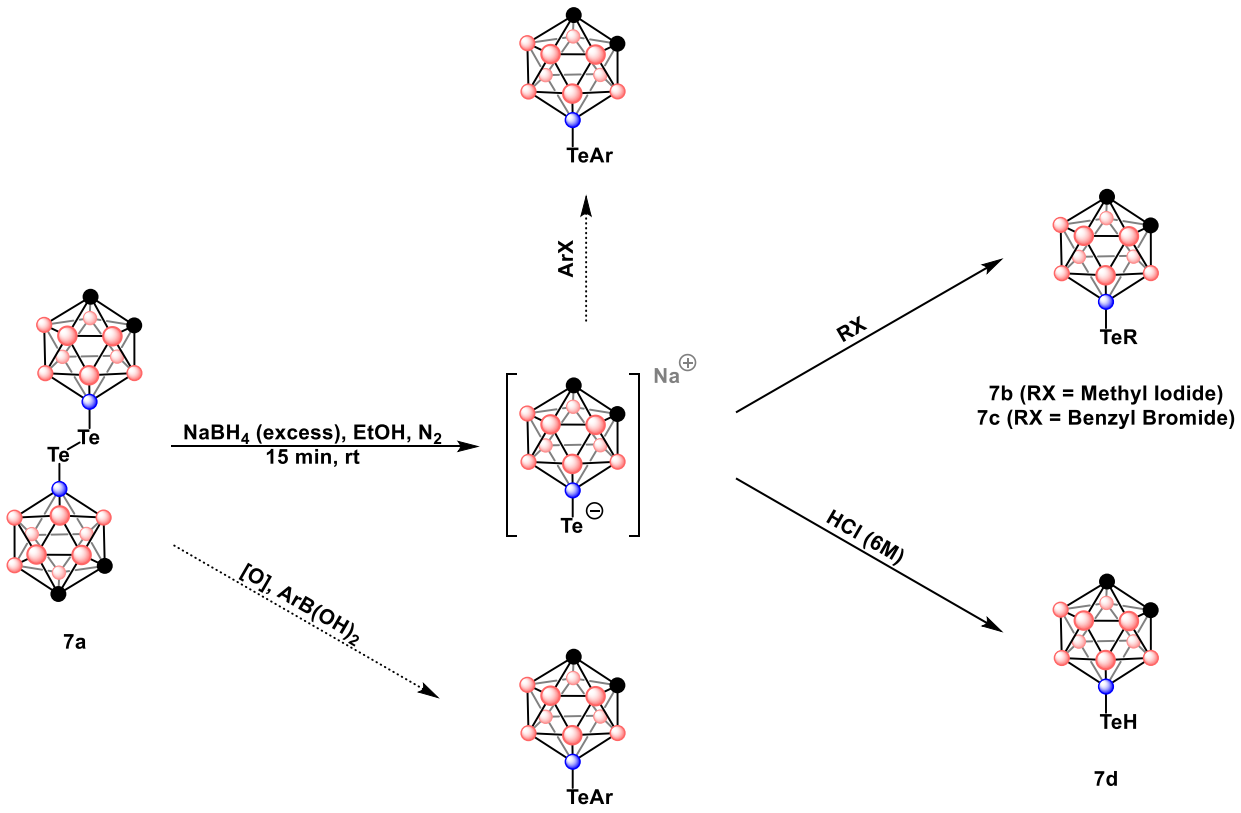

Figure 2-6. Synthetic scheme for the nucleophilic reactivity of the *orhto*-carboranyl tellurolate anion

	Entry	[O] (eq)	$ArB(OH)_2$ (eq)	Solvent	Temperature	Time	Result
Oxidative Coupling	**1**	$AgNO_3$ (0.20)	$PhB(OH)_2$ (2)	1,4-Dioxane	100 ˚C	6 hr	A
	2	$CuCl_2$ (2.25)	*p*-tolyl $B(OH)_2$ (2)	Et_2O	Room temp.	16 hr	B
	3	$Mn(OAc)_3$ (2.4)	*p*-tolyl $B(OH)_2$ (2)	THF	Room temp.	16 hr	A
	4	$Mn(OAc)_3$ (2.4)	*p*-tolyl $B(OH)_2$ (2)	THF	80 ˚C	16 hr	B
	5	$Mn(OAc)_3$ (2.4)	*p*-tolyl $B(OH)_2$ (2)	THF	50 ˚C	16 hr	B
	6	$Mn(OAc)_3$ (2.4)	*p*-tolyl $B(OH)_2$ (2)	AcOH	60 ˚C	16 hr	B
	7	CuI•bpy (0.05)	*p*-tolyl $B(OH)_2$ (2)	DMSO	100 ˚C	16 hr	A
	8	_	*p*-tolyl $B(OH)_2$ (2)	DMSO	100 ˚C	16 hr	A
	Entry	**ArX**		**Solvent**	**Temperature**	**Time**	**Result**
S_NAr	**9**	4-iodotoluene		EtOH	Room temp.	16 hr	C
	10	4-chlorotoluene		EtOH	Room temp.	16 hr	C
	11	Perfluorotoluene		DMF	Room temp.	16 hr	C

Table 2-2. Reaction conditions for attempted generation of aryl tellurides through S_NAr and oxidative coupling. All reactions were run on a 0.05 mmol scale with respect to **compound 7a**. **Results: A: no reaction; B: trace product by GCMS; C: no reaction, reforms ditelluride upon exposure to air**

Finally, **Figure 2-7** shows a reaction whereby the *meta*-carboranyl tellurolate was generated by reduction with $NaBH_4$ and then reacted with propylene oxide to produce 9-*meta*-carboranyl(2-hydroxypropyl)telluride.

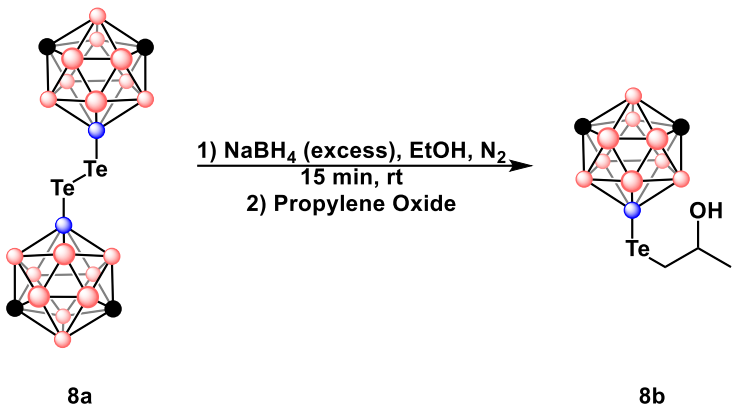

Figure 2-7. Reaction scheme for the synthesis of a *meta*-carboranyl telluroether (**compound 8b**)

2.2.6. Electrophilic Chemistry of Tellurium-Based Carboranyl Compounds

This section examines the electrophilic reactivity of tellurium-based *meta*-carboranyl reagents. The first explored mode of reactivity is with organolithium species. Lithium-Tellurium exchange is a well-studied branch of chemistry and represents one of the most common uses for Tellurium in synthetic chemistry. In fact, Li-Te exchange is known to be one of the fastest metal-lithium exchange reactions[16]. We wanted to conduct preliminary studies into the reactivity of carboranyl tellurides with organolithiums and explore whether Te-Te, Te-B, or Te-C bond cleavage occurred. One issue is that the carborane C-H vertices posed an issue since they are acidic enough to also react with organolithiums. As a result, the methyl-protected *meta*-carboranyl ditelluride and *meta*-carboranyl methyl telluride seen in **Figure 2-8** were both synthesized and then stirred with an excess of *n*-butyllithium (nBuLi) for 15 minutes. The results were probed by GCMS, and it was observed that the Te-Te bond in the ditelluride is quantitatively cleaved by nBuLi to form the butyl telluride (**Figure 2-8**). On the other hand, the methyl telluride was much slower to react with nBuLi, only forming the butyl telluride in 7% conversion after 15 minutes.

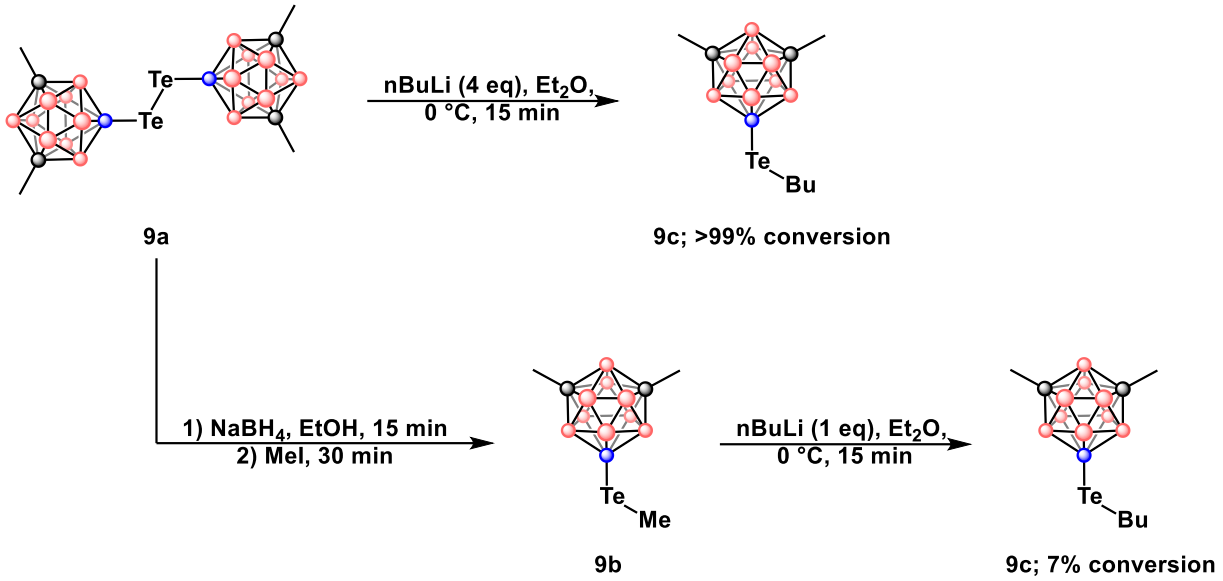

Figure 2-8. Reaction scheme for probing the Li-Te exchange properties of the *meta*-carboranyl tellurides

The second explored mode of electrophilic reactivity of tellurium-based *meta*-carboranyl species is the addition to alkenes and alkynes. The specific class of carboranyl-tellurium reagents chosen for this was the carboranyl tellurium trihalides. **Figure 2-9** shows the reaction scheme for the synthesis of a variety of *meta*-carboranyl tellurium trihalides. Ultimately, **compound 10a** was chosen as the model electrophile because it offers the highest electrophilicity due to the electronegativity of the chlorine atoms. **Figure 2-10** shows the reaction scheme between **compound 10a** and several nucleophiles. There is clean conversion to **compounds 11a and 12a** after the reaction with phenylacetylene and norbornene, respectively. Furthermore, these Te(IV) species can be reduced to their Te(II) counterparts upon treatment with an aqueous solution of sodium thiosulfate. This can be monitored by tracking the upfield change in the ^{125}Te NMR resonances as well as the well-resolved splitting in the Te(II) species that are not broadened out due to having two chlorines on the tellurium atom anymore.

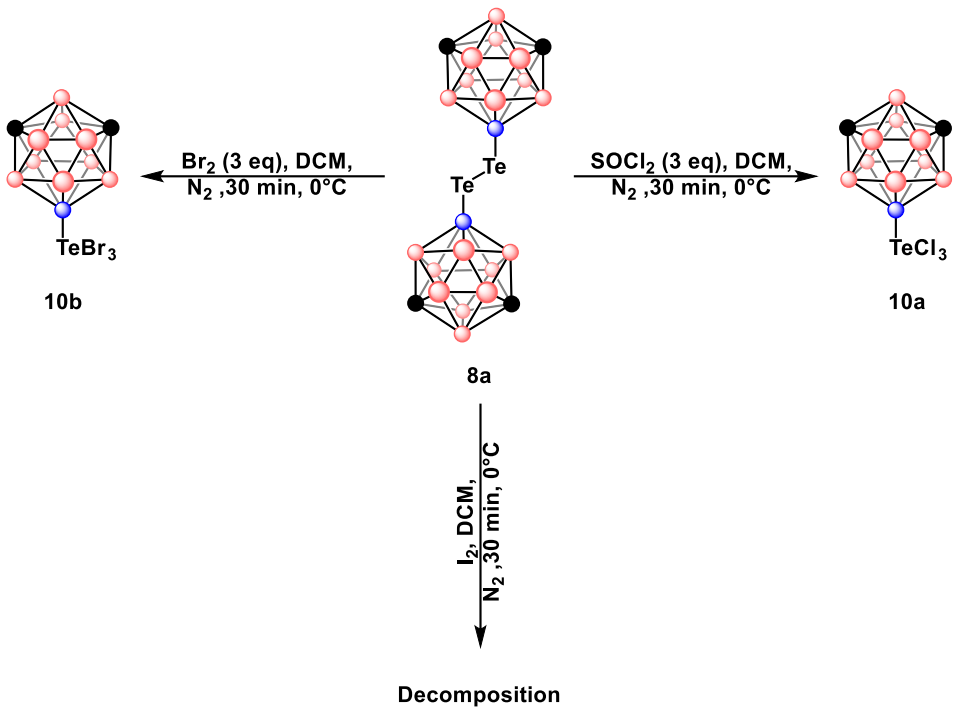

Figure 2-9. Reaction scheme for the synthesis attempts of various *meta*-carboranyl tellurium trihalides

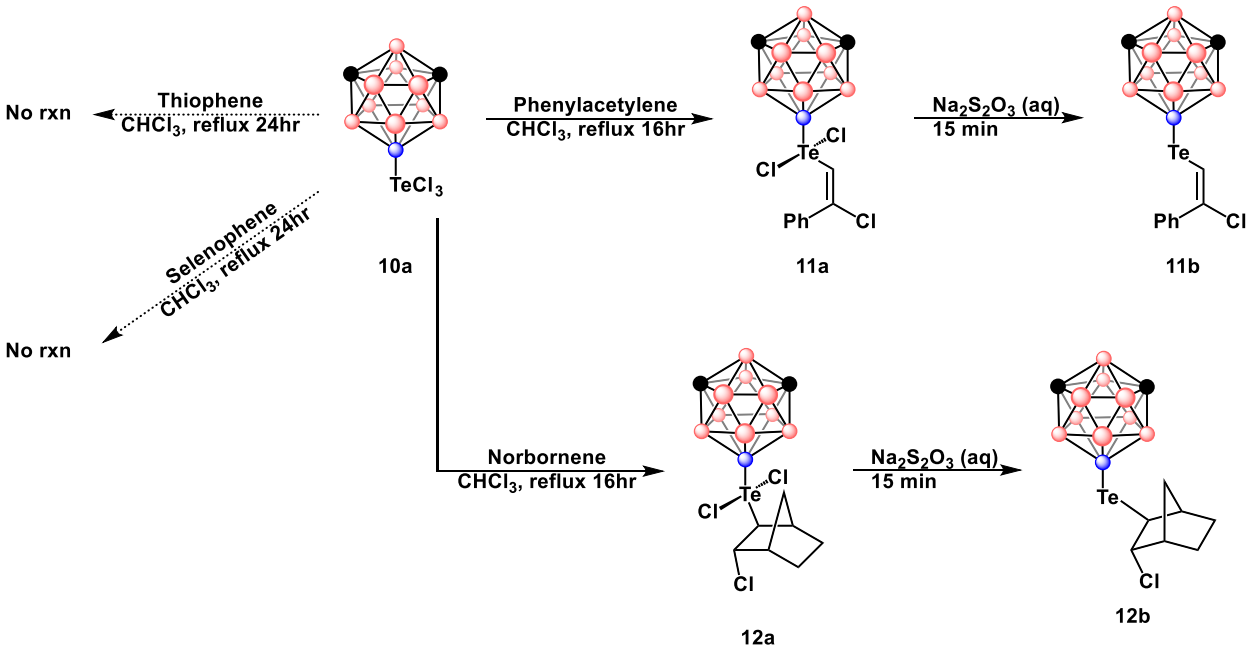

Figure 2-10. Reaction scheme for the reactivity of the *meta*-carboranyl tellurinyl (IV) trichloride (**compound 10a**). Note that only one isomer is shown but the isomer that represents the true major product is not known yet.

2.3. Results

2.3.1. Nucleophilic Chemistry of Selenium-Based Carboranyl Compounds

The 9-*ortho*-carboranyl selenol (**compound 4b**) was characterized by ^{1}H (**Figure 2-11**) and ^{11}B (**Figure 2-12**) NMR spectroscopy. The (2-hydroxypropyl) 9-*meta*-carboranyl selenide (**compound 5b**) was characterized by ^{1}H (**Figures 2-13, 2-14**), ^{13}C (**Figures 2-15, 2-16**), ^{11}B (**Figure 2-17**), $^{11}B\{^{1}H\}$ (**Figure 2-18**), ^{125}Te (**Figure 2-19**), and ^{1}H-^{1}H COSY (**Figure 2-20**) NMR spectroscopy.

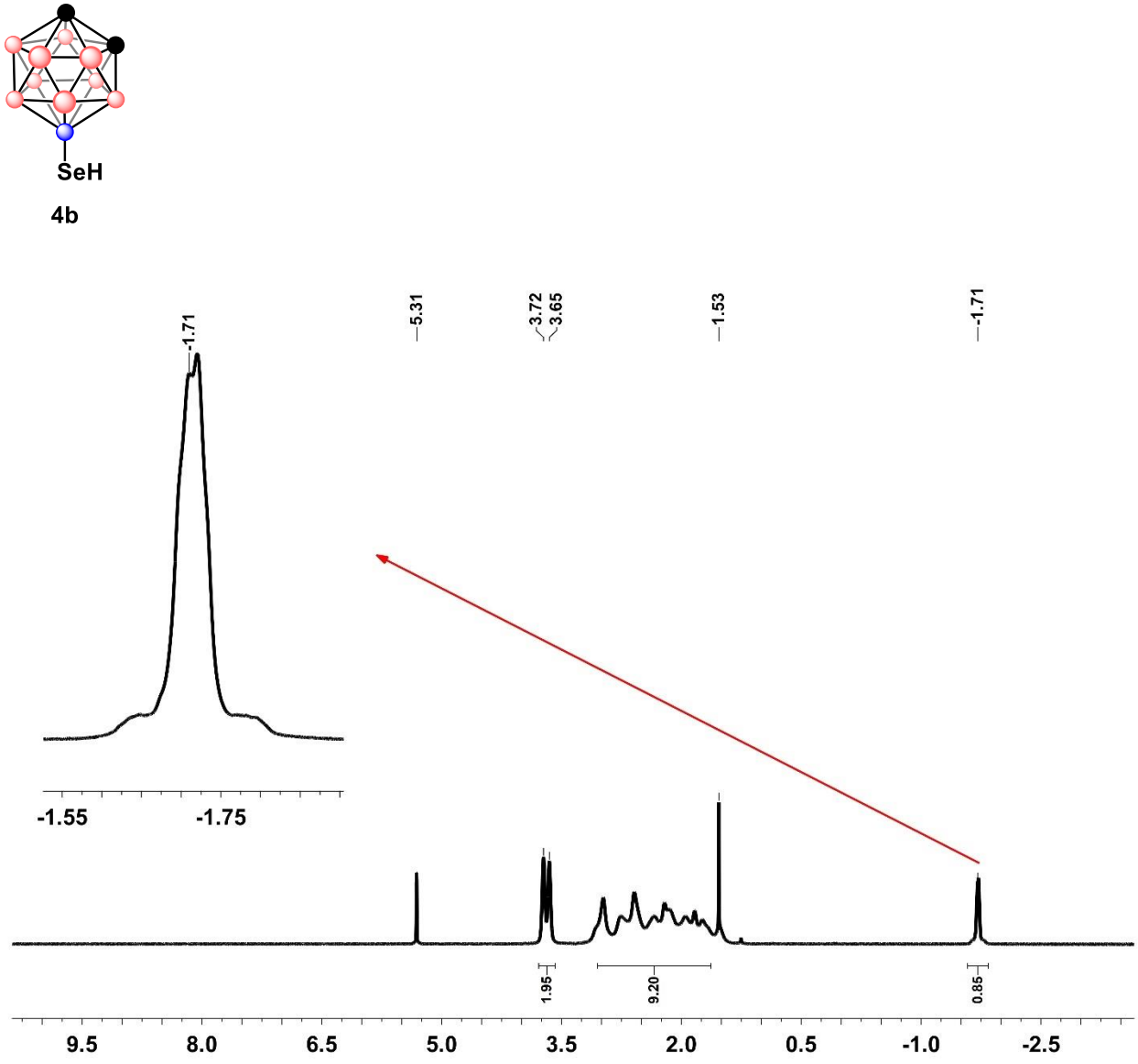

Figure 2-11. ^{1}H NMR spectrum of **compound 4b** in CD_2Cl_2

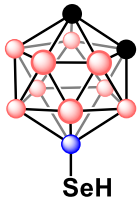

4b

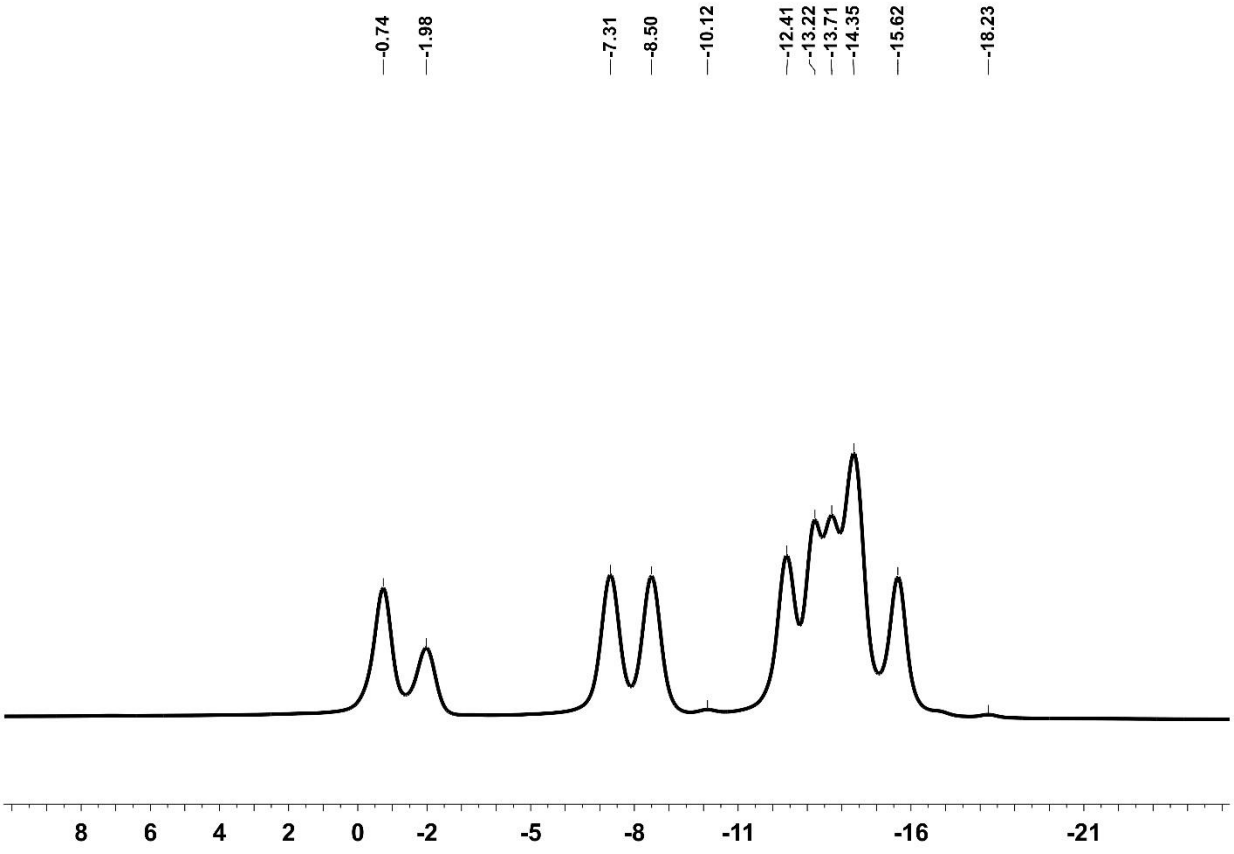

Figure 2-12. ^{11}B NMR spectrum of **compound 4b** in CD_2Cl_2

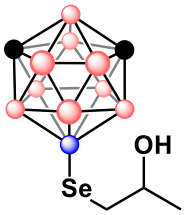

5b

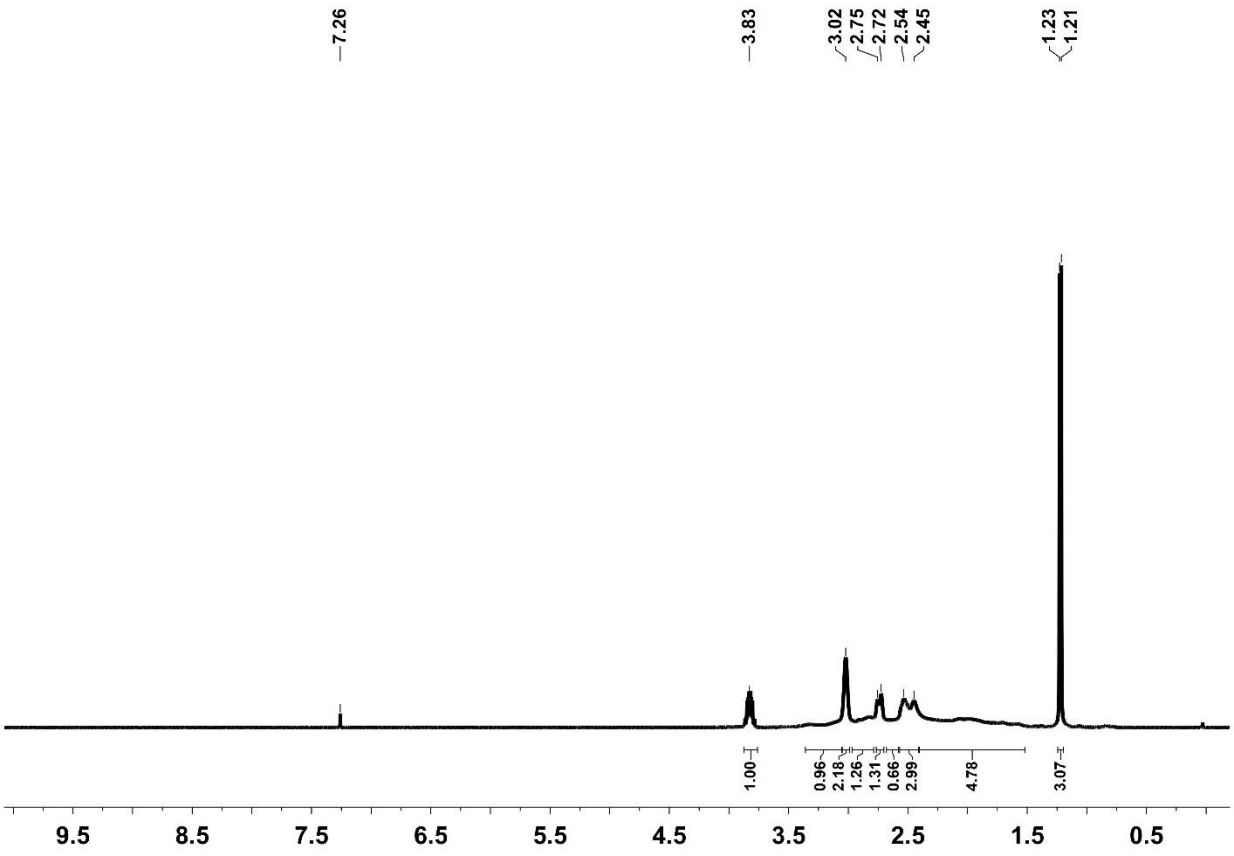

Figure 2-13. ^{1}H NMR spectrum of **compound 5b** in $CDCl_3$

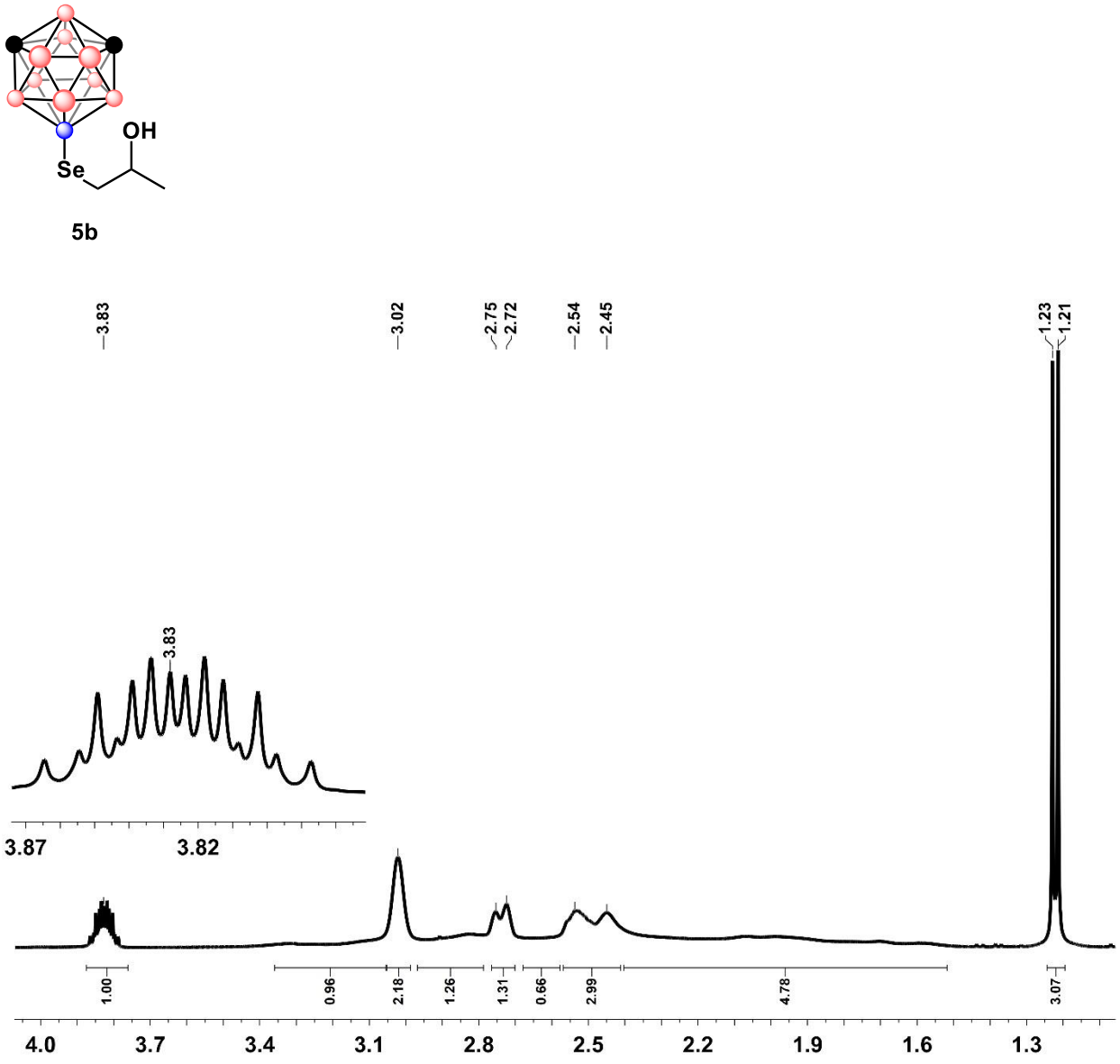

Figure 2-14. Zoomed-in ^{1}H NMR spectrum of **compound 5b** in $CDCl_3$

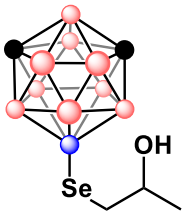

5b

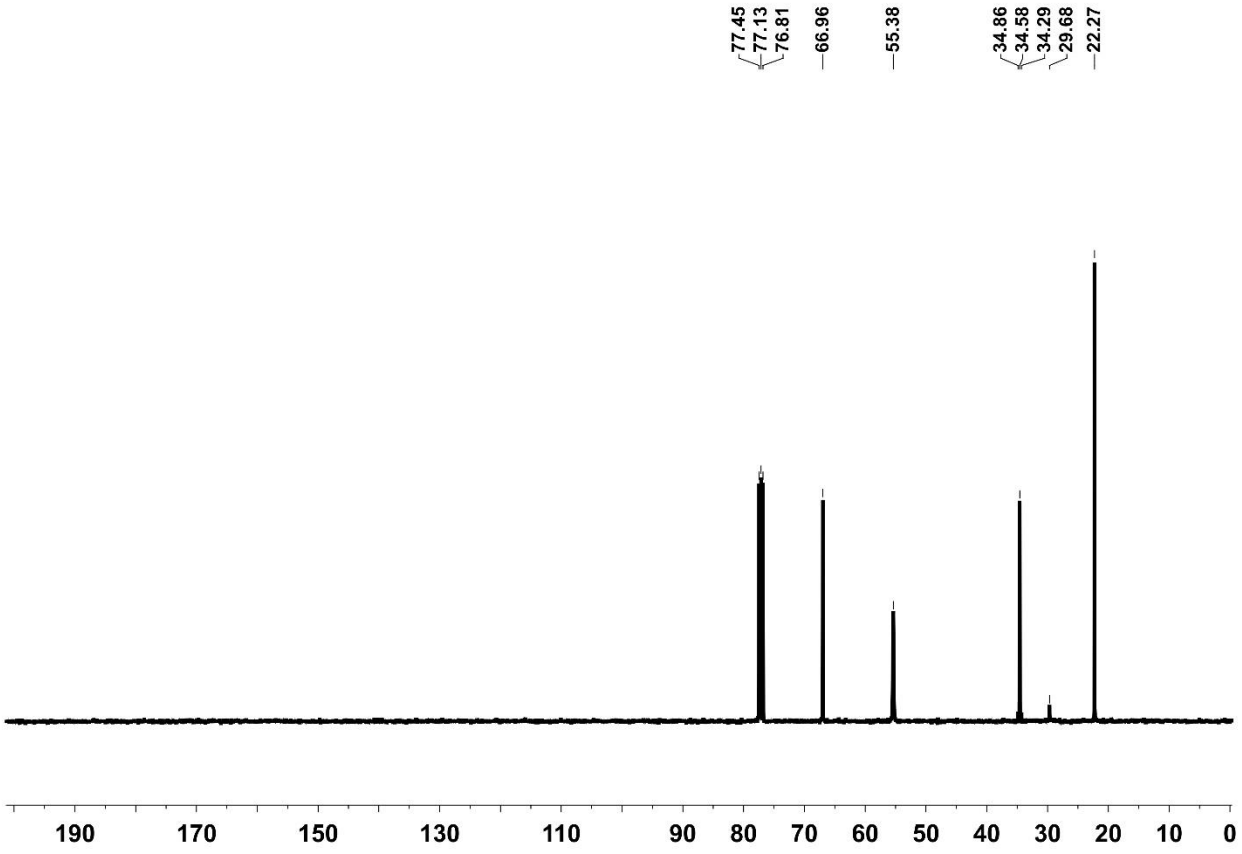

Figure 2-15. ^{13}C NMR spectrum of **compound 5b** in $CDCl_3$

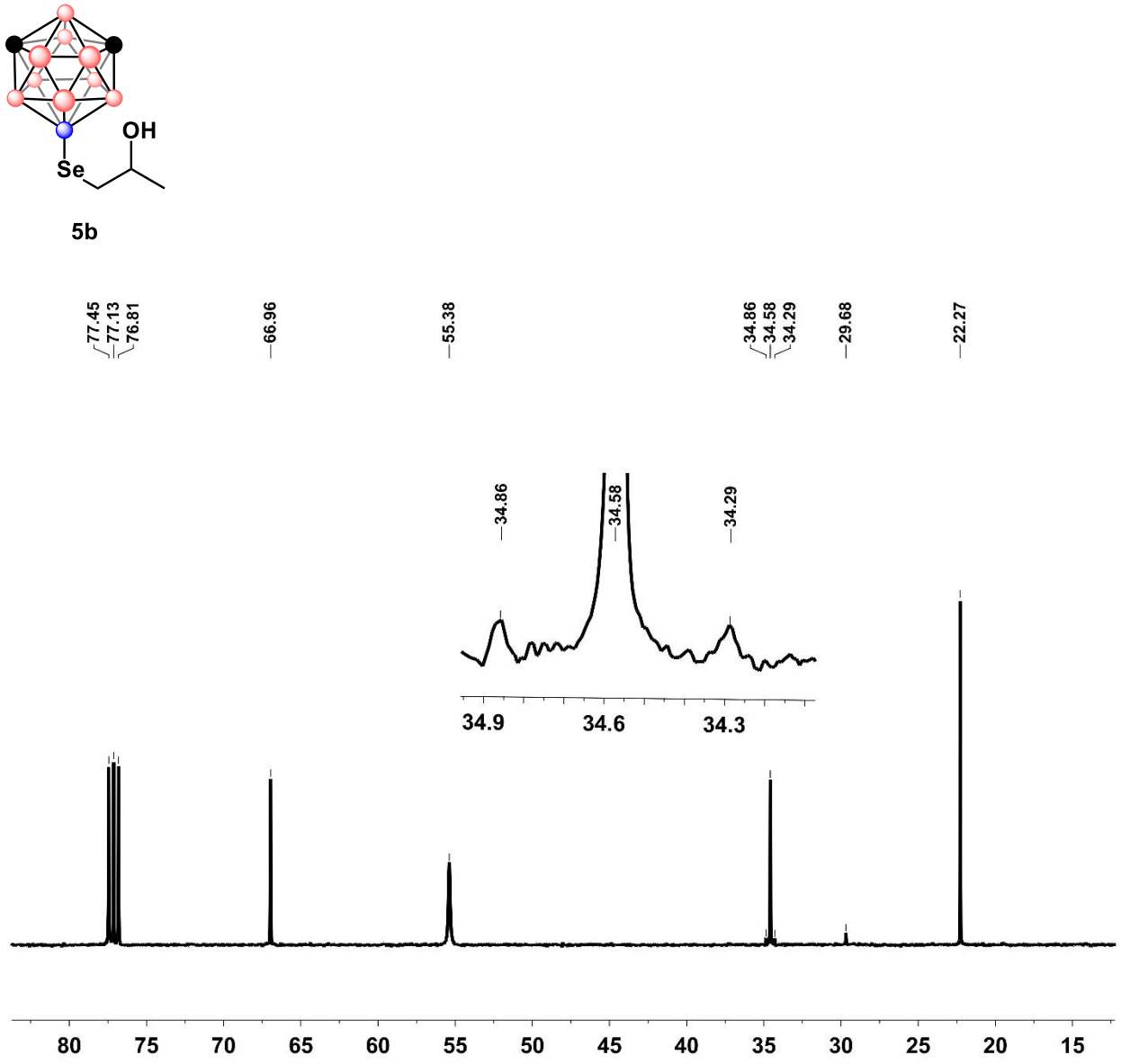

Figure 2-16. Zoomed-in ^{13}C NMR spectrum of **compound 5b** in $CDCl_3$

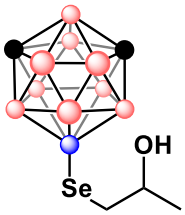

5b

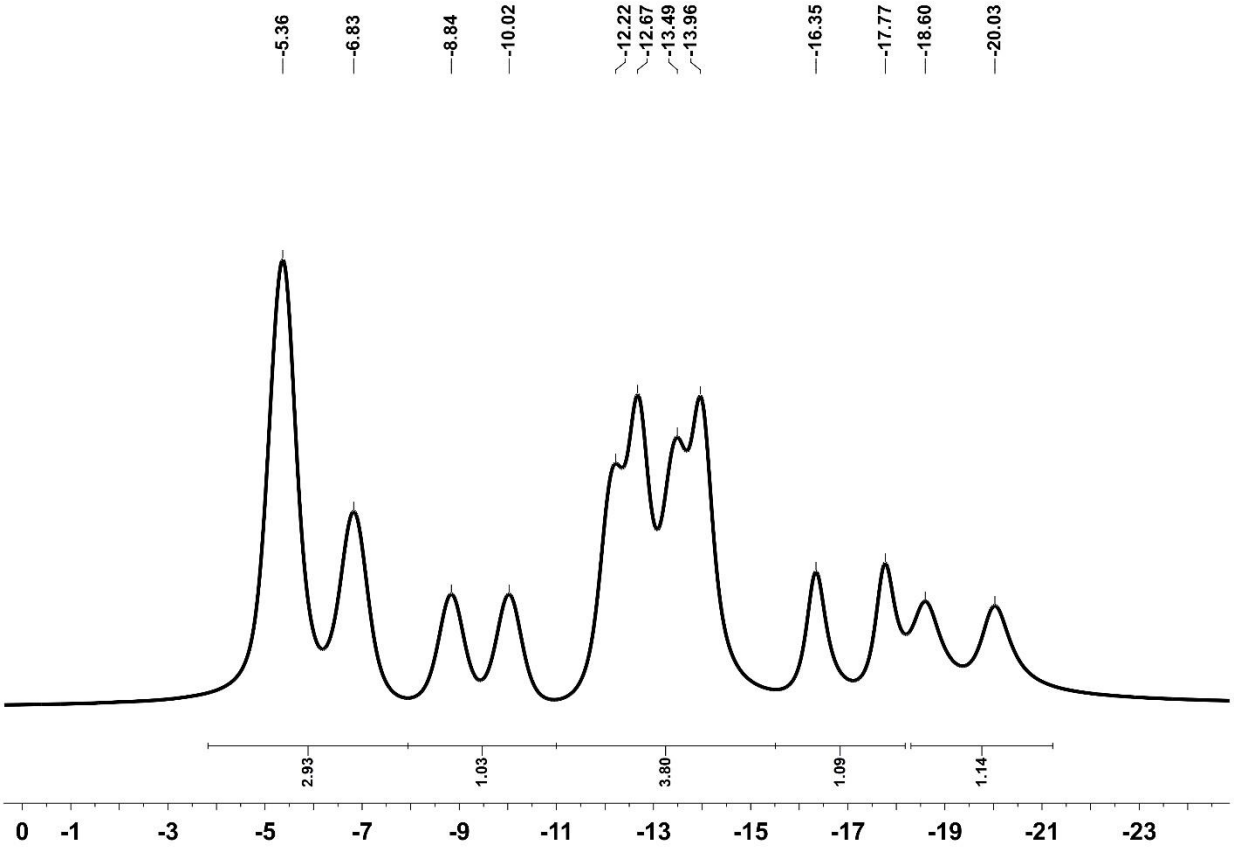

Figure 2-17. ^{11}B NMR spectrum of **compound 5b** in $CDCl_3$

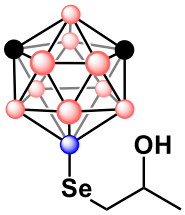

5b

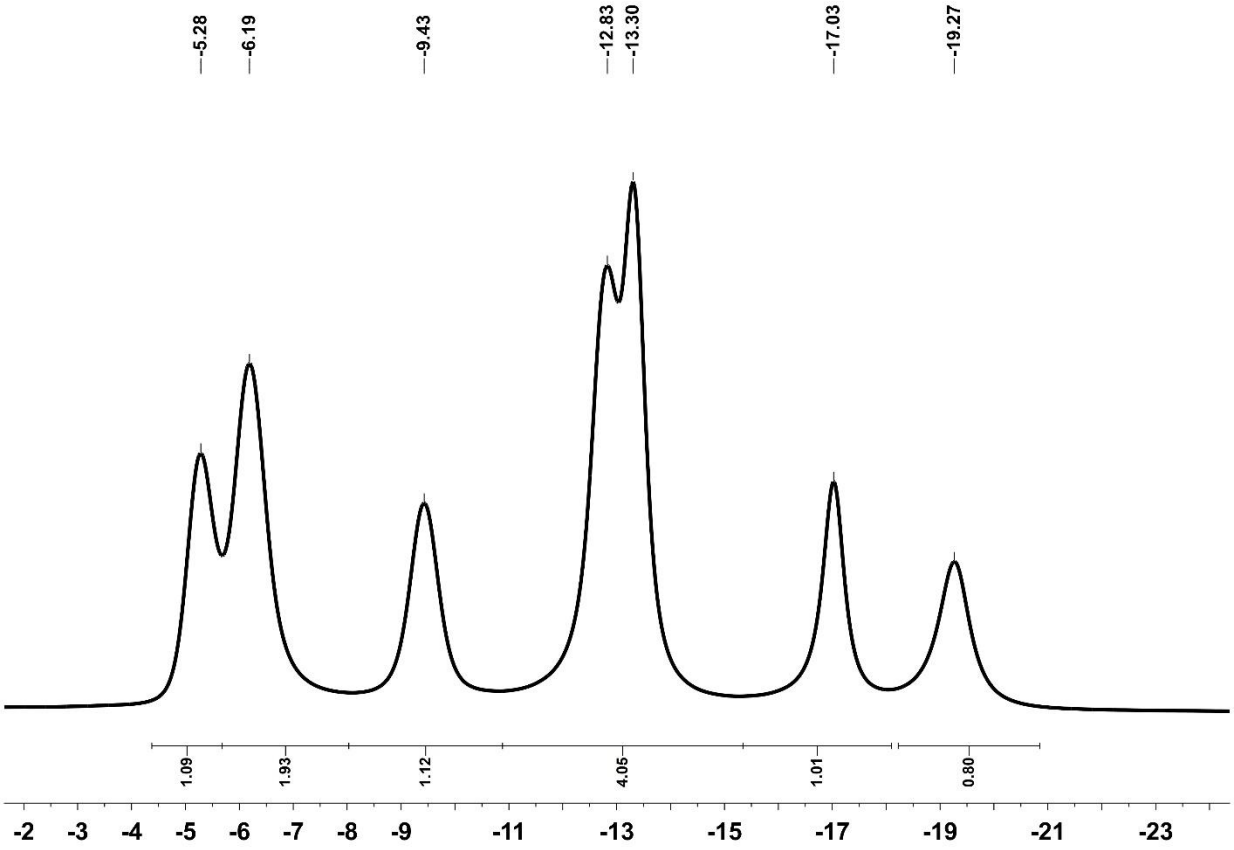

Figure 2-18. $^{11}B\{^{1}H\}$ NMR spectrum of **compound 5b** in $CDCl_3$

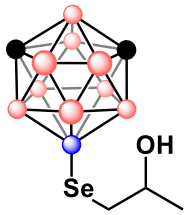

5b

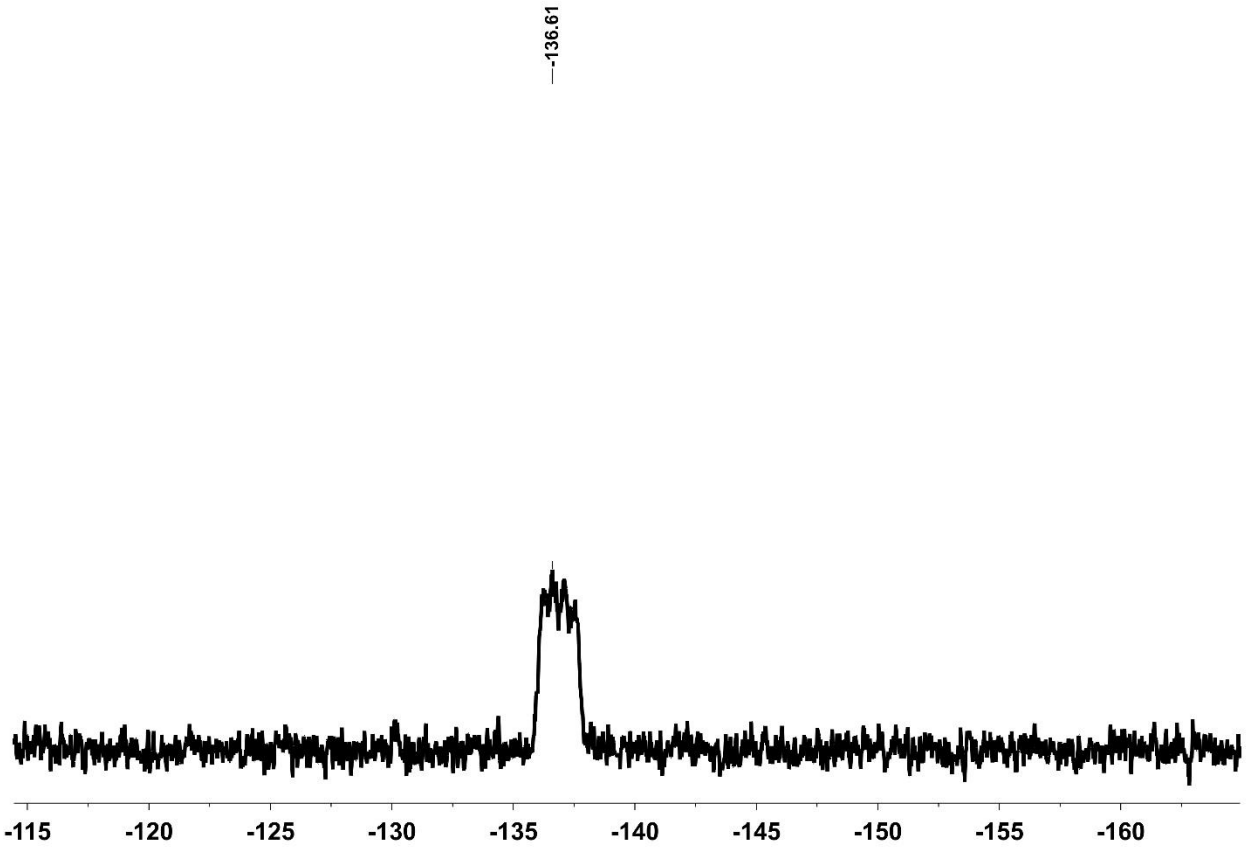

Figure 2-19. ^{77}Se NMR spectrum of **compound 5b** in $CDCl_3$

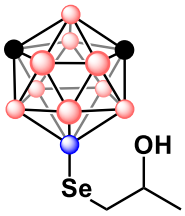

5b

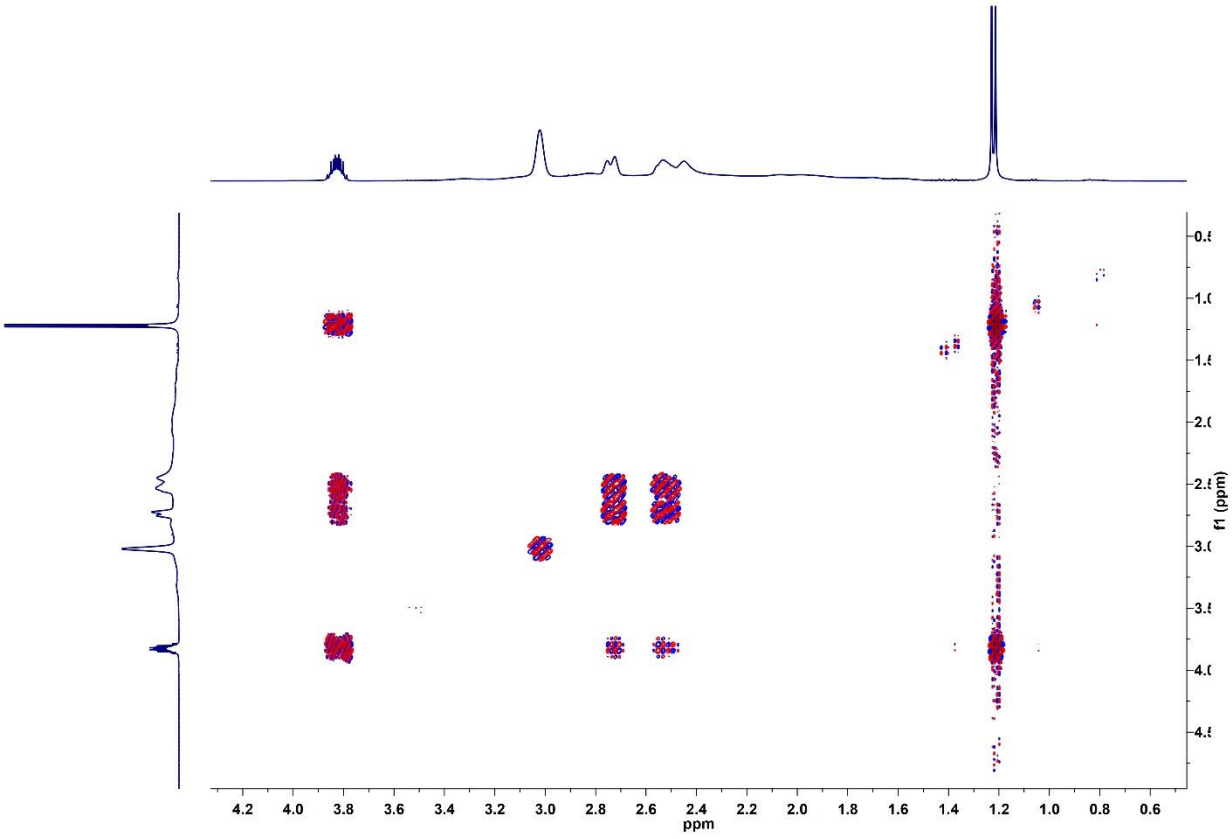

Figure 2-20. ^{1}H-^{1}H COSY NMR spectrum of **compound 5b** in $CDCl_3$

2.3.2. Electrophilic Chemistry of Selenium-Based Carboranyl Compounds

The products (**compound 6b**) resulting from the reaction of 9-*meta*-carboranyl selenyl (II) chloride (**compounds 6a**) and 5-hexen-2-one were characterized by GCMS (**Figure 2-21**). The products (**compound 6c**) resulting from the reaction of 9-*meta*-carboranyl selenyl (II) chloride (**compound 6a**) and cycloheptanone were characterized by GCMS (**Figure 2-22**).

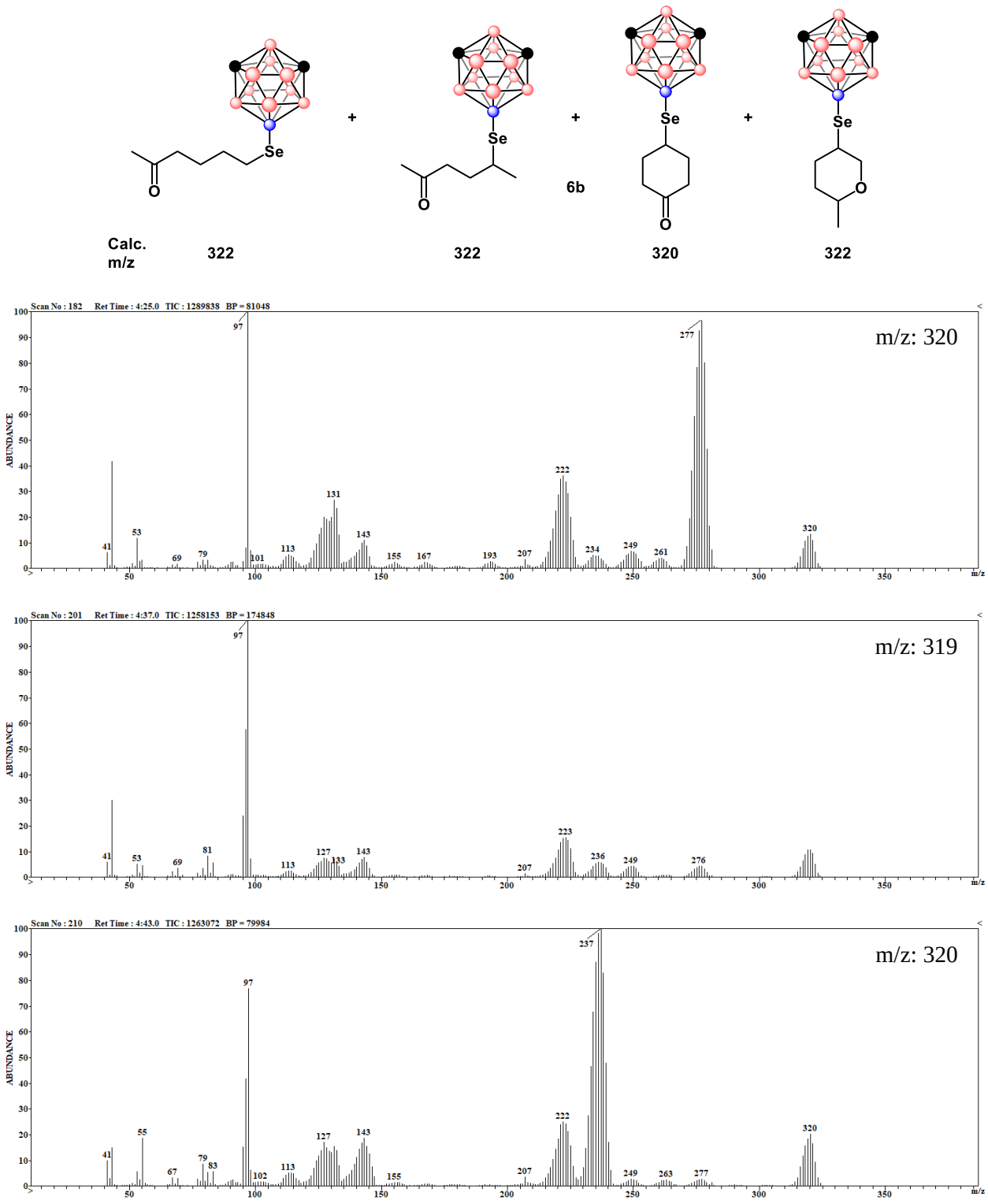

Figure 2-21. GCMS spectra of **compound 6b** (Note: there are three retention times corresponding to product; the parent ion masses all correspond to either an extra double bond in the two structures to the left or a cyclization like seen in the two structures to the right)

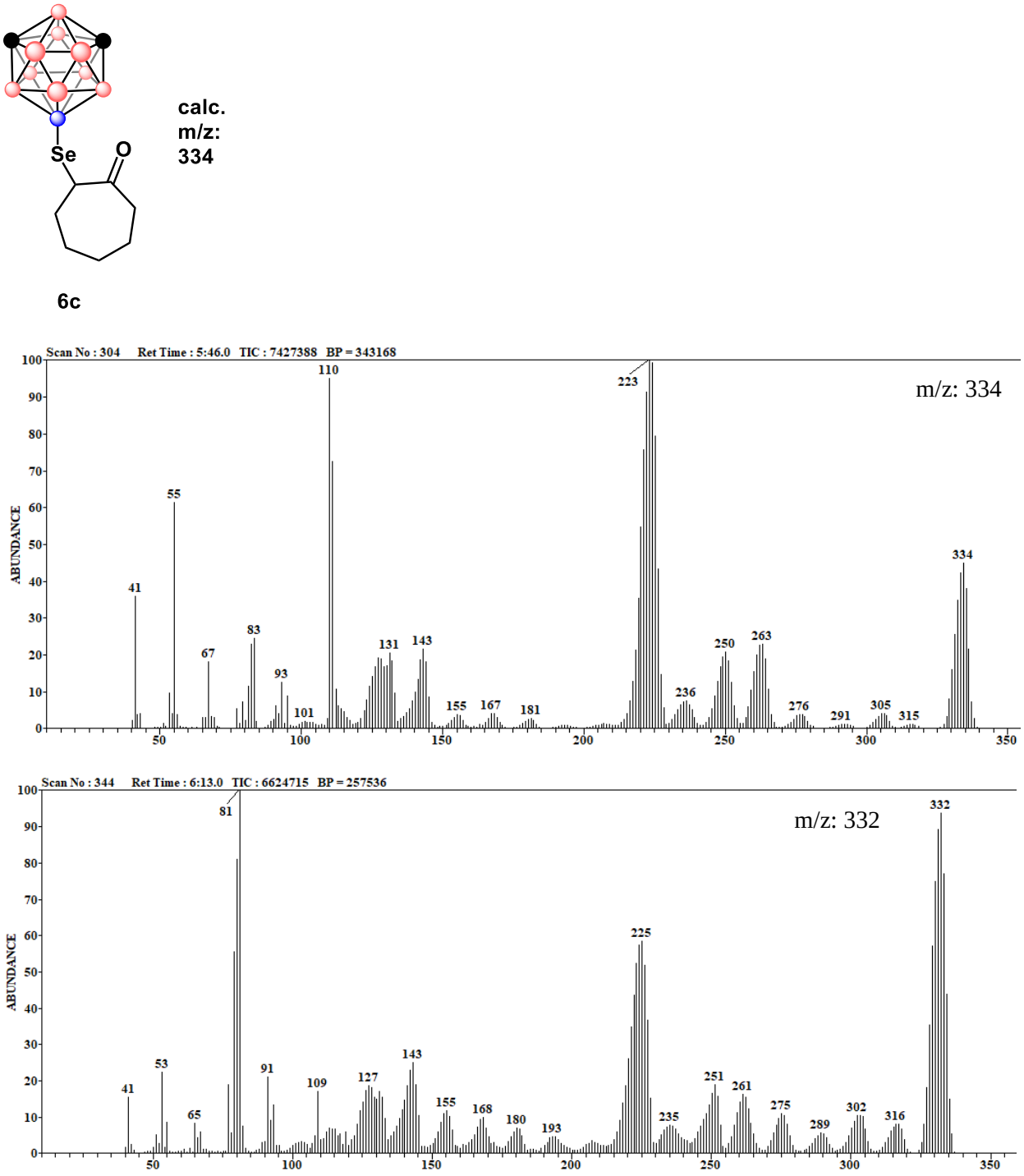

Figure 2-22. GCMS spectra of **compound 6c** (Note: both retention times corresponding to the product are shown; the second one likely corresponds to an extra double bond in the ring since the calculated mass of product 6c as shown is 332 m/z)

2.3.3. Nucleophilic Chemistry of Tellurium-Based Carboranyl Compounds

The bis(9-*ortho*-carboranyl) ditelluride (**compound 7a**) was characterized by ^{1}H (**Figure 2-23, 2-28**), ^{13}C (**Figure 2-24**), ^{11}B (**Figure 2-25, 2-29**), ^{11}B{^{1}H} (**Figure 2-26, 2-30**), and ^{125}Te (**Figure 2-27**) NMR spectroscopy. The 9-*ortho*-carboranyl methyl telluride (**compound 7b**) was characterized by ^{1}H (**Figure 2-31, 2-32, 2-37**), ^{13}C (**Figure 2-33**), ^{11}B (**Figure 2-34**), ^{11}B{^{1}H} (**Figure 2-35, 2-38**), and ^{125}Te (**Figure 2-36**) NMR spectroscopy as well as GCMS (**Figure 2-39**). The 9-*ortho*-carboranyl benzyl telluride (**compound 7c**) was characterized by ^{1}H (**Figure 2-40**), ^{11}B (**Figure 2-41**), and ^{11}B{^{1}H} (**Figure 2-42**) NMR spectroscopy. The 9-*ortho*-carboranyl tellurol (**compound 7d**) was characterized by ^{1}H (**Figure 2-43**), ^{13}C (**Figure 2-44**), ^{11}B (**Figure 2-45**), ^{11}B{^{1}H} (**Figure 2-46**), and ^{125}Te (**Figure 2-47**) NMR spectroscopy. Due to decomposition, several extra resonances can be seen for **compound 7d**. The (2-hydroxypropyl) 9-*meta*-carboranyl telluride (**compound 8b**) was characterized by ^{1}H (**Figures 2-48, 2-49**), ^{13}C (**Figures 2-50, 2-51**), ^{11}B (**Figure 2-52**), ^{11}B{^{1}H} (**Figure 2-53**), ^{125}Te (**Figure 2-54**), and ^{1}H-^{1}H COSY (**Figure 2-55**) NMR spectroscopy.

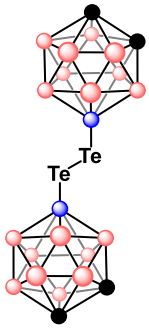

7a

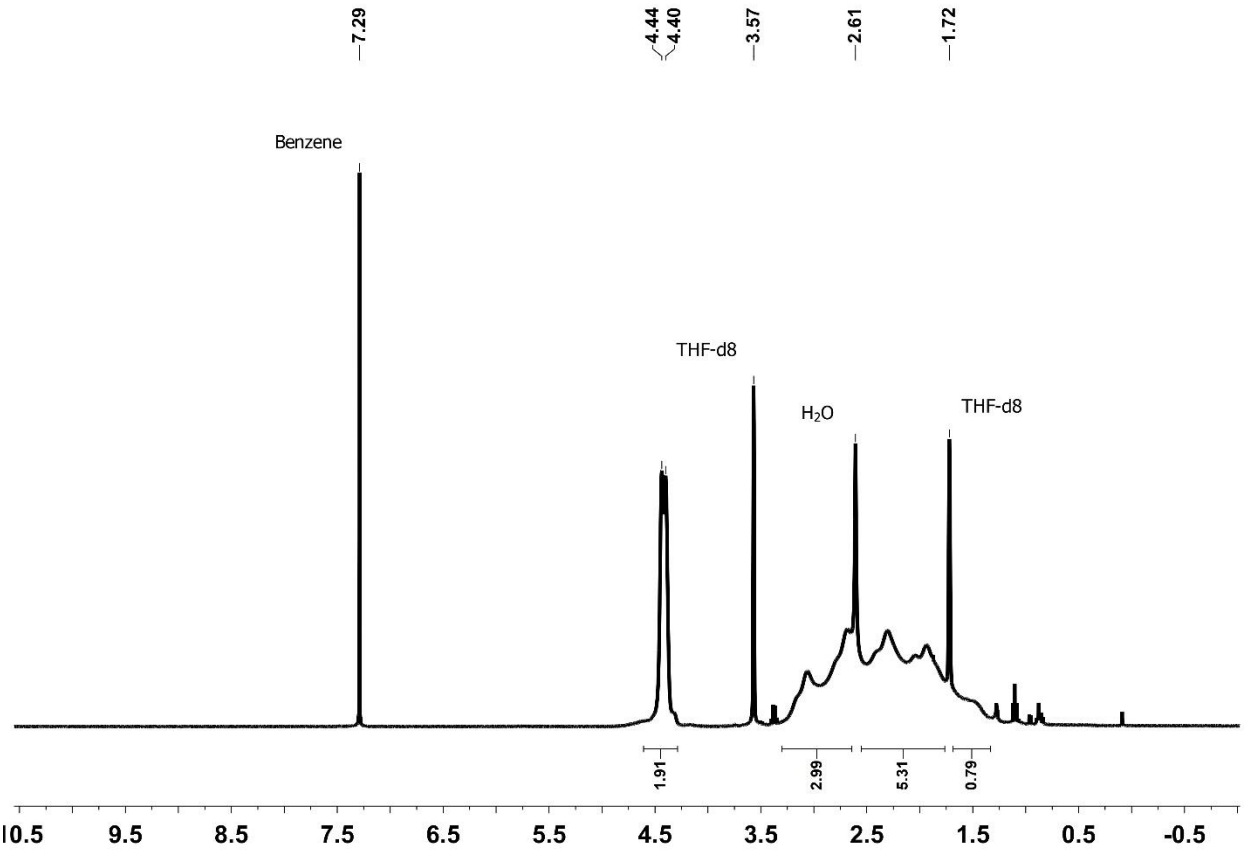

Figure 2-23. ^{1}H NMR spectrum of **compound 7a** in THF-d8

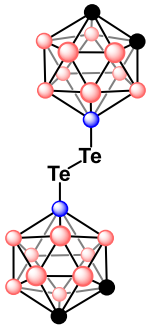

7a

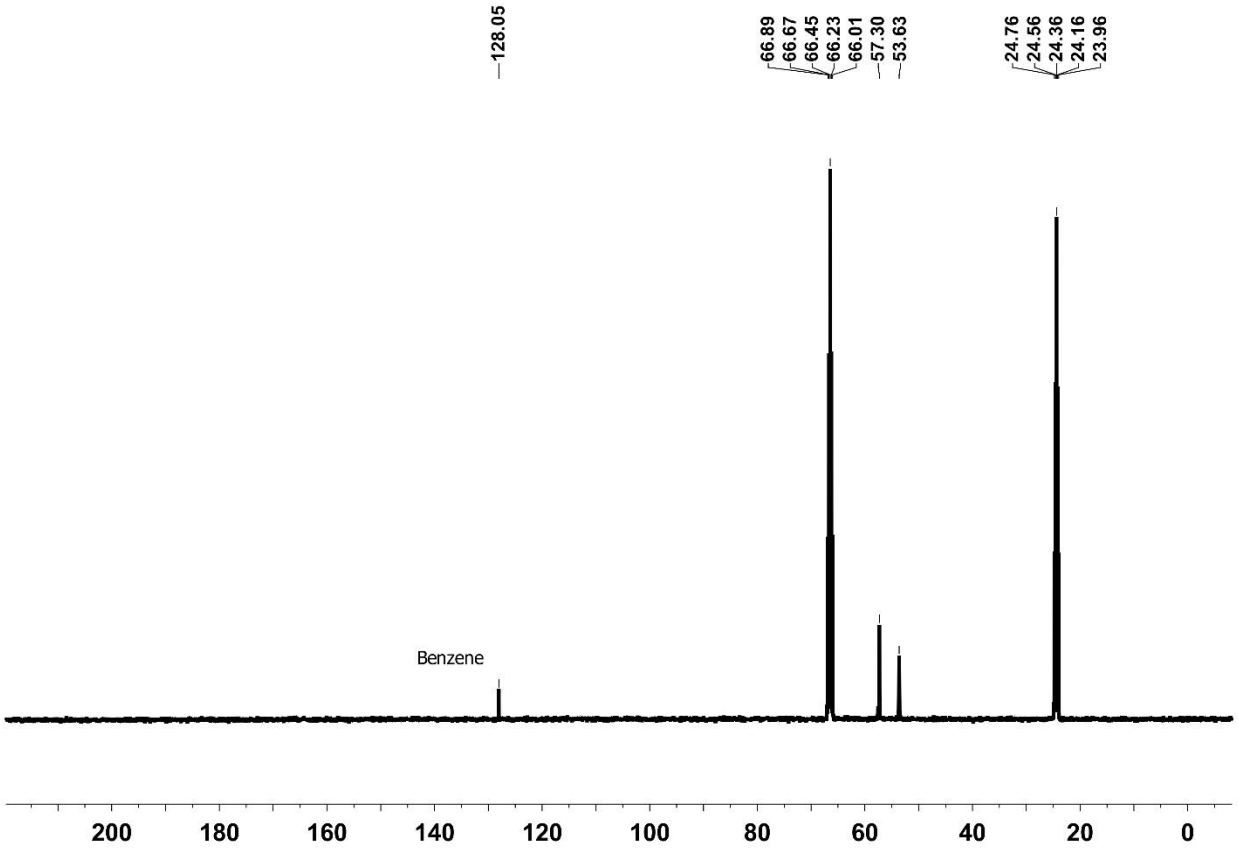

Figure 2-24. ^{13}C NMR spectrum of **compound 7a** in THF-d8

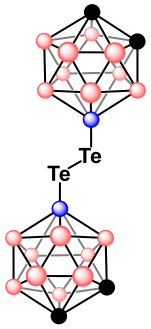

7a

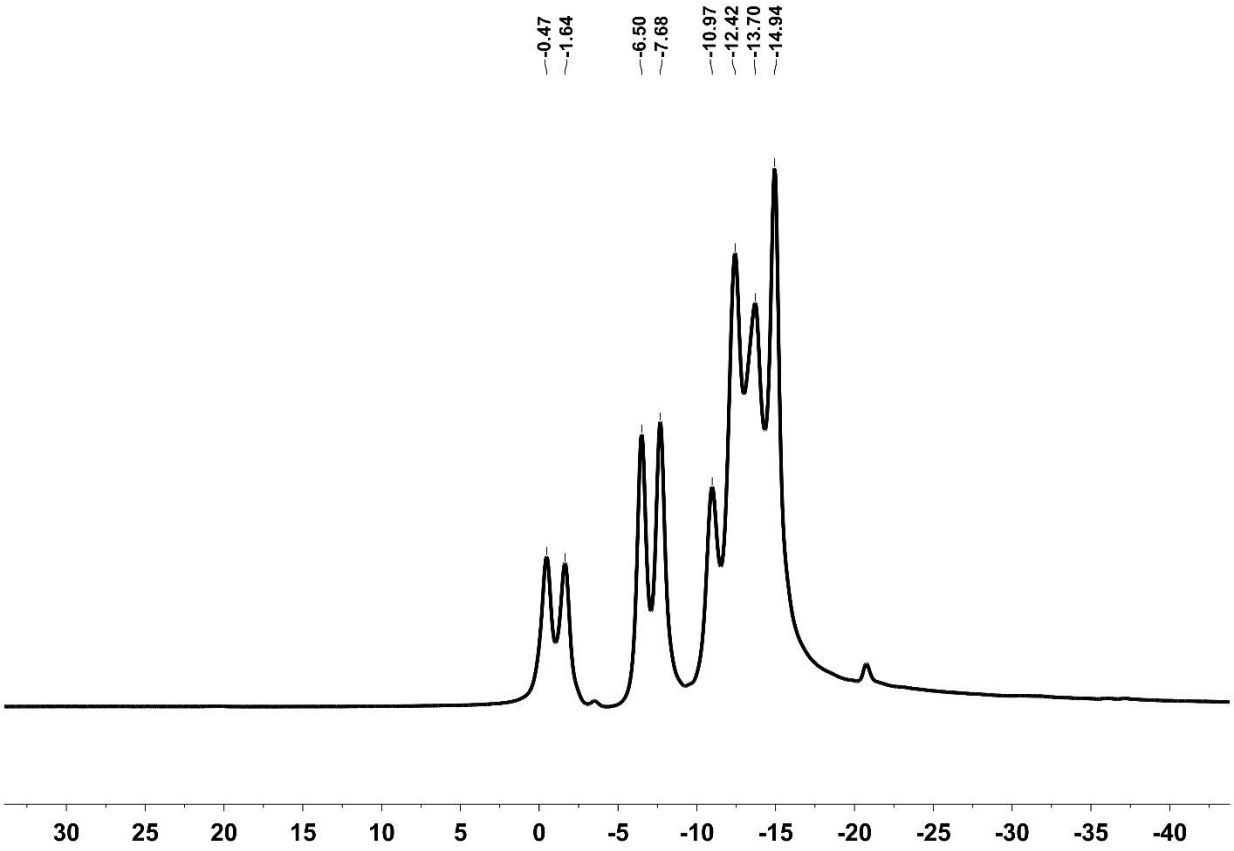

Figure 2-25. ^{11}B NMR spectrum **of compound 7a** in THF-d8

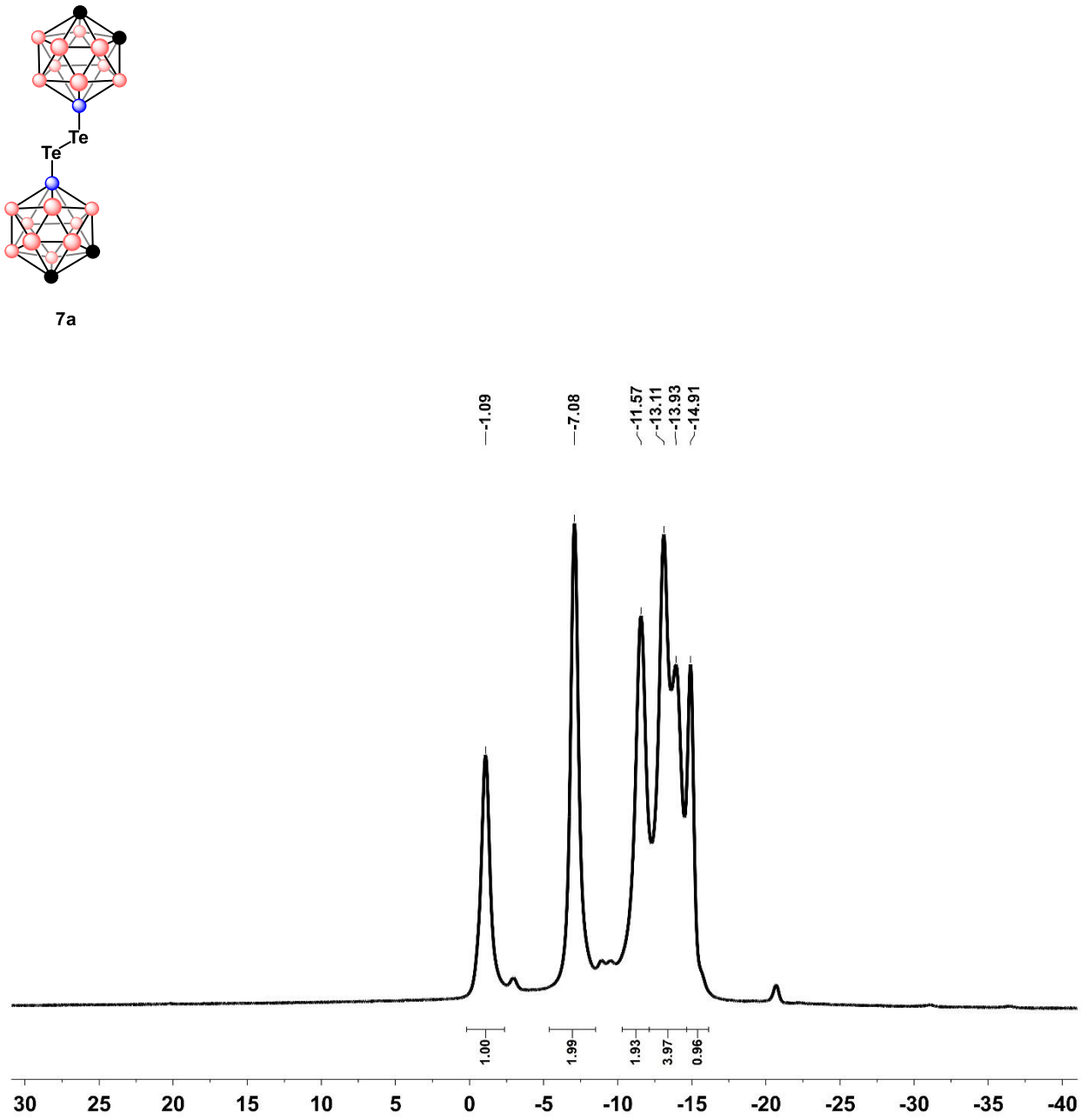

Figure 2-26. $^{11}B\{^{1}H\}$ NMR spectrum of **compound 7a** in THF-d8

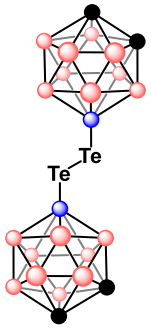

7a

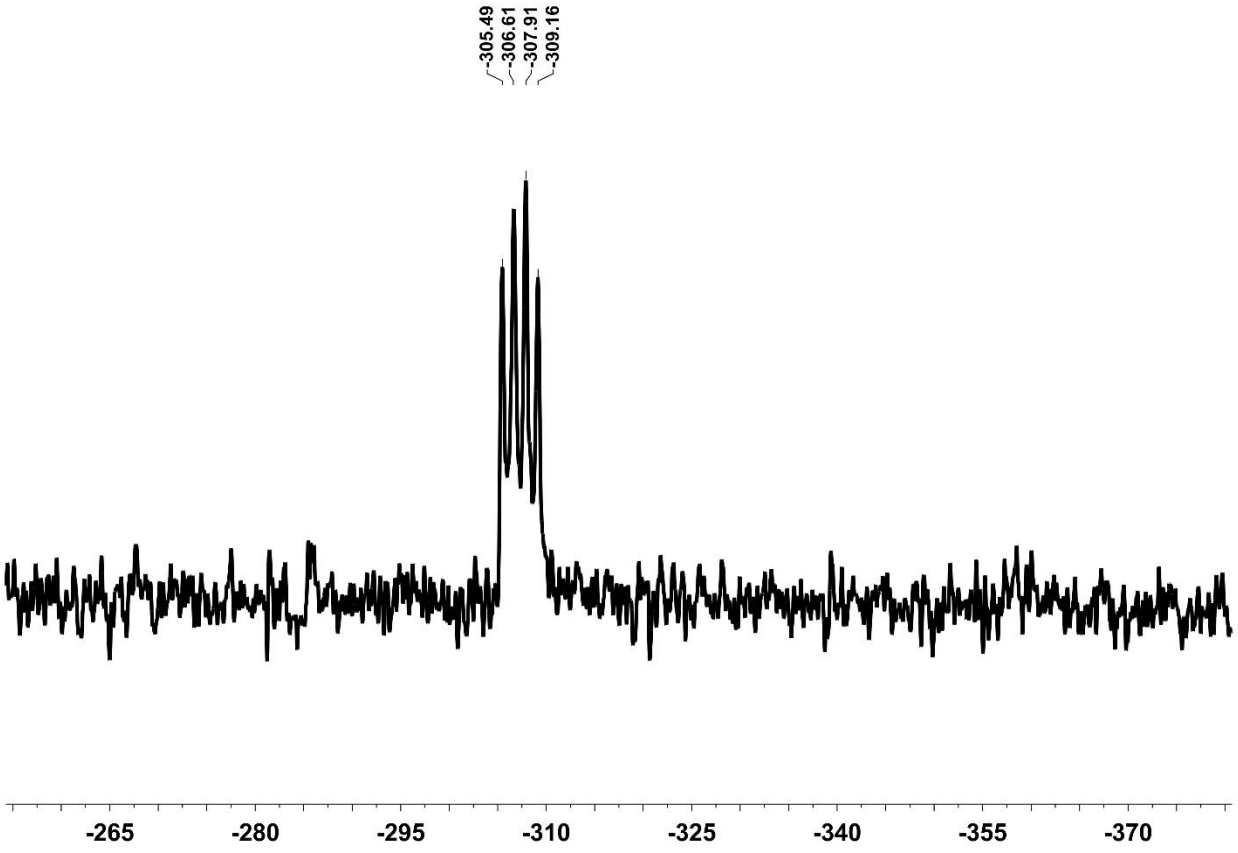

Figure 2-27. ^{125}Te NMR spectrum of **compound 7a** in THF-d8 (apodization applied; lb = 25 Hz)

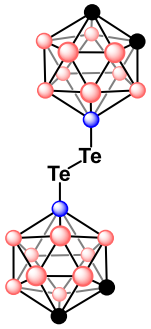

7a

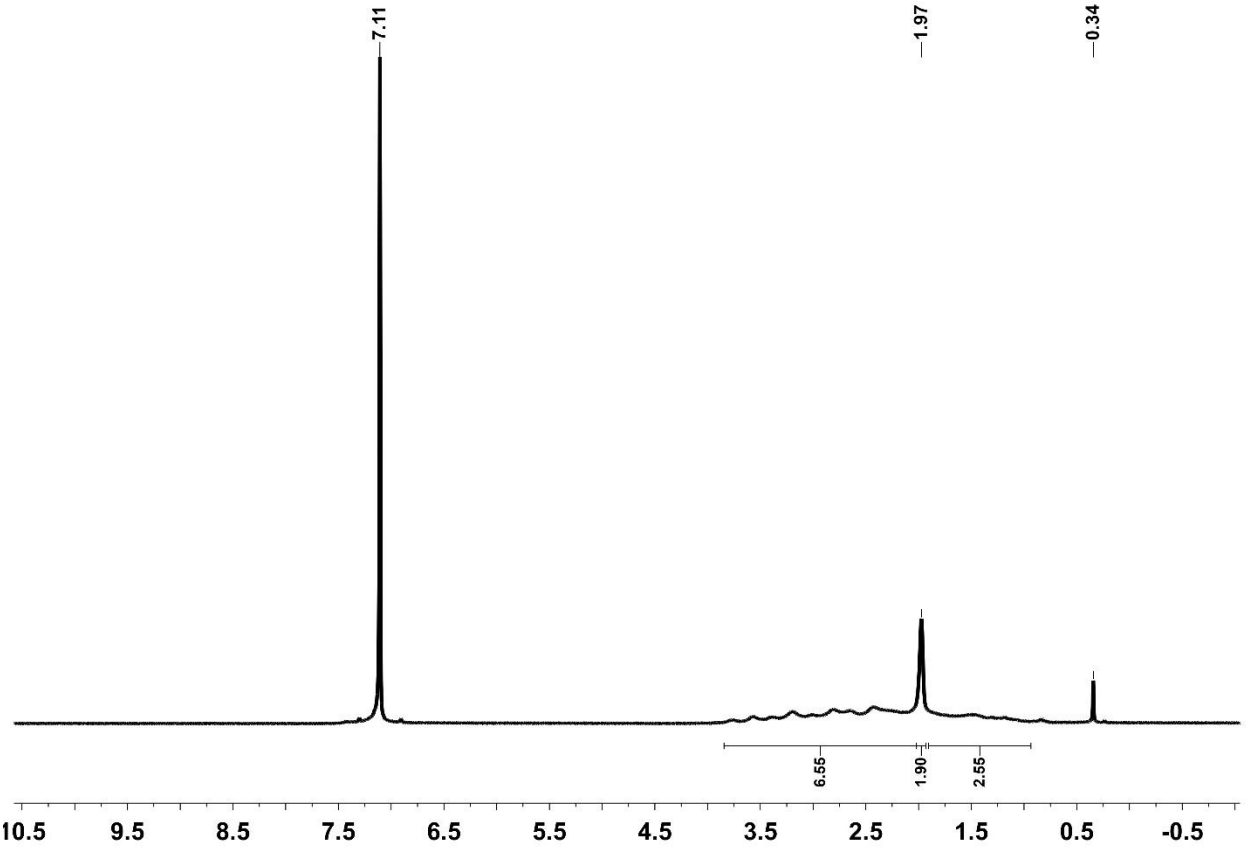

Figure 2-28. ^{1}H NMR spectrum of **compound 7a** in C_6D_6

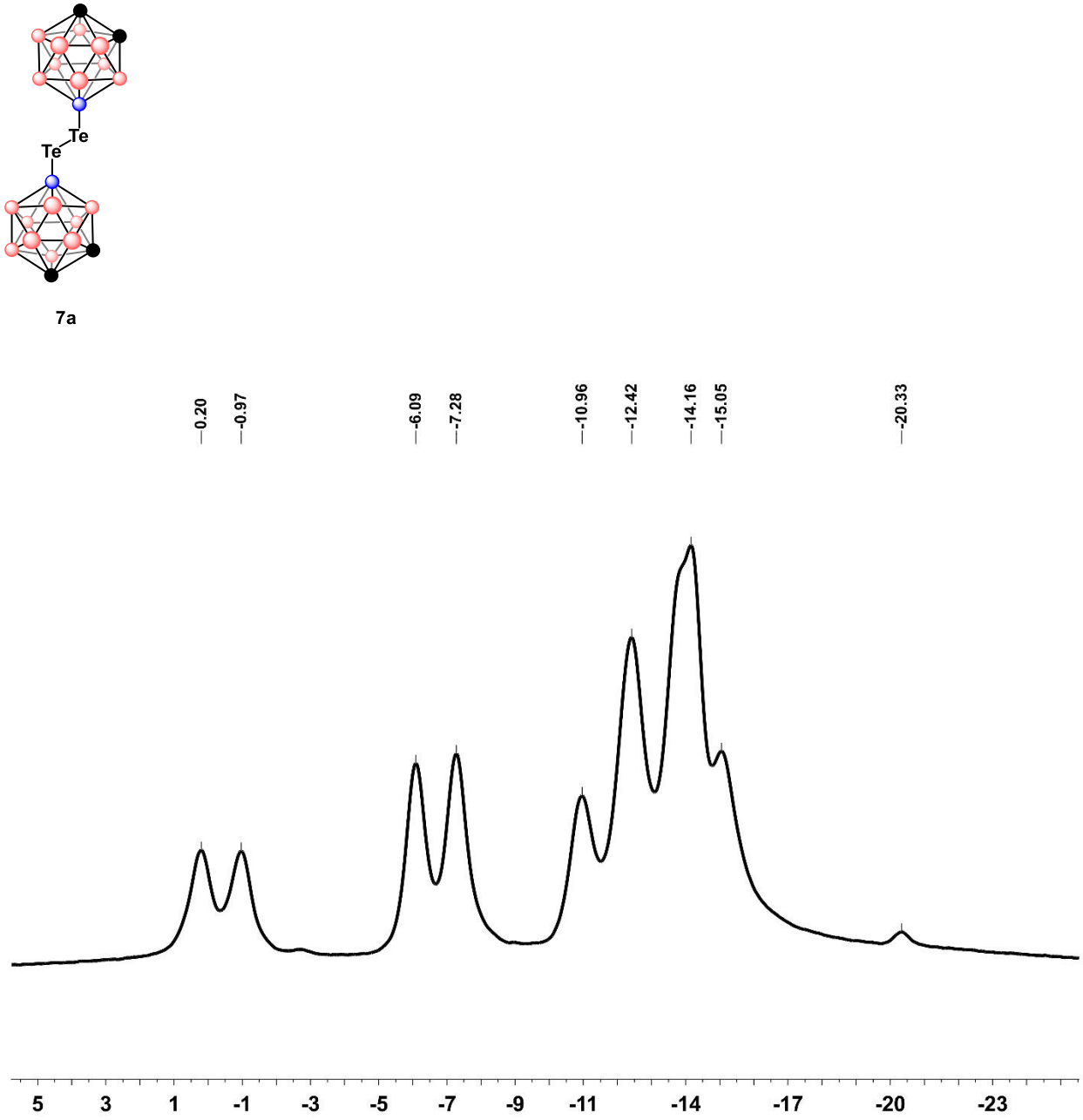

Figure 2-29. ^{11}B NMR spectrum of **compound 7a** in C_6D_6

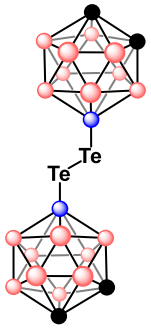

7a

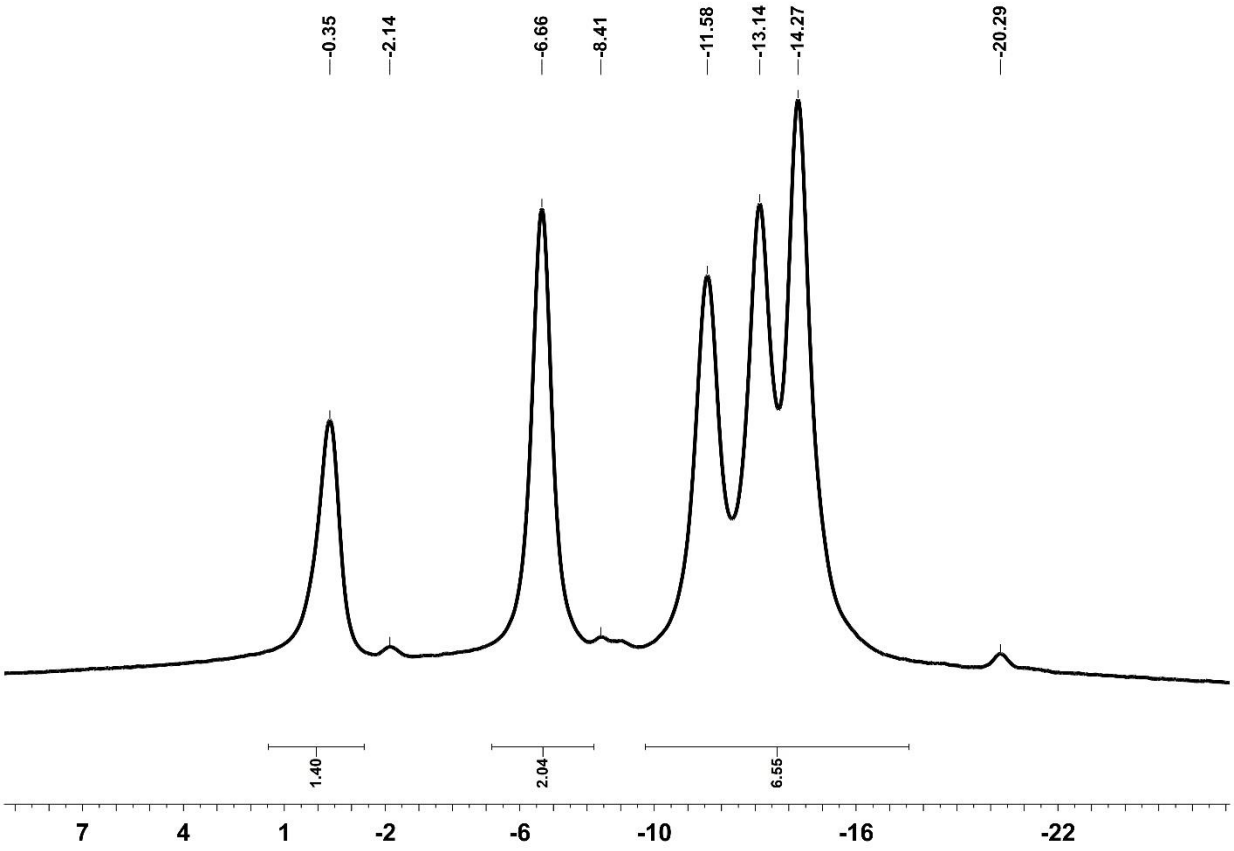

Figure 2-30. $^{11}B\{^{1}H\}$ NMR spectrum of **compound 7a** in C_6D_6

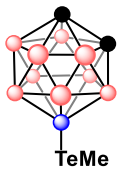

7b

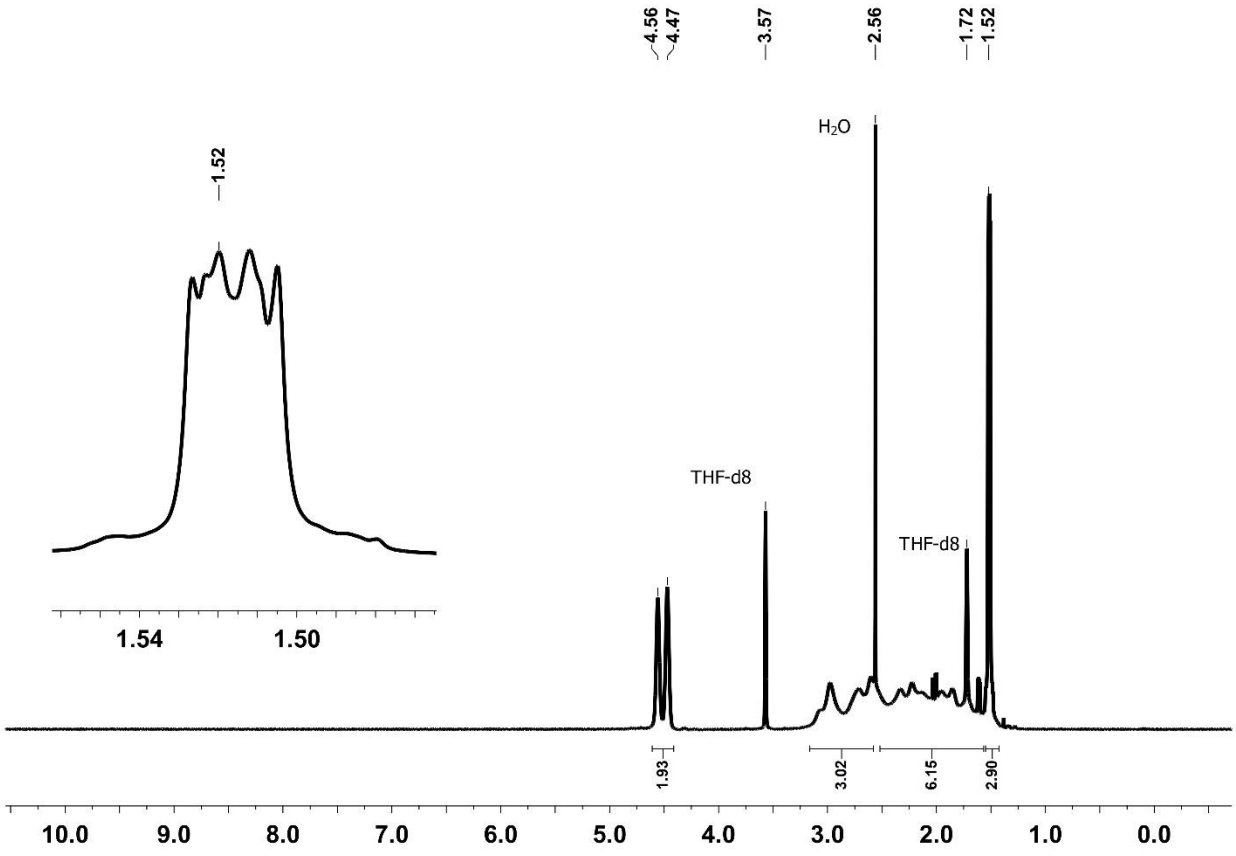

Figure 2-31. ^{1}H NMR spectrum of **compound 7b** in THF-d8

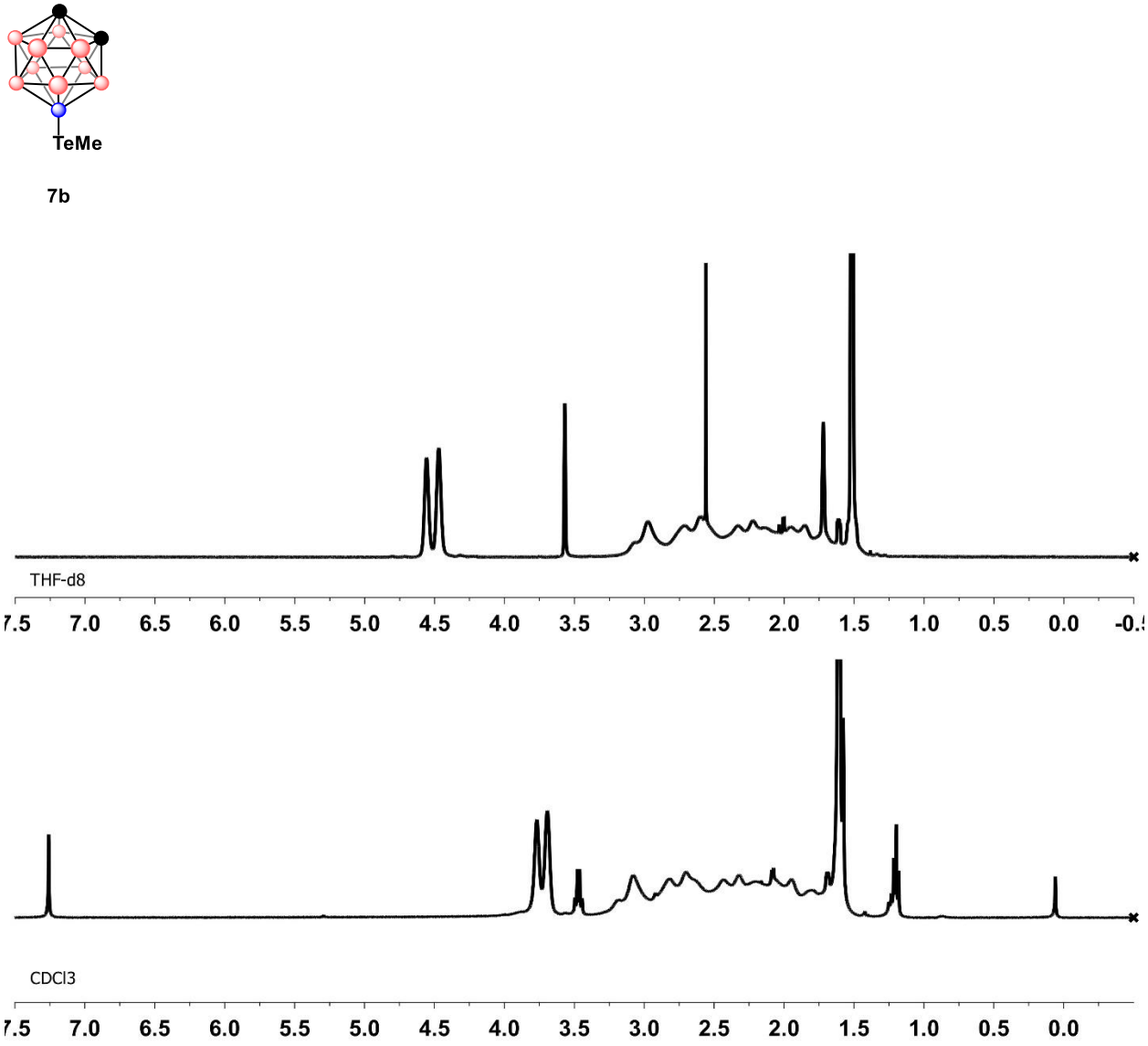

Figure 2-32. ^{1}H NMR spectra comparison of **compound 7b** in $CDCl_3$ and THF-d8

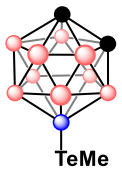

7b

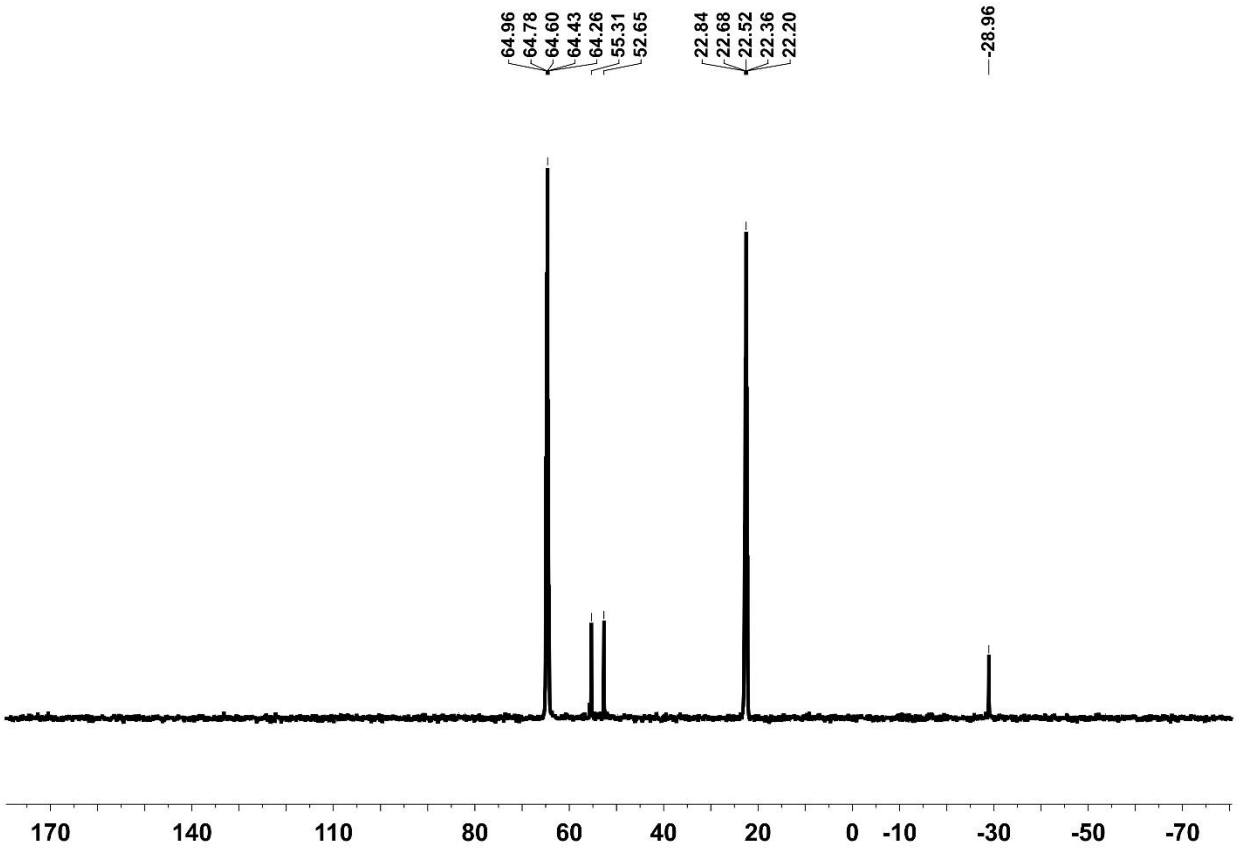

Figure 2-33. ^{13}C NMR spectrum of **compound 7b** in THF-d8

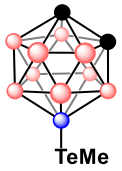

7b

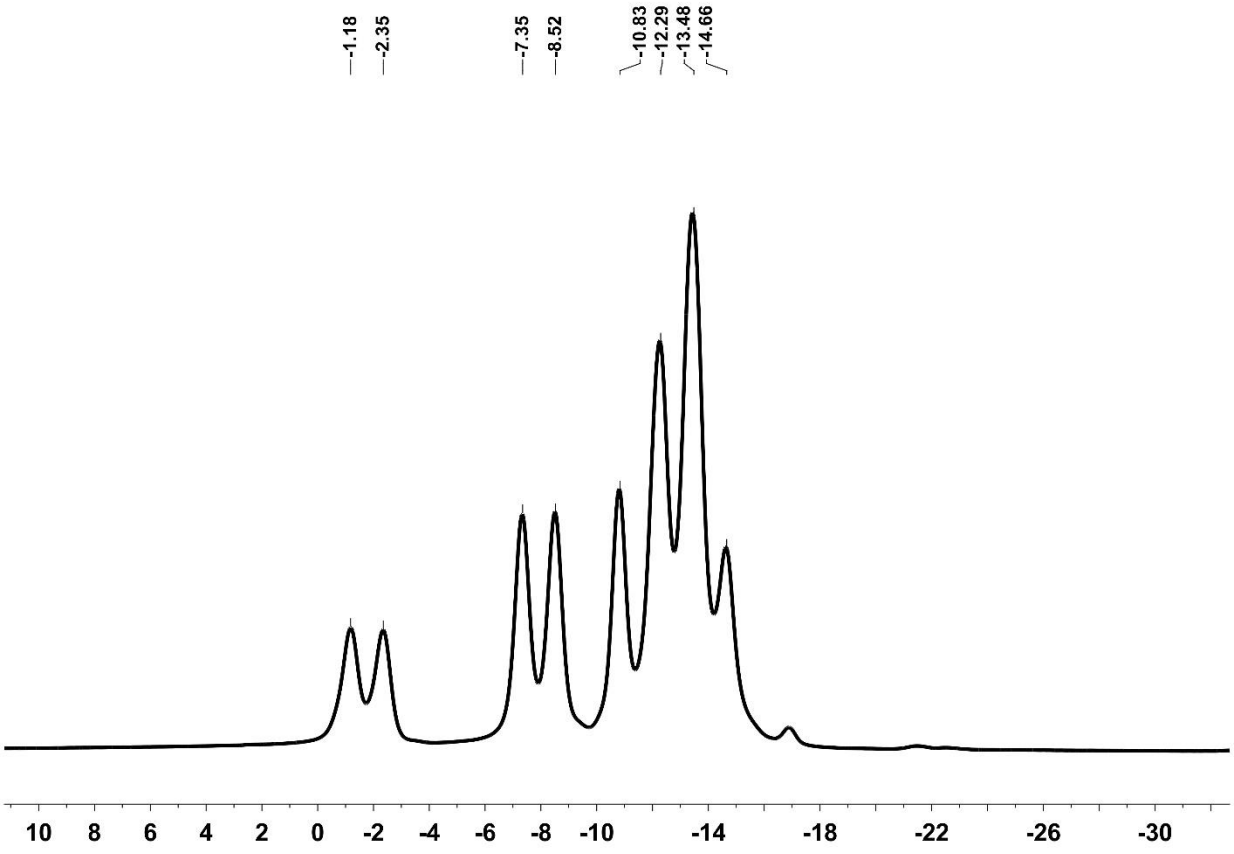

Figure 2-34. ^{11}B NMR spectrum of **compound 7b** in THF-d8

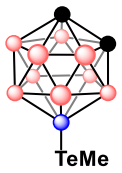

7b

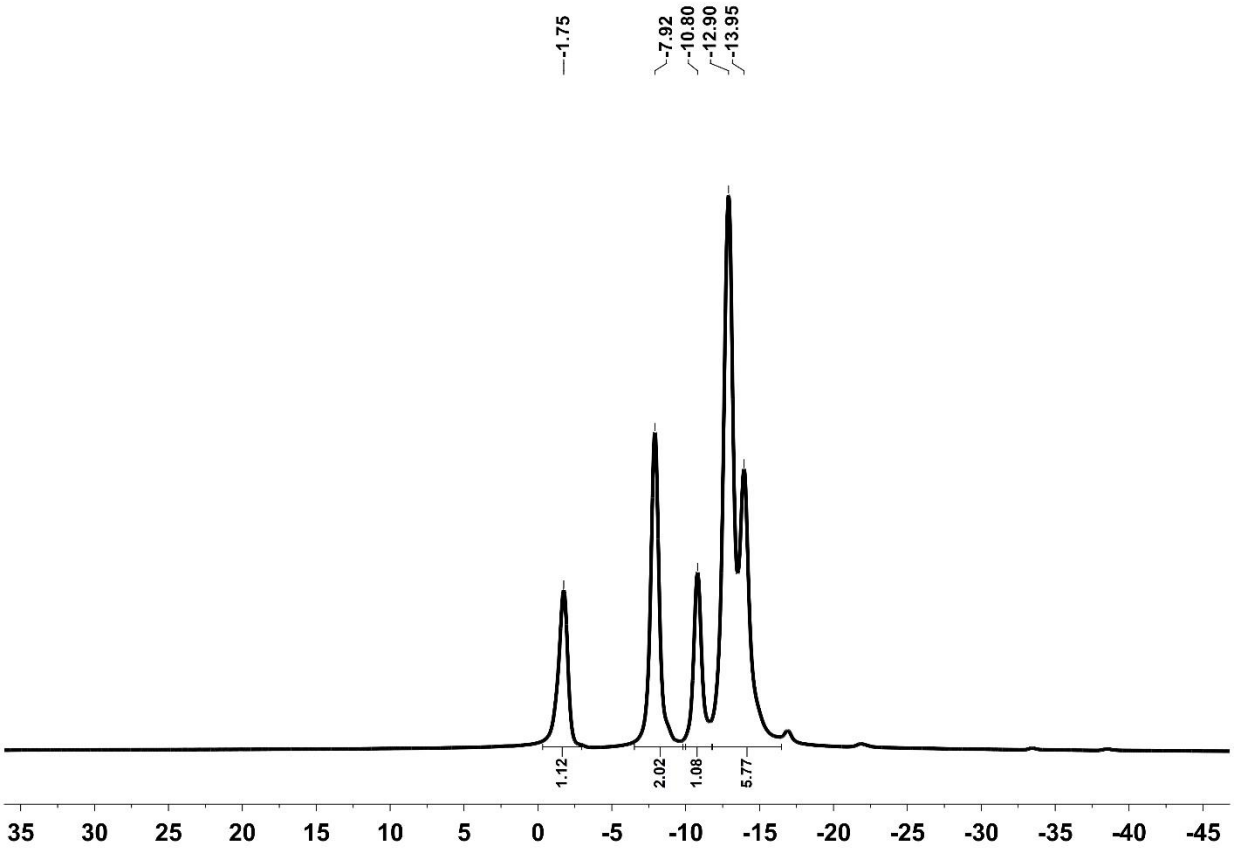

Figure 2-35. $^{11}B\{^{1}H\}$ NMR spectrum of **compound 7b** in THF-d8

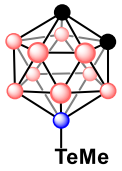

7b

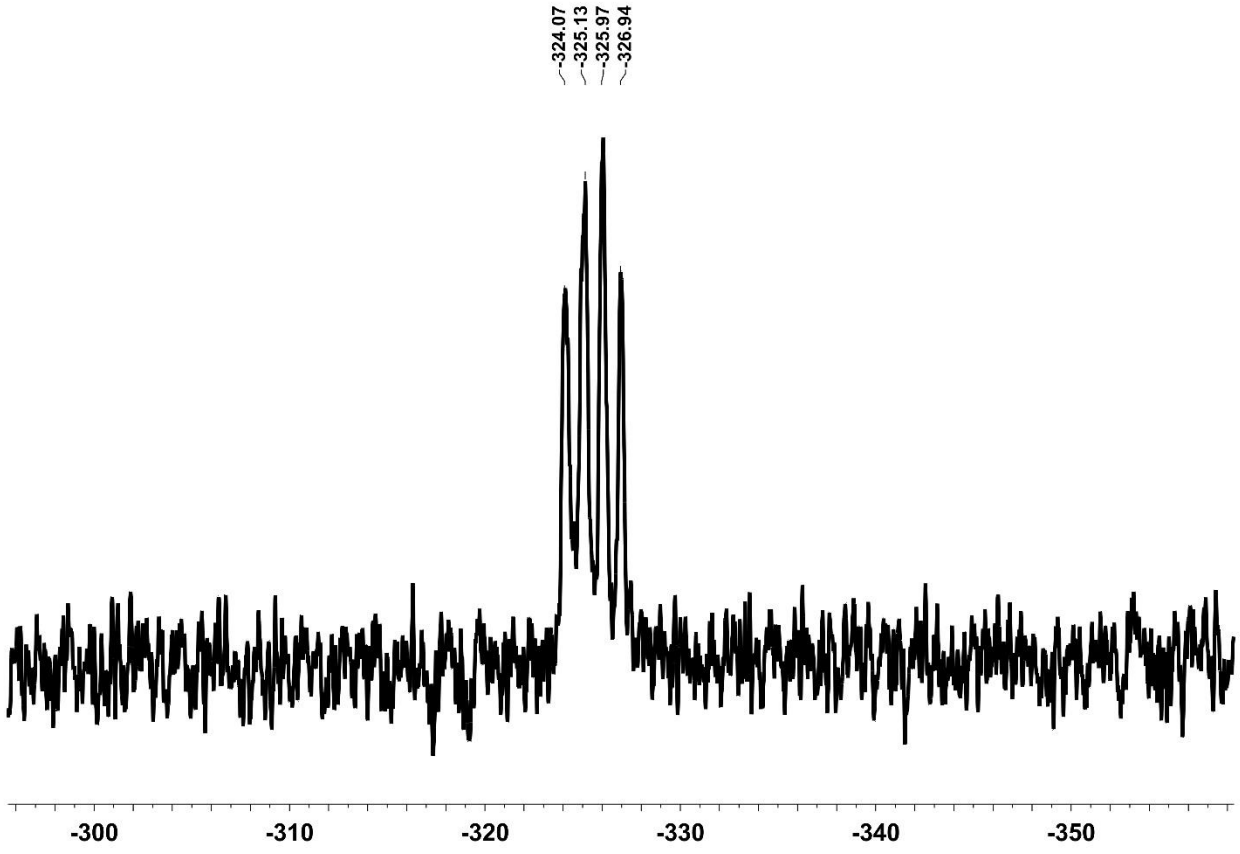

Figure 2-36. ^{125}Te NMR spectrum of **compound 7b** in THF-d8 (apodization applied; lb = 4 Hz; gb = 4 Hz)

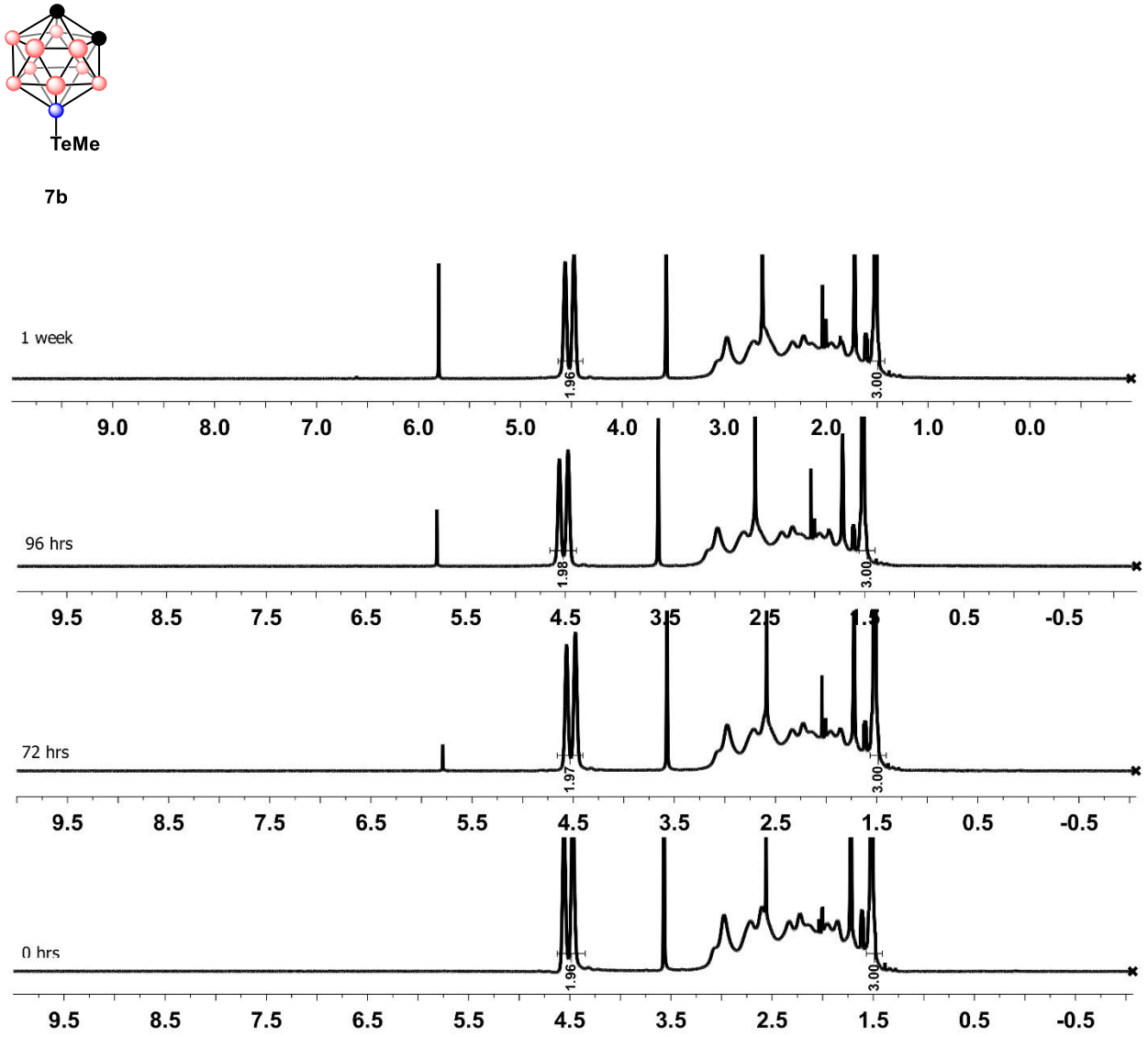

Figure 2-37. ^{1}H NMR spectrum stability study of **compound 7b** in THF-d8

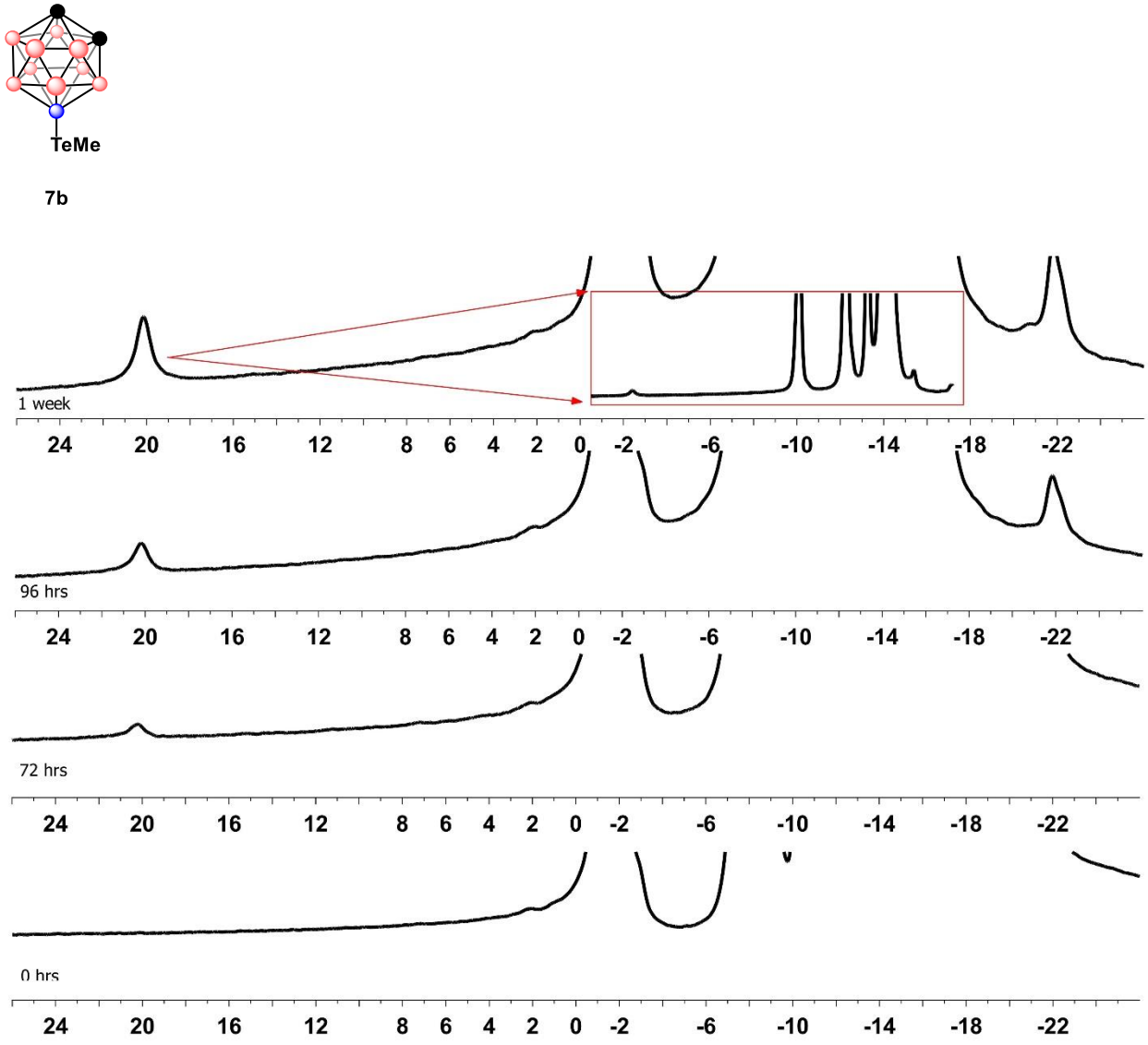

Figure 2-38. $^{11}B\{^{1}H\}$ NMR spectrum stability study of **compound 7b** in THF-d8

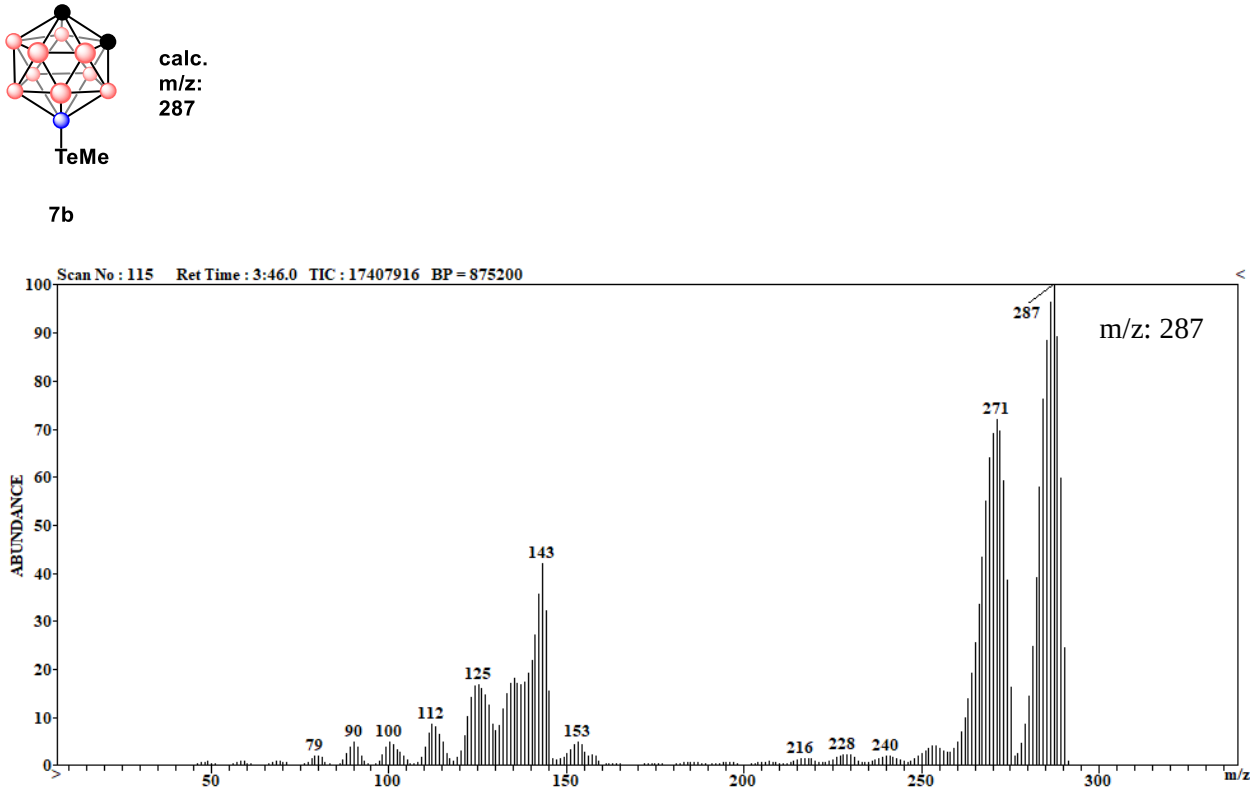

Figure 2-39. GCMS spectrum of **compound 7b**

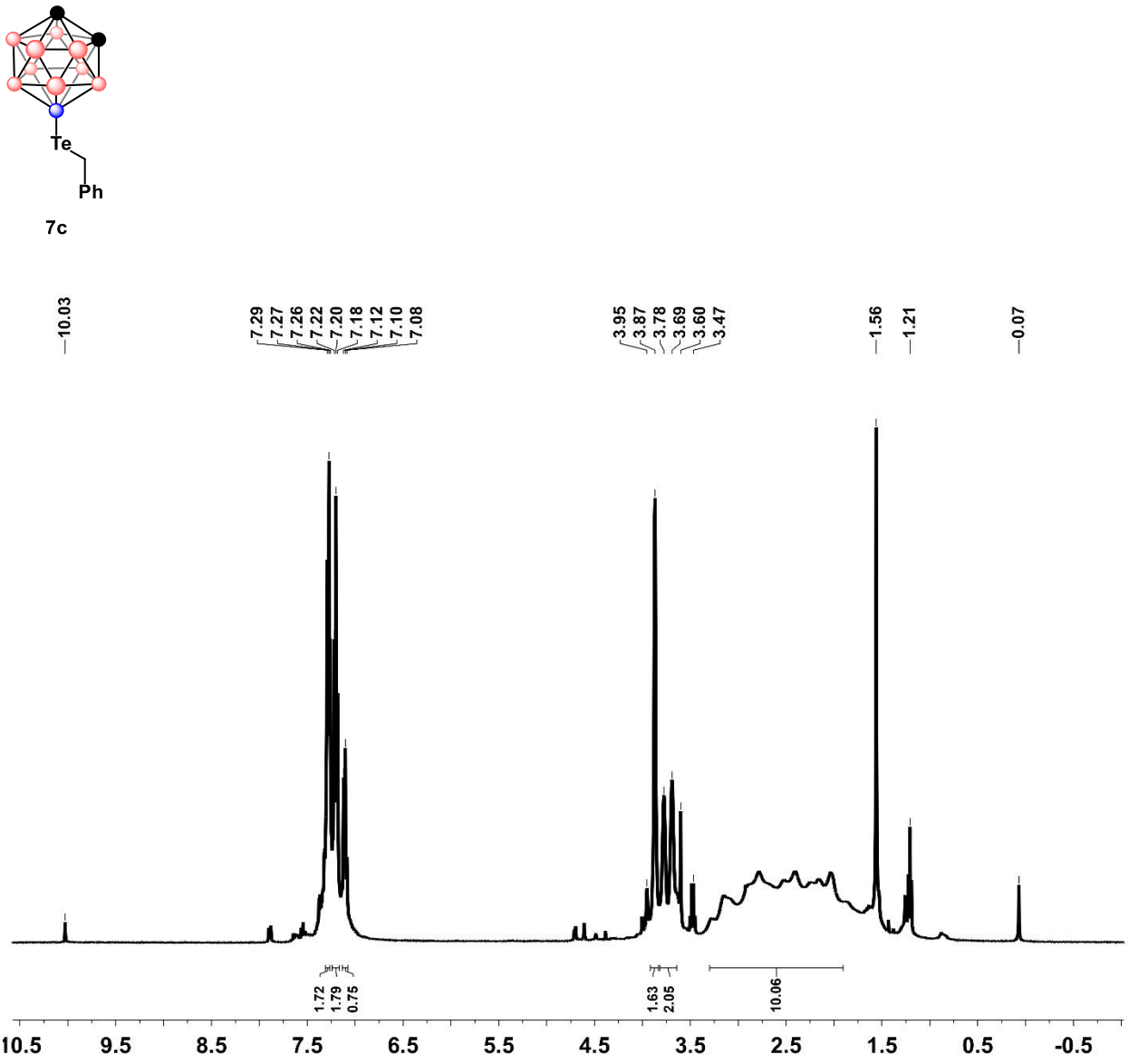

Figure 2-40. ^{1}H NMR spectrum of **compound 7c** in $CDCl_3$

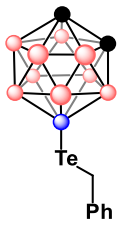

7c

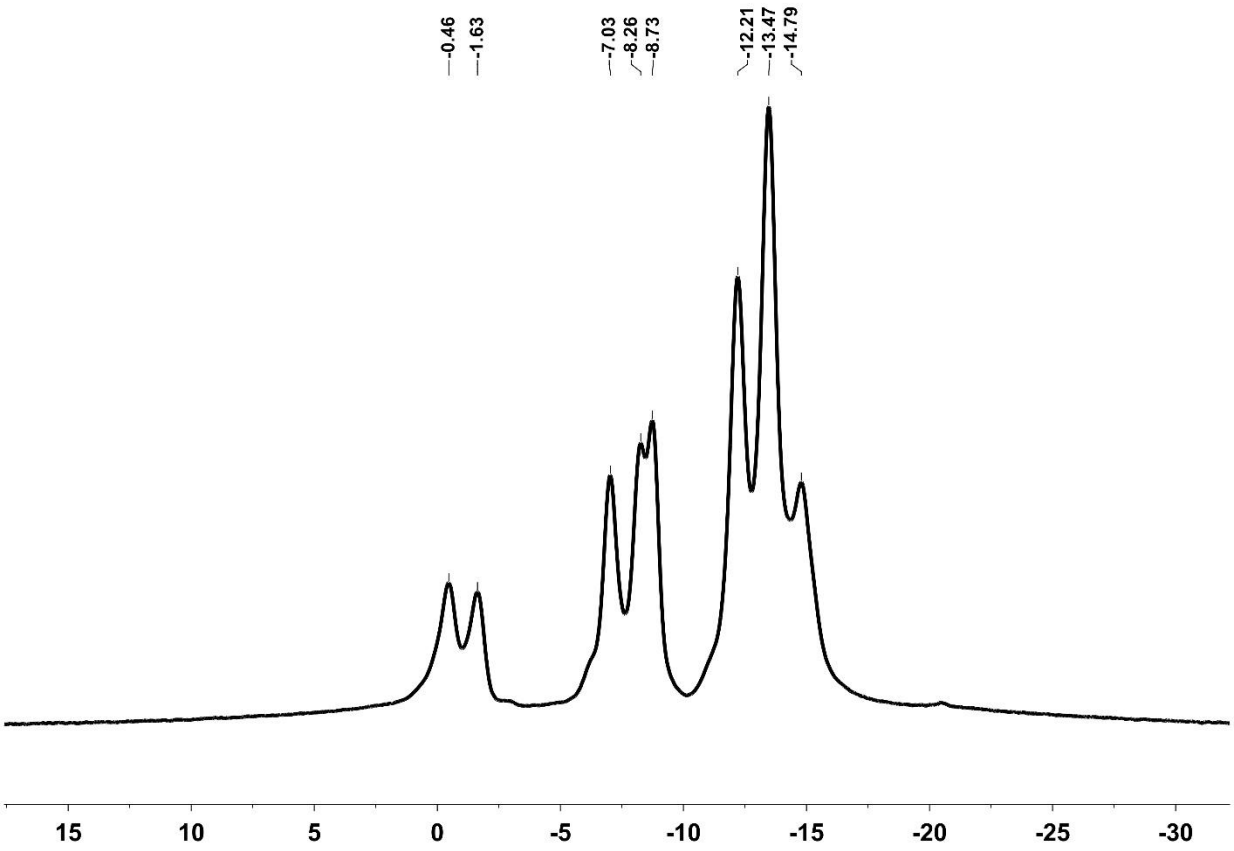

Figure 2-41. ^{11}B NMR spectrum of **compound 7c** in $CDCl_3$

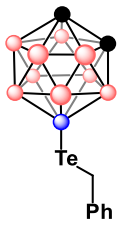

7c

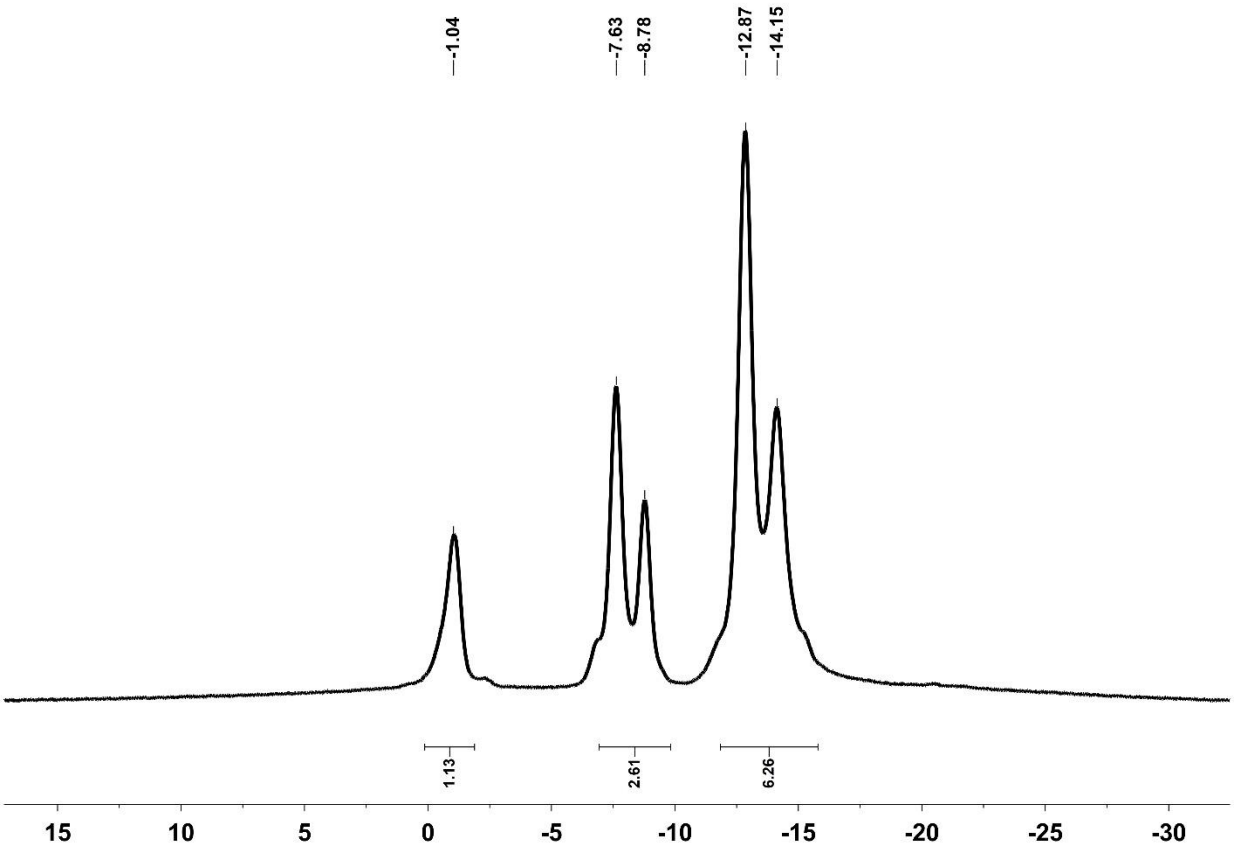

Figure 2-42. $^{11}B\{^{1}H\}$ NMR spectrum of **compound 7c** in $CDCl_3$

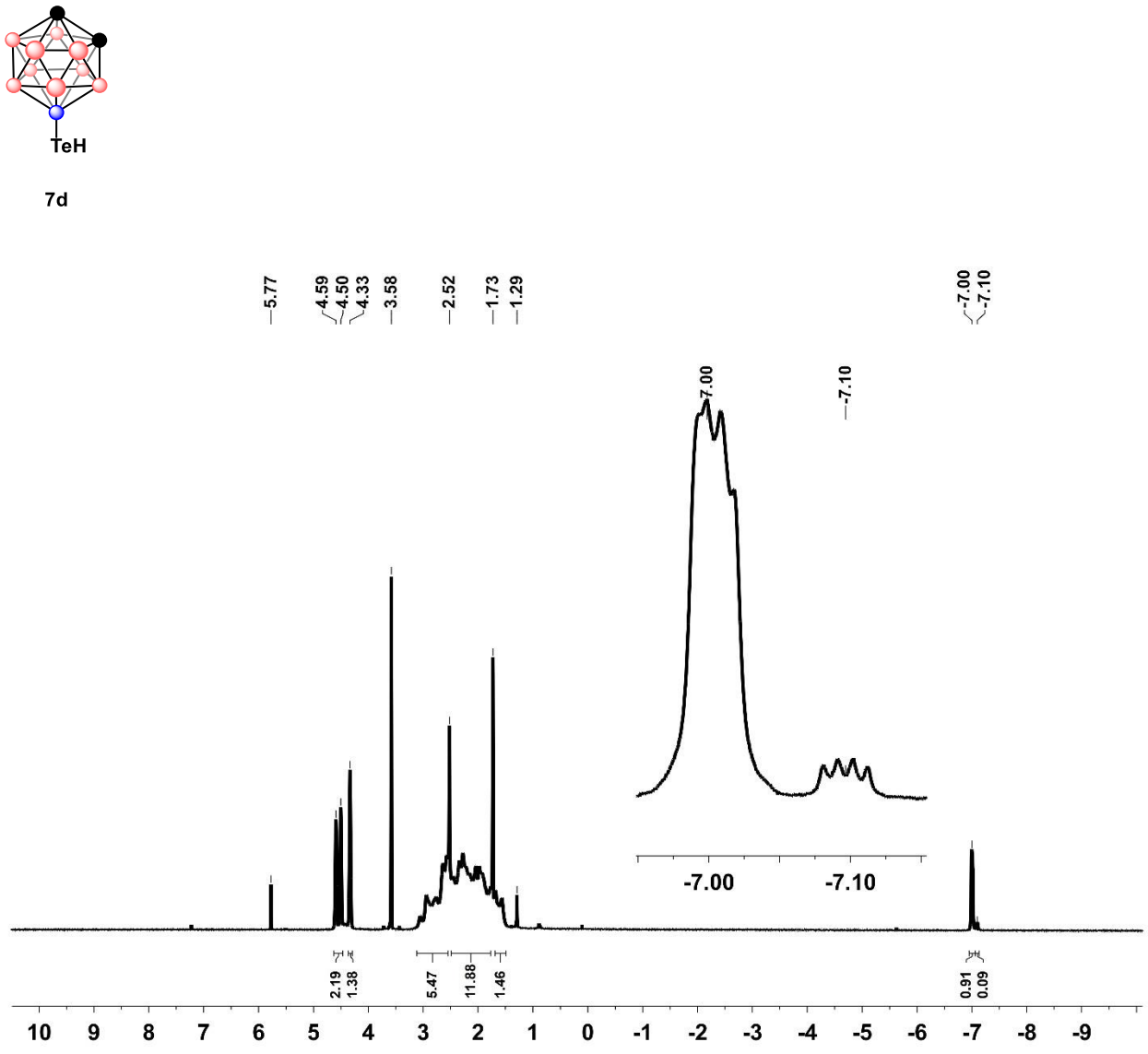

Figure 2-43. ^{1}H NMR spectrum of **compound 7d** (with expansion) in THF-d8

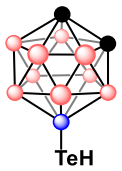

7d

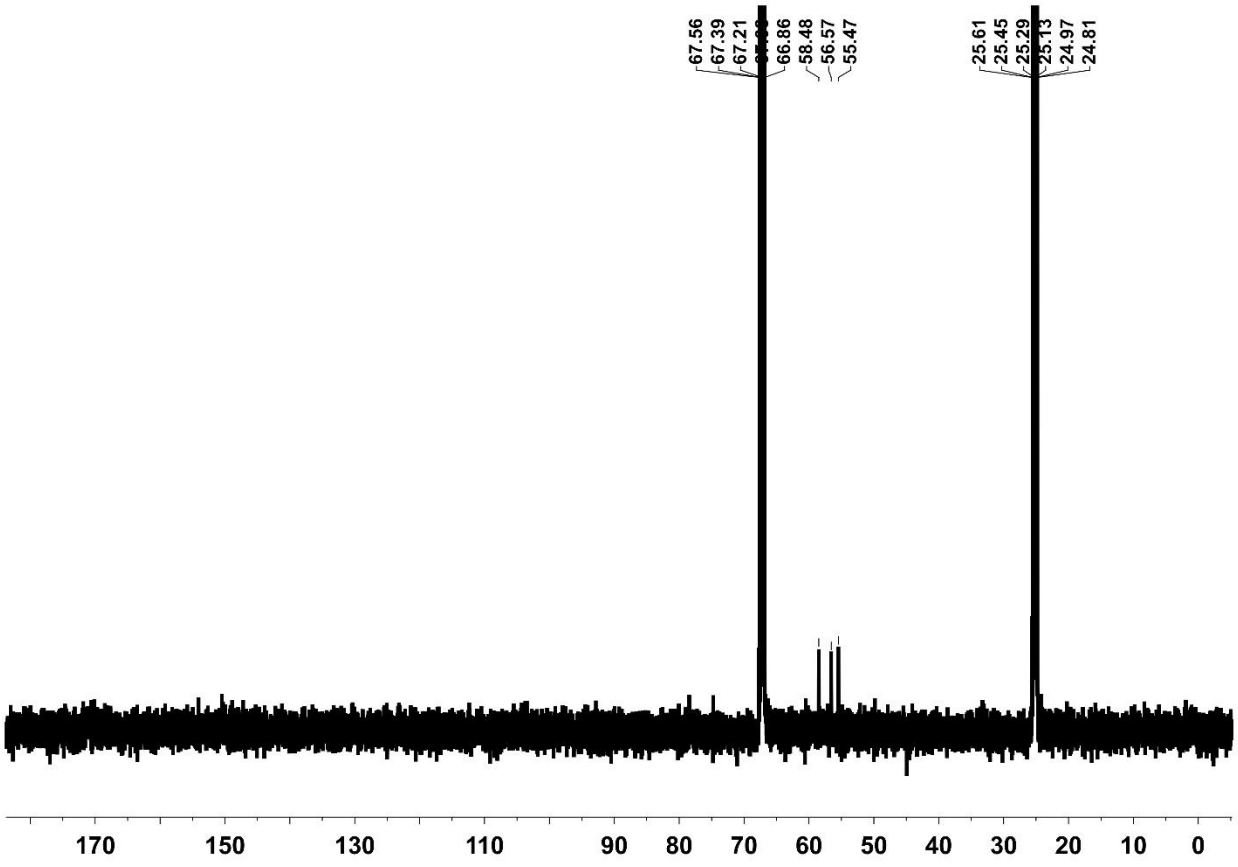

Figure 2-44. ^{13}C NMR spectrum of **compound 7d** in THF-d8

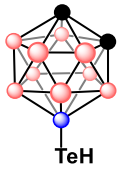

7d

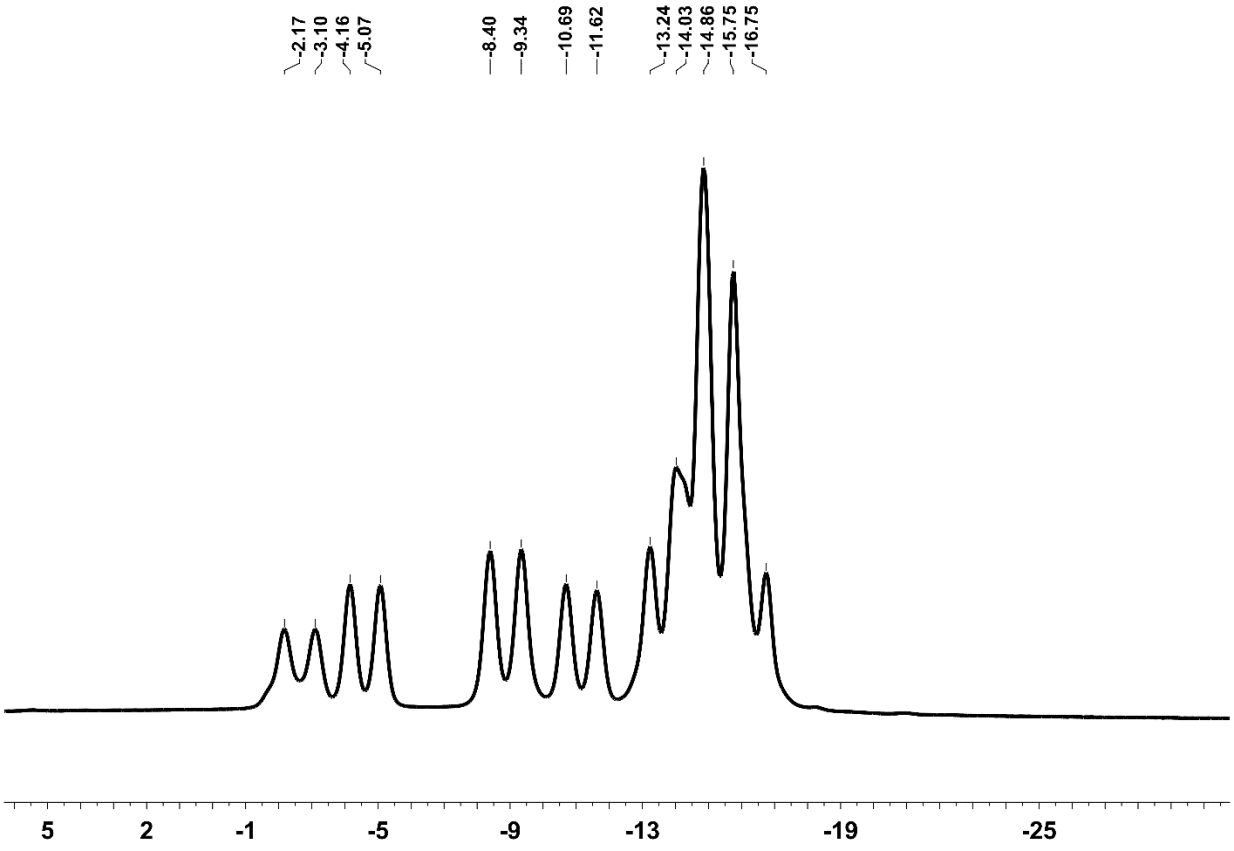

Figure 2-45. ^{11}B NMR spectrum of **compound 7d** in THF-d8

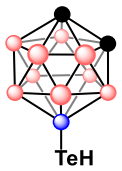

7d

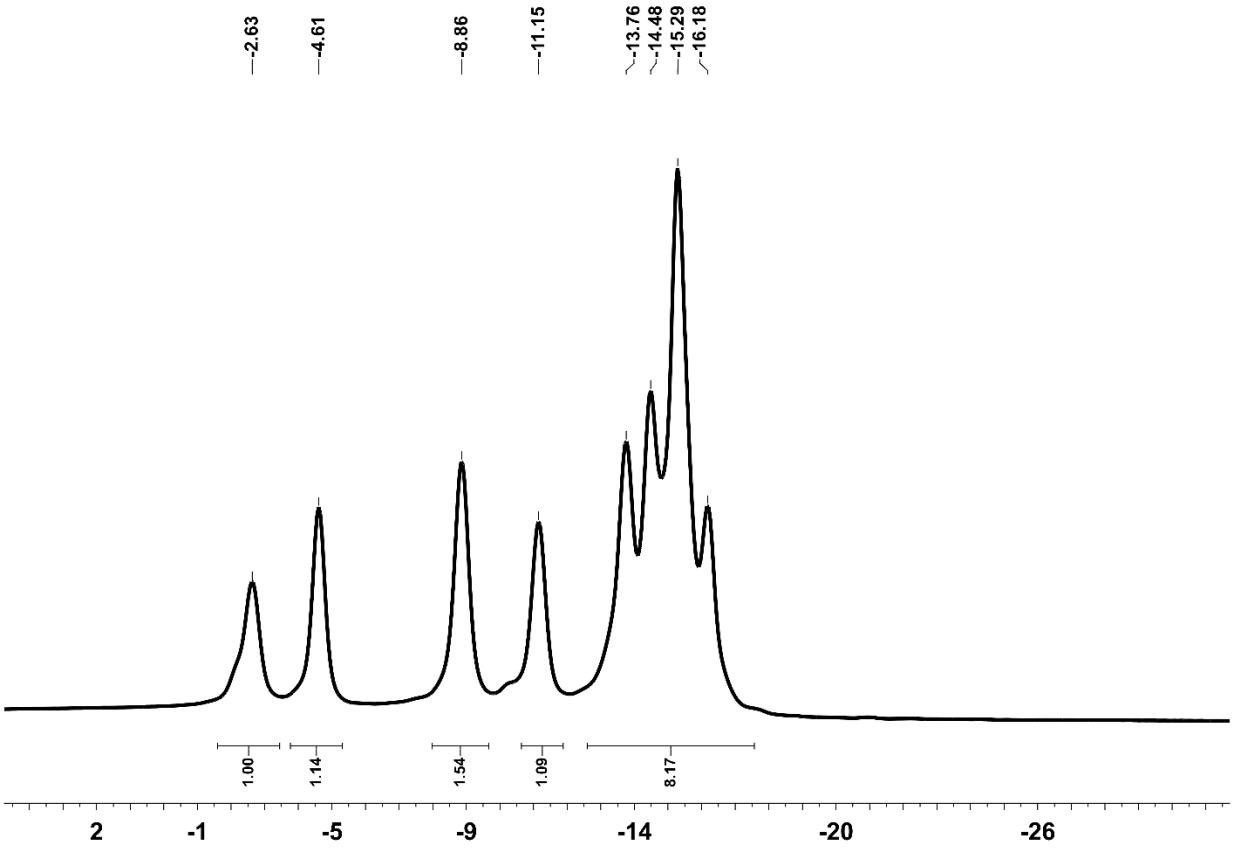

Figure 2-46. $^{11}B\{^{1}H\}$ NMR spectrum of **compound 7d** in THF-d8

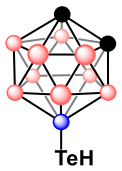

7d

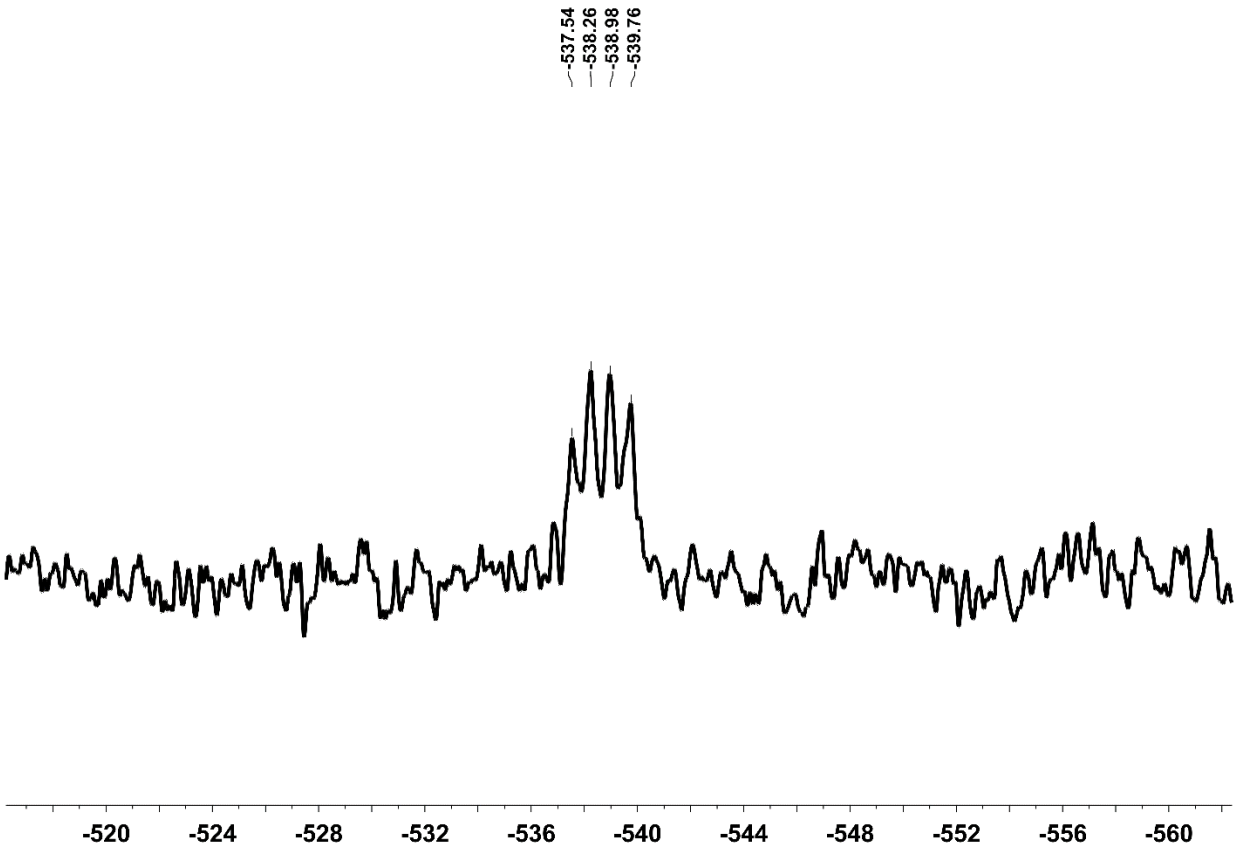

Figure 2-47. ^{125}Te NMR spectrum of **compound 7d** in THF-d8 (Apodization applied; lb = 25 Hz)

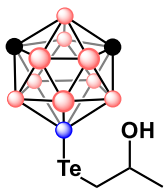

8b

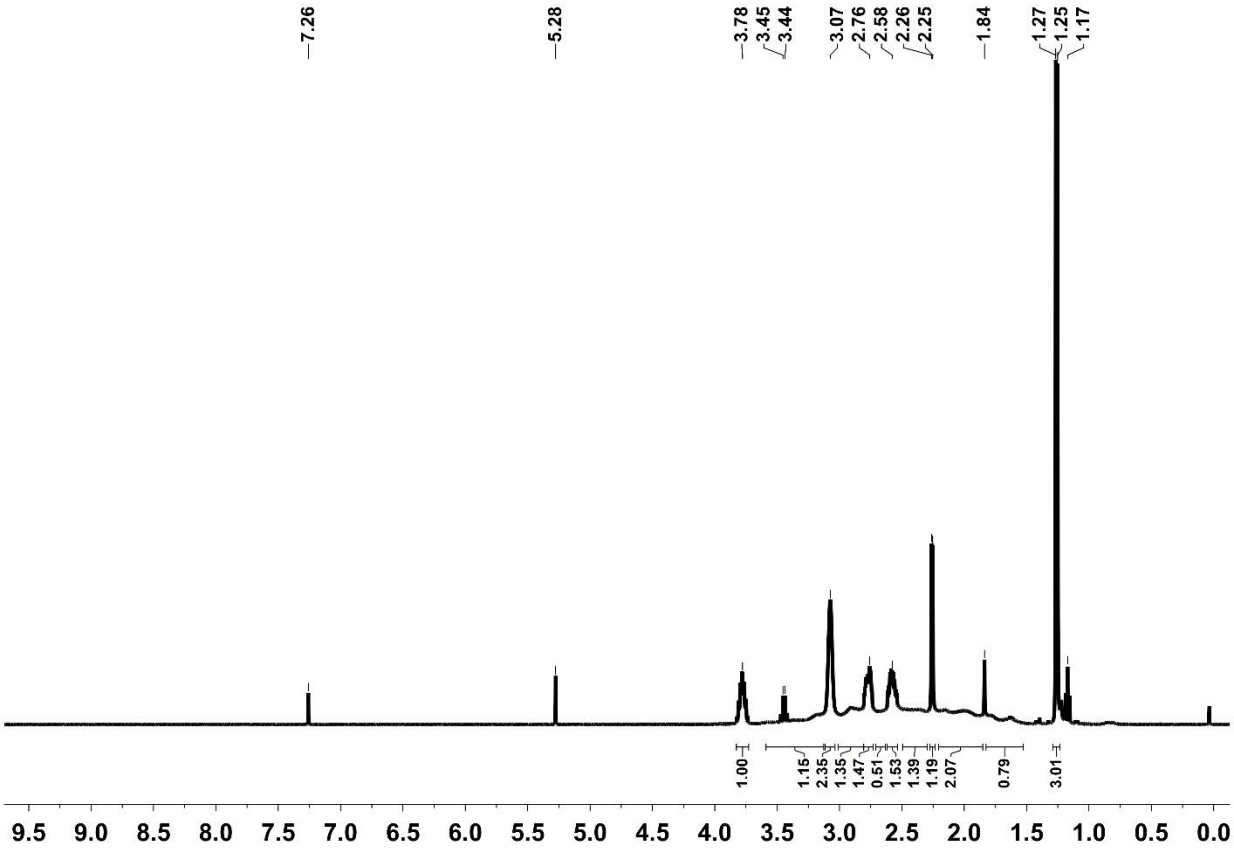

Figure 2-48. ^{1}H NMR spectrum of **compound 8b** in $CDCl_3$

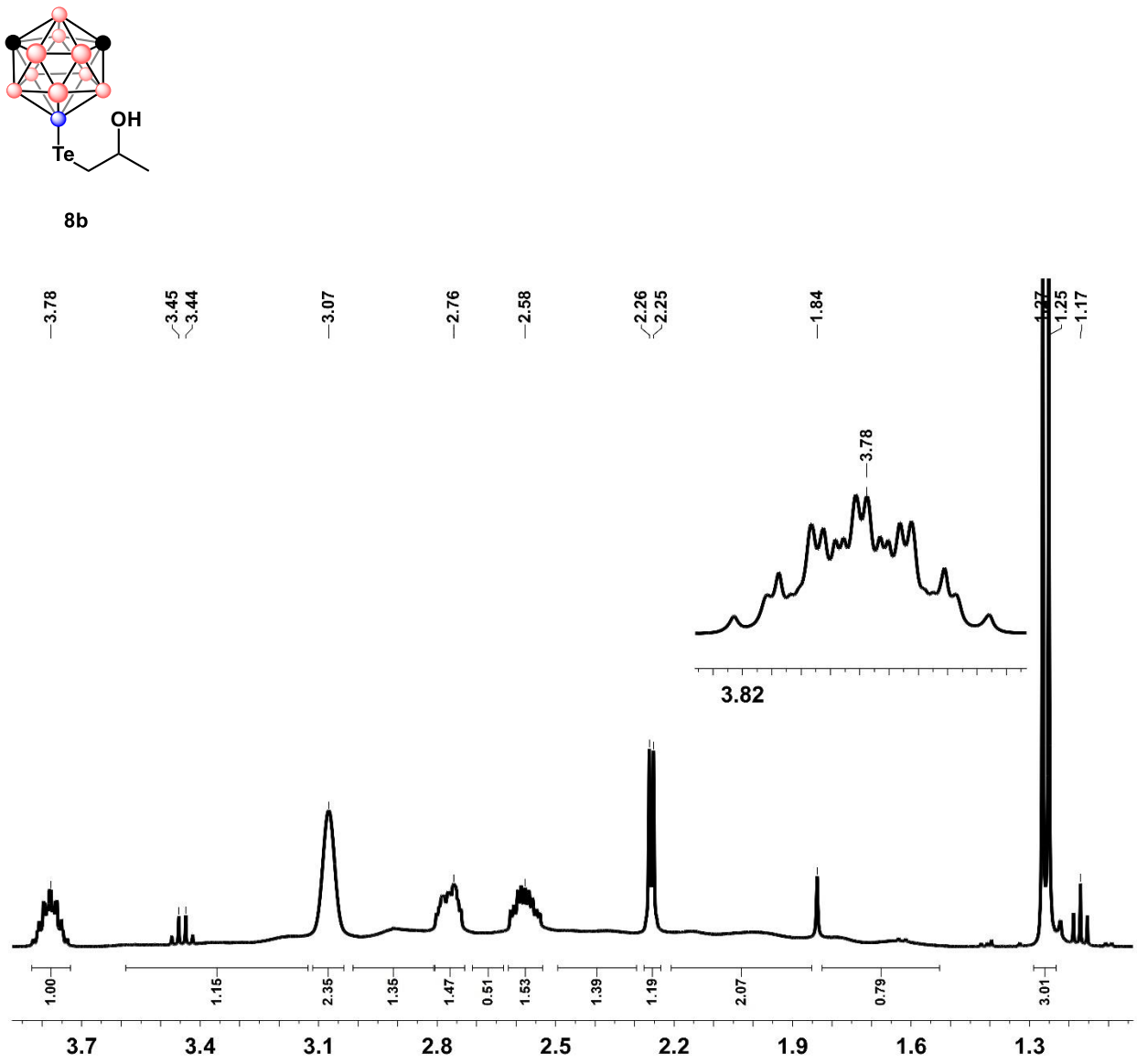

Figure 2-49. Zoomed-in ^{1}H NMR spectrum of **compound 8b** in $CDCl_3$

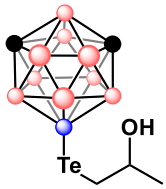

8b

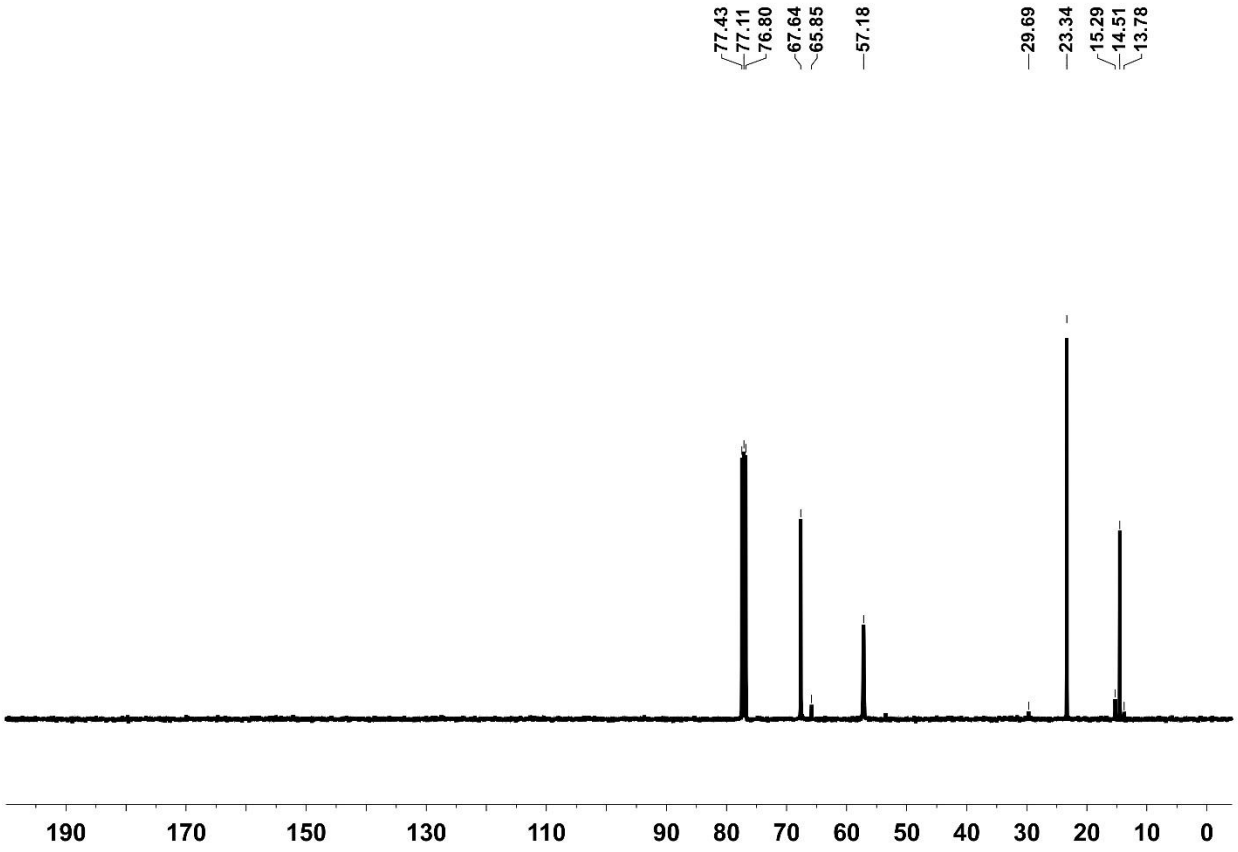

Figure 2-50. ^{13}C NMR spectrum of **compound 8b** in $CDCl_3$

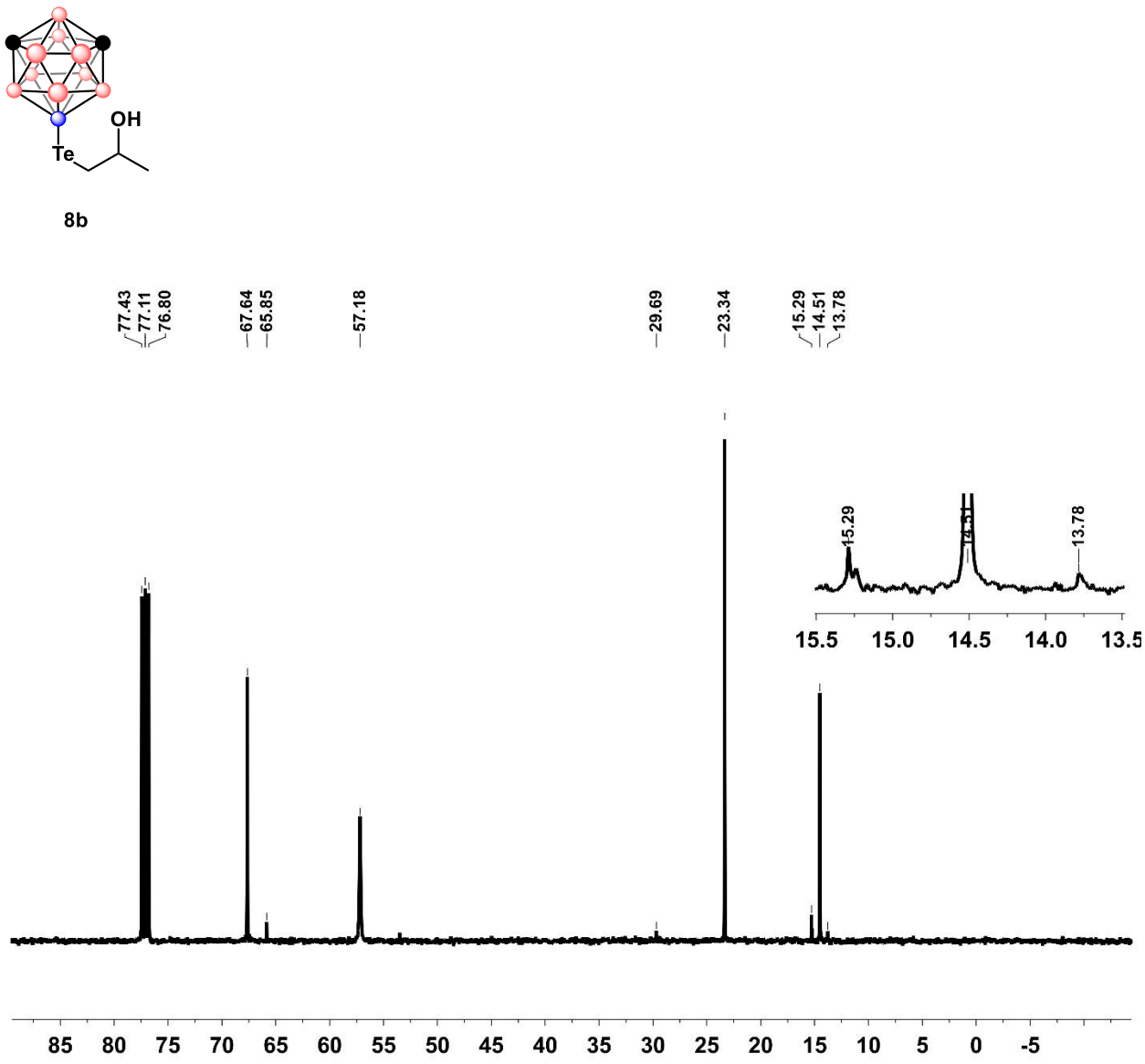

Figure 2-51. Zoomed-in ^{13}C NMR spectrum of **compound 8b** in $CDCl_3$

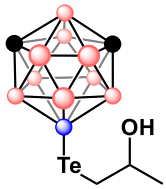

8b

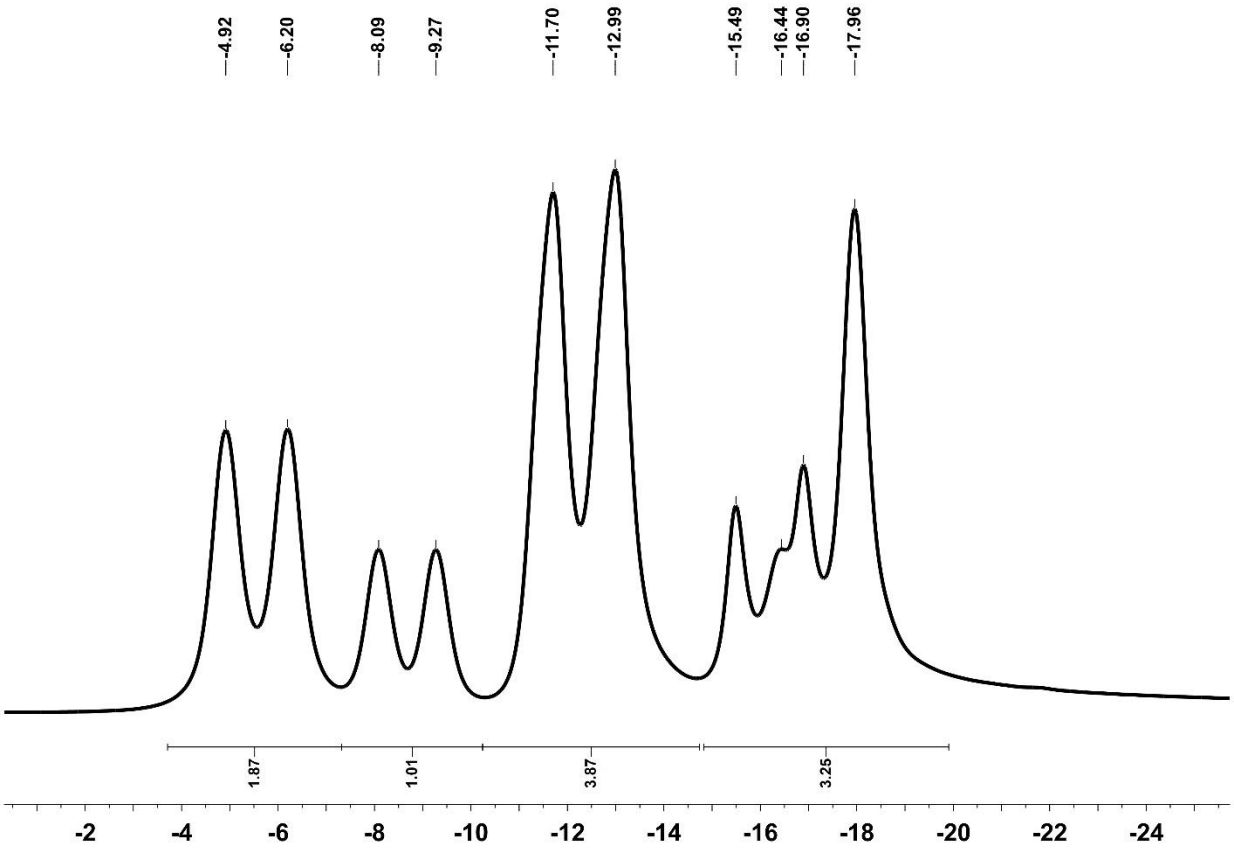

Figure 2-52. ^{11}B NMR spectrum of **compound 8b** in $CDCl_3$

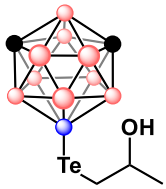

8b

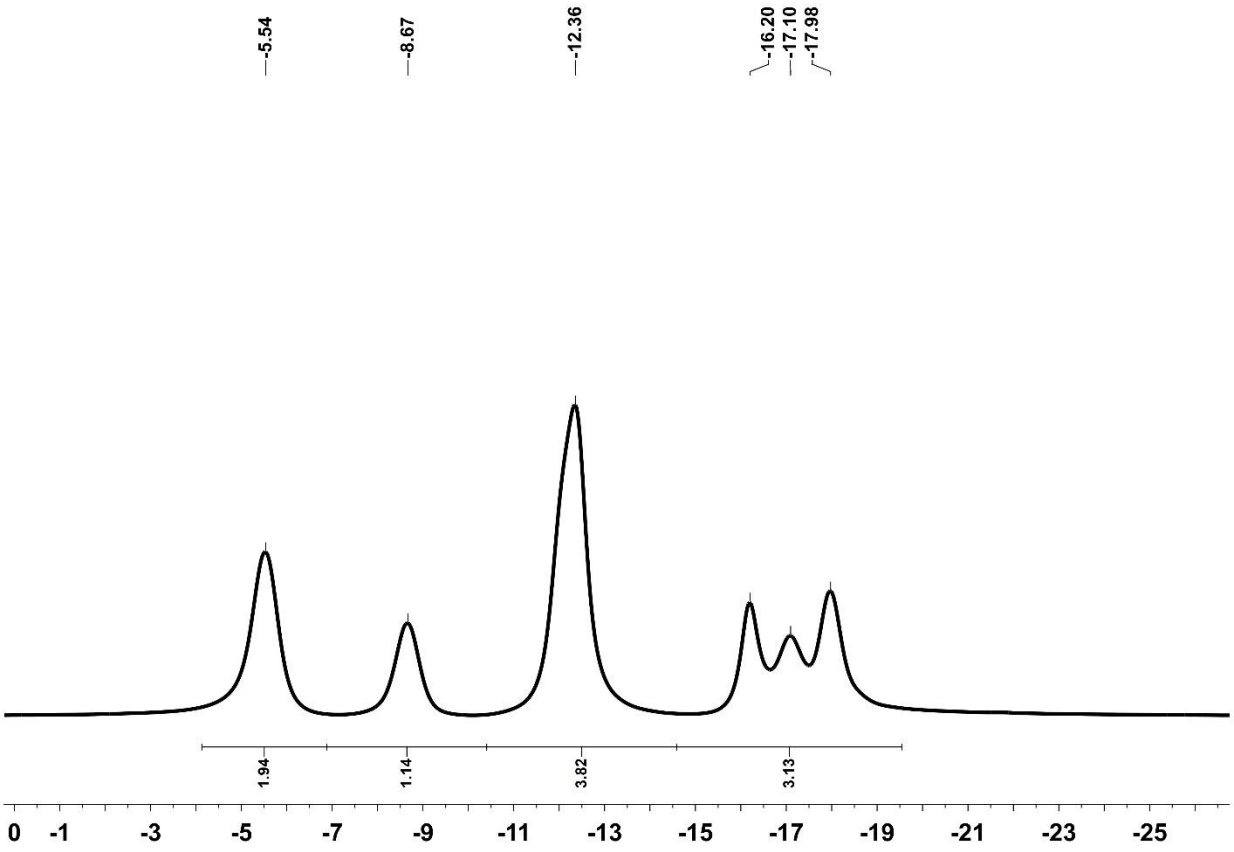

Figure 2-53. $^{11}B\{^{1}H\}$ NMR spectrum of **compound 8b** in $CDCl_3$

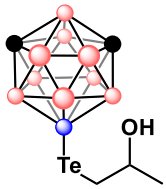

8b

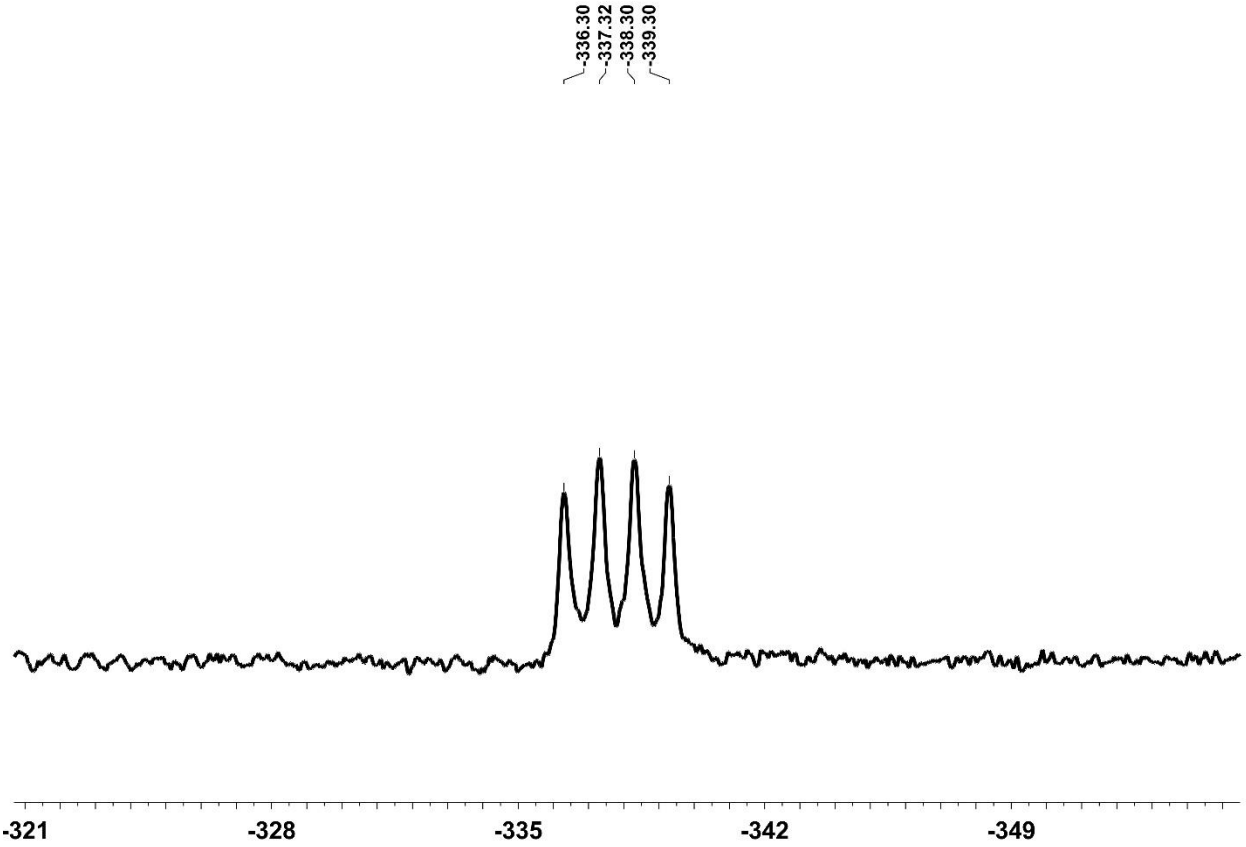

Figure 2-54. ^{125}Te NMR spectrum of **compound 8b** in $CDCl_3$ (Apodization applied; lb = 12 Hz)

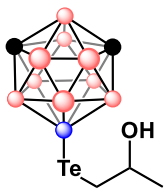

8b

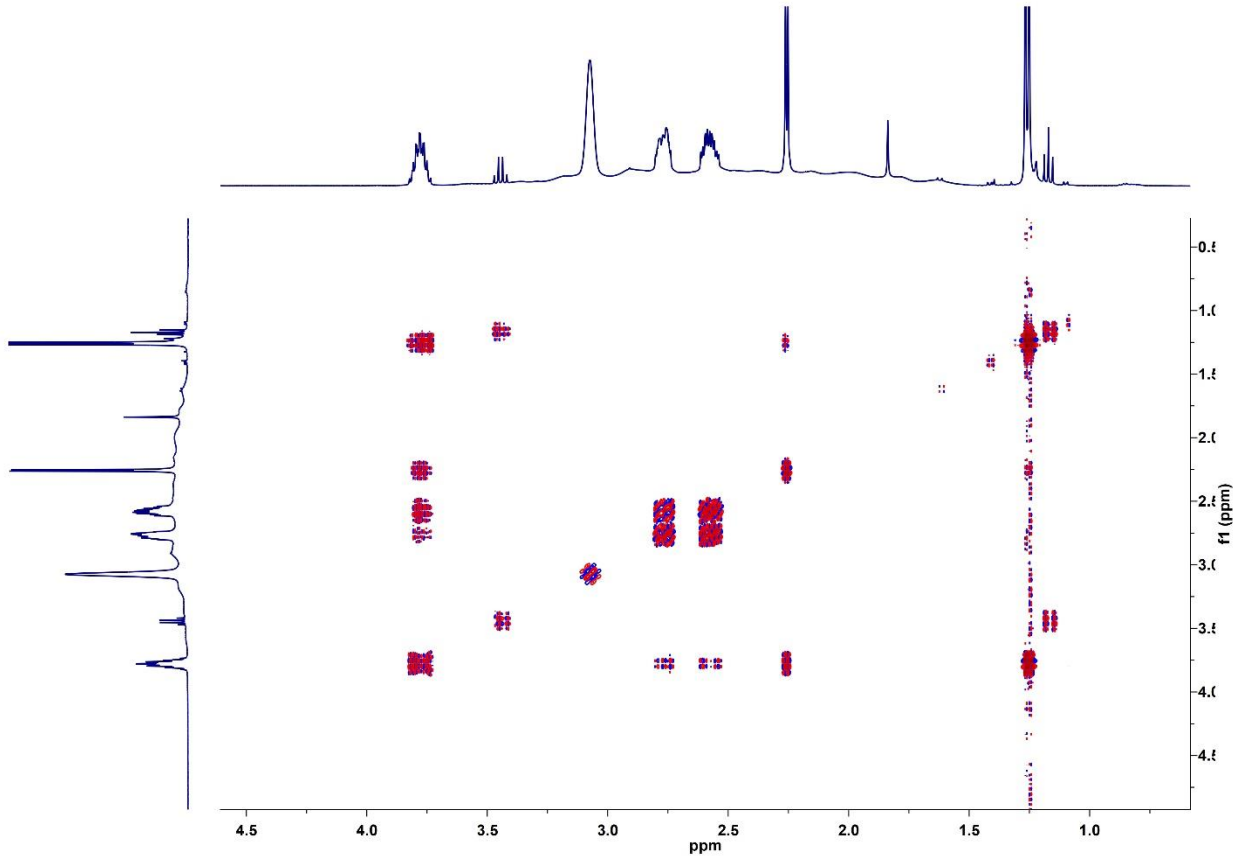

Figure 2-55. ^{1}H-^{1}H COSY NMR spectrum of **compound 8b** in $CDCl_3$

2.3.4. Electrophilic Chemistry of Tellurium-Based Carboranyl Compounds

The product (**compound 9c**) of the lithiation reaction of the bis(9-*meta*-1,7-dimethylcarboranyl) ditelluride (**compound 9a**) was characterized by GCMS (**Figure 2-56**). The product (**compound 9c**) of the lithiation reaction of the (9-*meta*-1,7-dimethylcarboranyl) methyl telluride (**compound 9b**) was characterized by GCMS (**Figure 2-57**). The 9-*meta*-carboranyl tellurinyl (IV) trichloride (**compound 10a**) was characterized by ^{1}H (**Figure 2-58**), ^{13}C (**Figure 2-59**), ^{11}B (**Figure 2-60**), ^{11}B{^{1}H} (**Figure 2-61**), and ^{125}Te (**Figure 2-62**) NMR spectroscopy. The 9-*meta*-carboranyl tellurinyl (IV) tribromide (**compound 10b**) was characterized by ^{1}H (**Figure 2-63**), ^{13}C (**Figure 2-64**), ^{11}B (**Figure 2-65**), ^{11}B{^{1}H} (**Figure 2-66**), and ^{125}Te (**Figure 2-67**) NMR spectroscopy. The product (**compound 11a**) of the reaction of the 9-*meta*-carboranyl tellurinyl (IV) trichloride (**compound 10a**) and phenylacetylene was characterized by ^{125}Te (**Figure 2-68**) NMR spectroscopy. The reduction product of **compound 11a** (**compound 11b**) was characterized by ^{125}Te (**Figure 2-69**) NMR spectroscopy. The product (**compound 12a**) of the reaction of the 9-*meta*-carboranyl tellurinyl (IV) trichloride (**compound 10a**) and norbornene was characterized by ^{125}Te (**Figure 2-70**) NMR spectroscopy. The reduction product of **compound 12a** (**compound 12b**) was characterized by ^{125}Te (**Figure 2-71)** NMR spectroscopy.

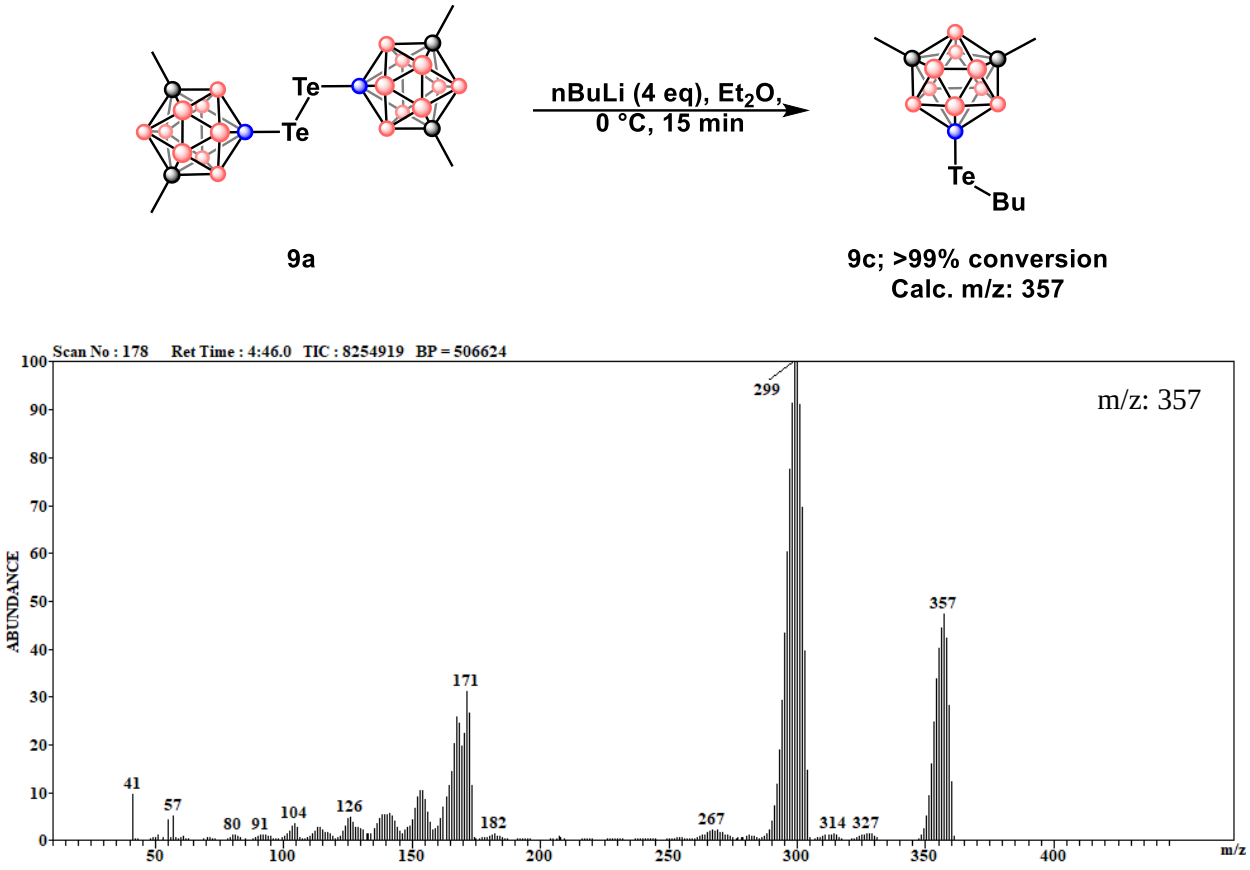

Figure 2-56. GCMS spectrum of **compound 9c** from lithiation of **compound 9a**

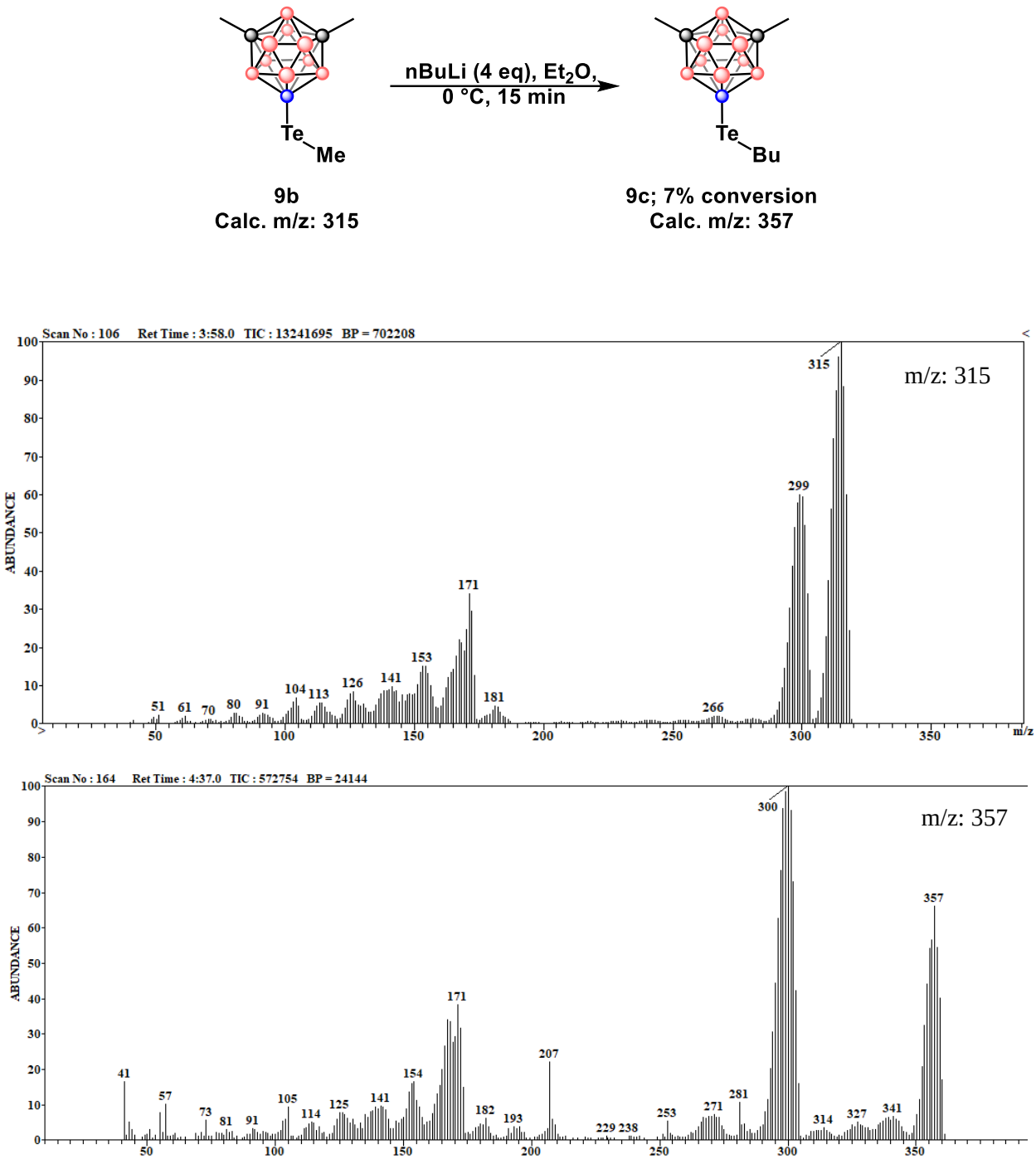

Figure 2-57. GCMS spectrum of **compound 9c** from lithiation of **compound 9b** (Note: the top mass spectrum corresponds to unreacted **compound 9b**)

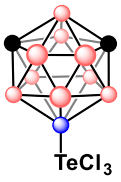

10a

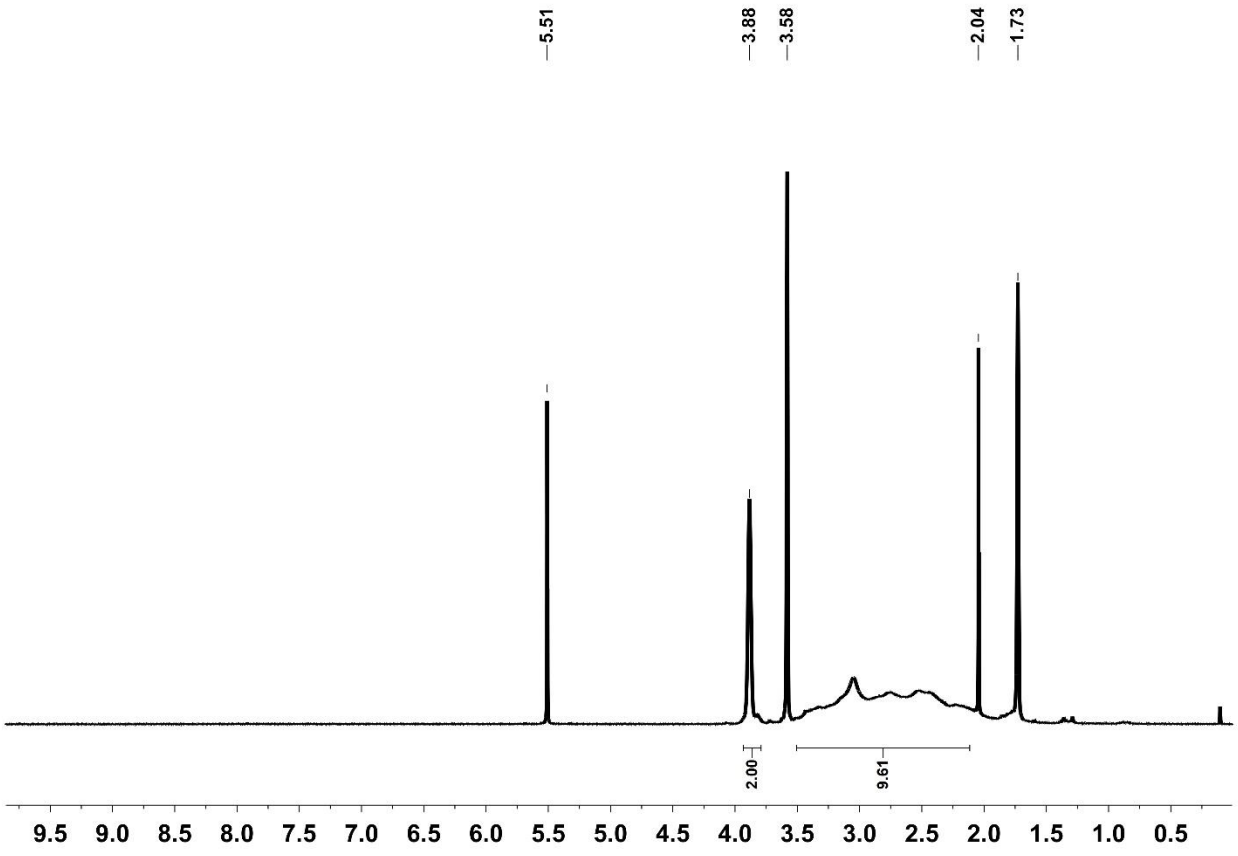

Figure 2-58. ^{1}H NMR spectrum of **compound 10a** in THF-d8

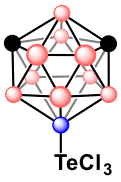

10a

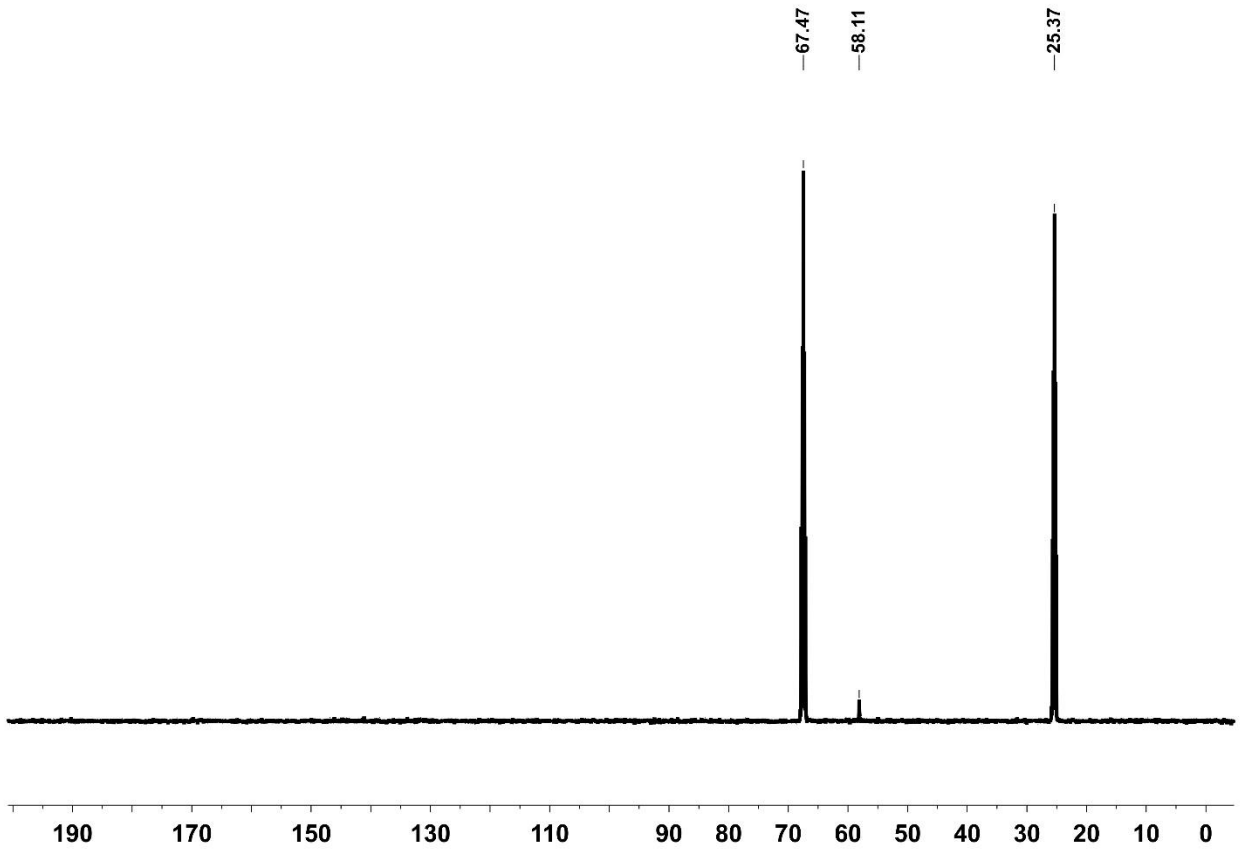

Figure 2-59. ^{13}C NMR spectrum of **compound 10a** in THF-d8

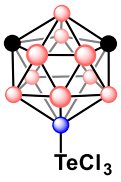

10a

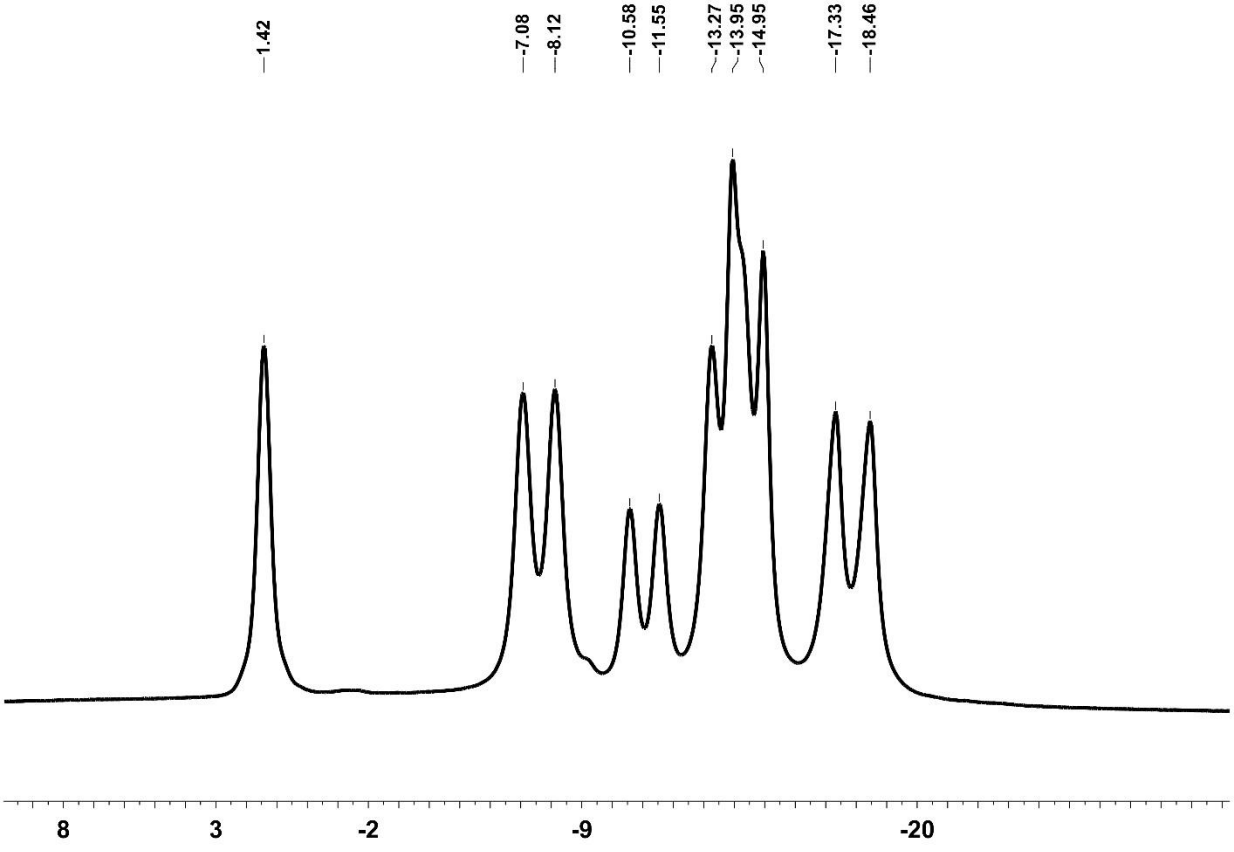

Figure 2-60. ^{11}B NMR spectrum of **compound 10a** in THF-d8

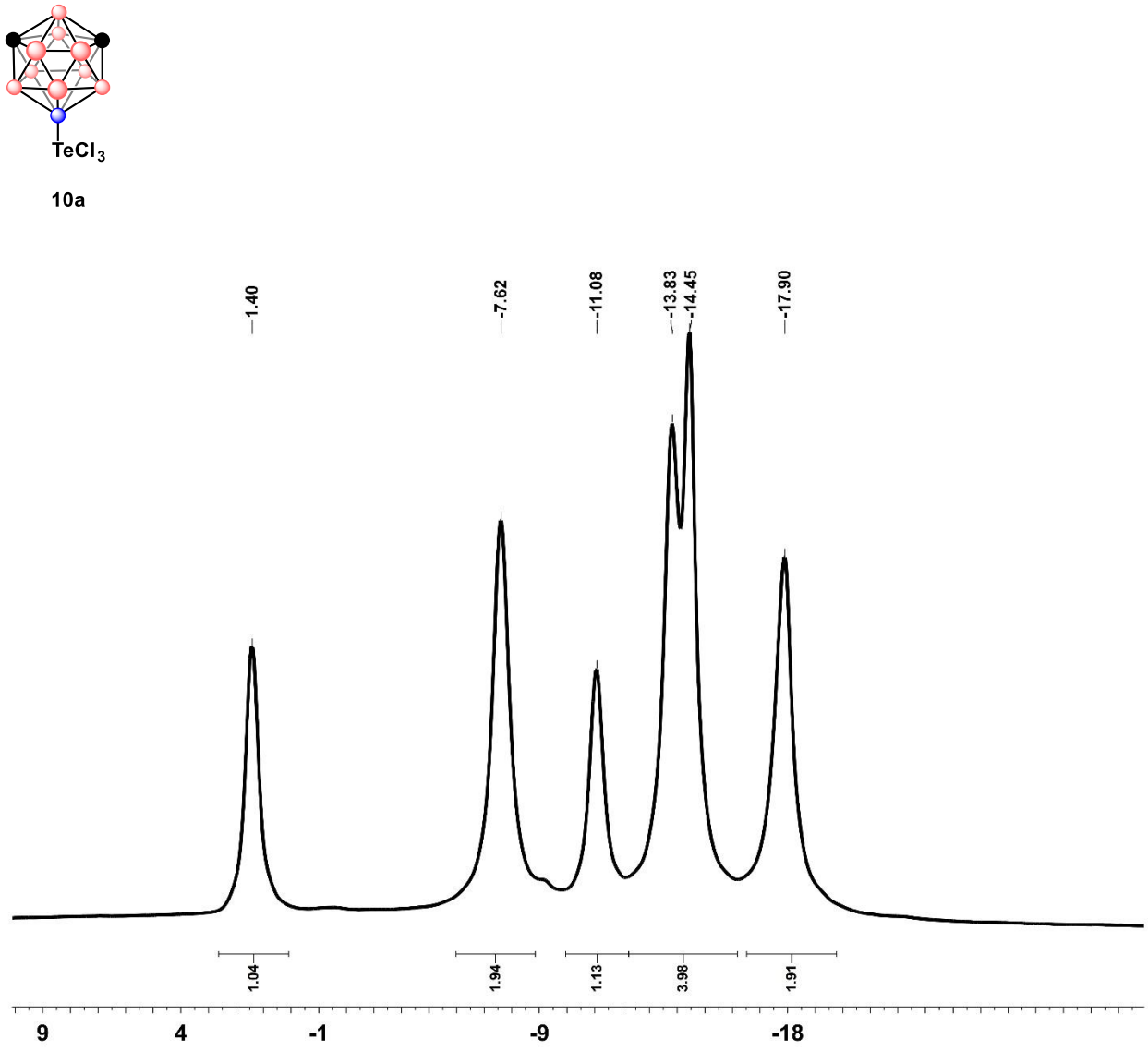

Figure 2-61. $^{11}B\{^{1}H\}$ NMR spectrum of **compound 10a** in THF-d8

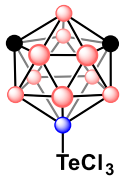

10a

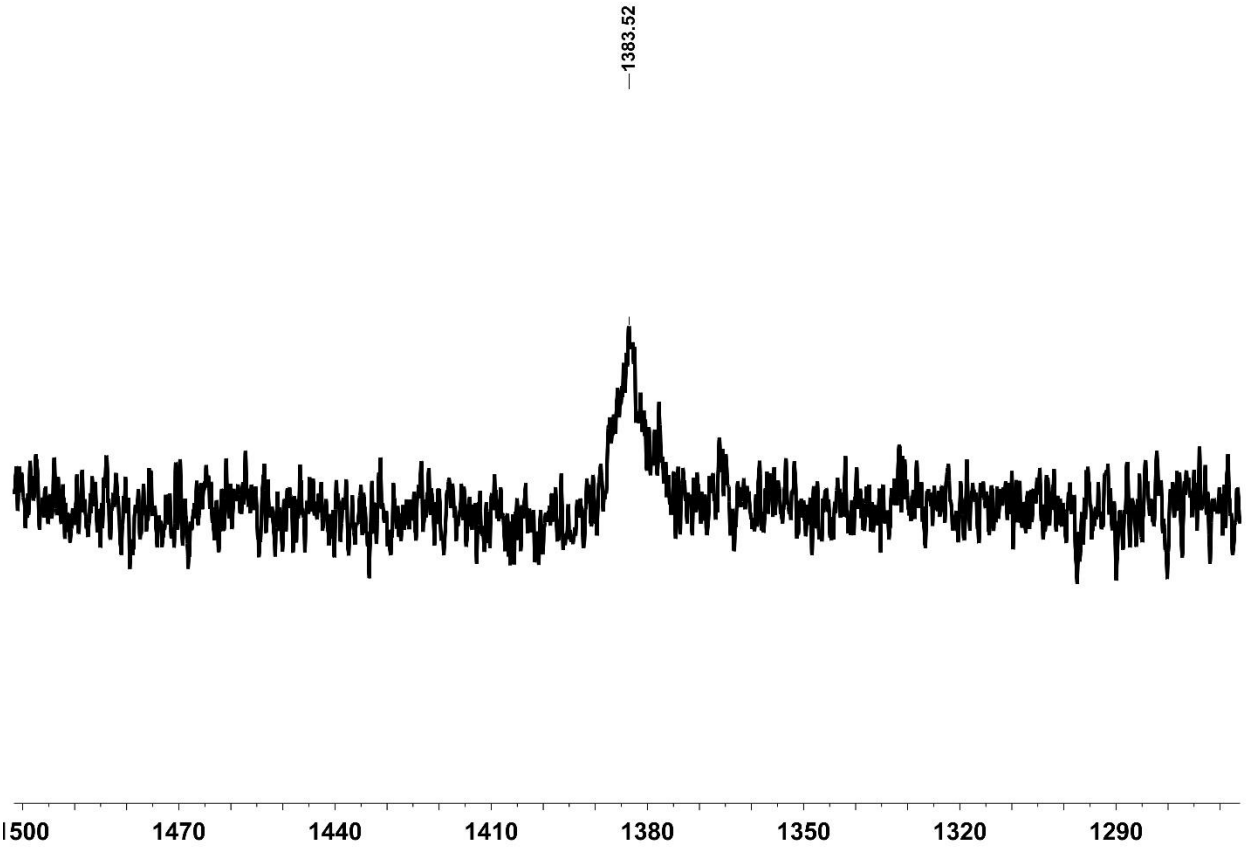

Figure 2-62. ^{125}Te NMR spectrum of **compound 10a** in THF-d8 (Apodization applied; lb = 35 Hz)

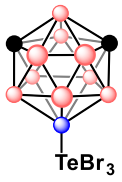

10b

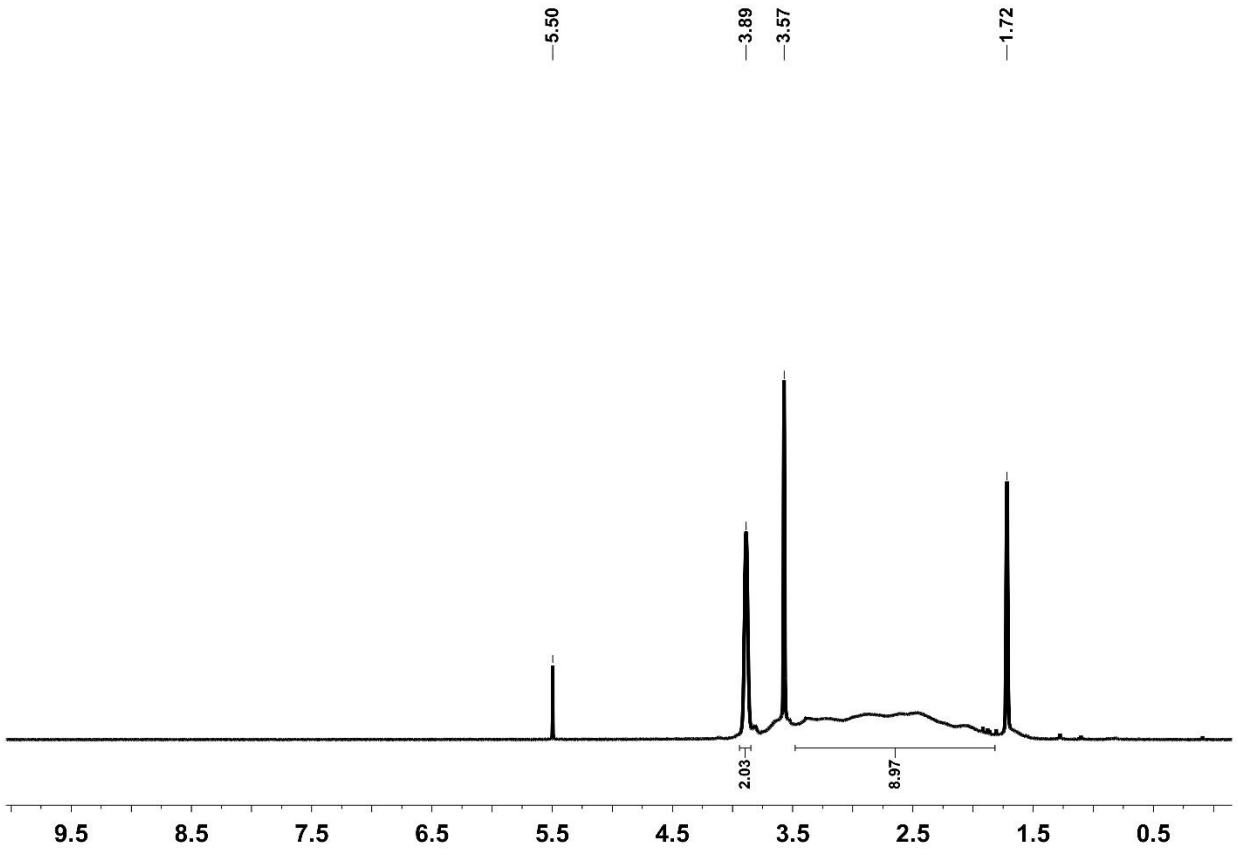

Figure 2-63. ^{1}H NMR spectrum of **compound 10b** in THF-d8

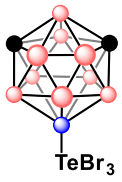

10b

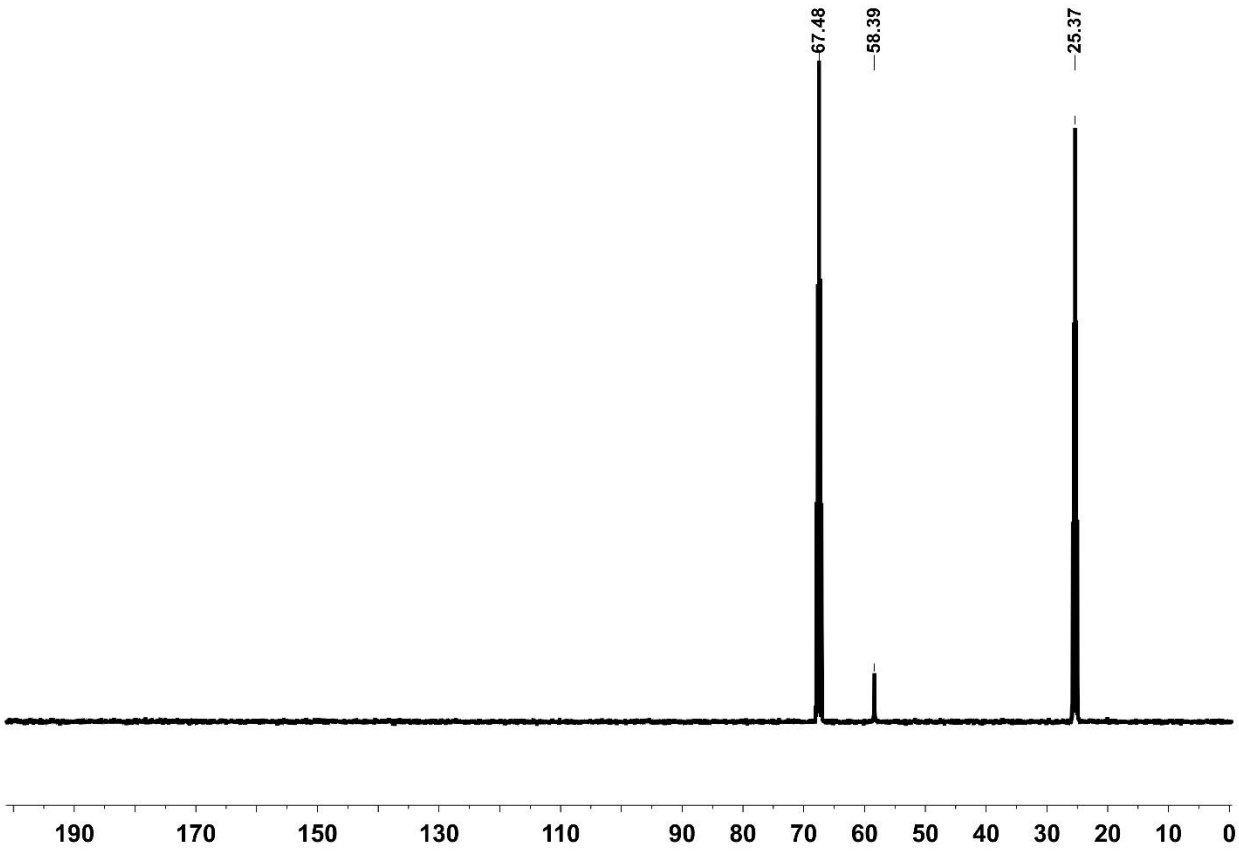

Figure 2-64. ^{13}C NMR spectrum of **compound 10b** in THF-d8

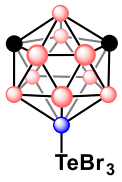

10b

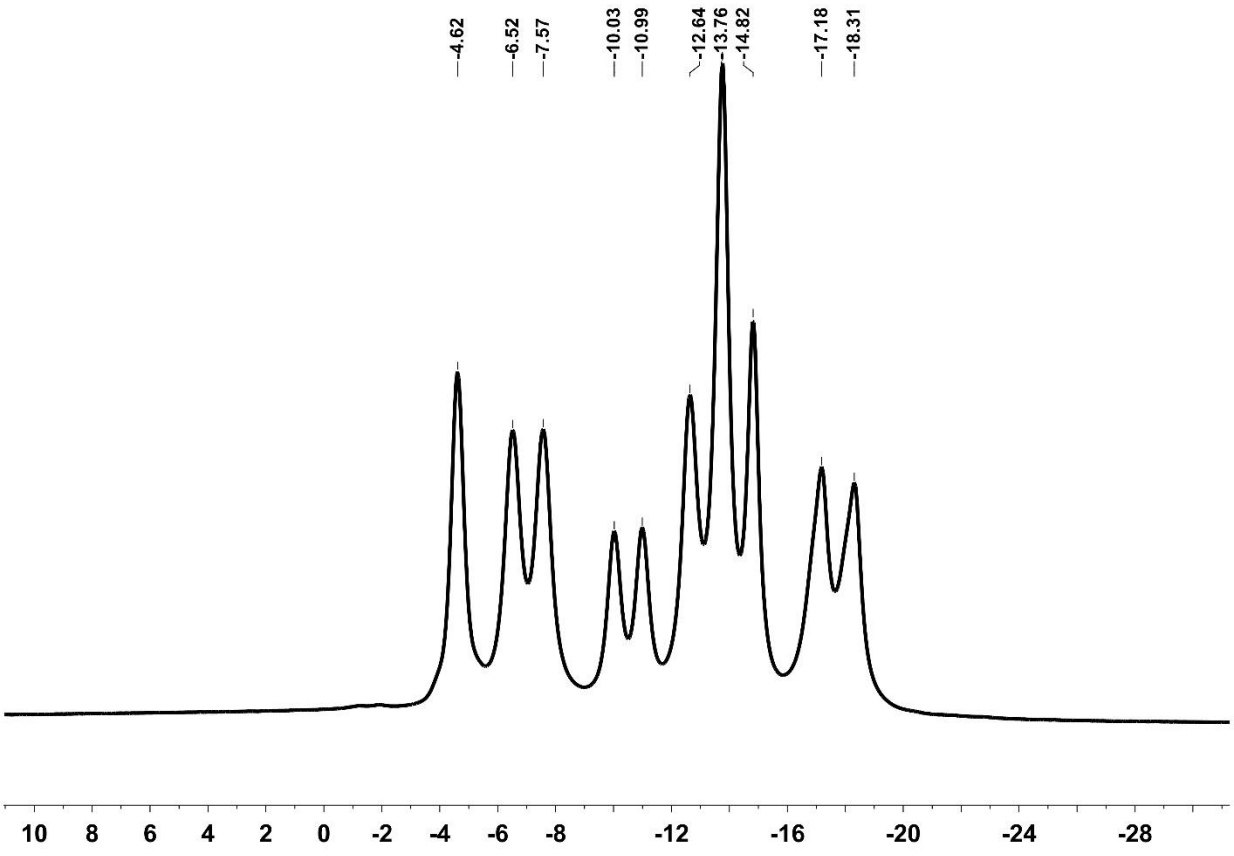

Figure 2-65. ^{11}B NMR spectrum of **compound 10b** in THF-d8

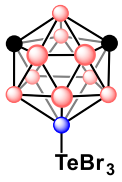

10b

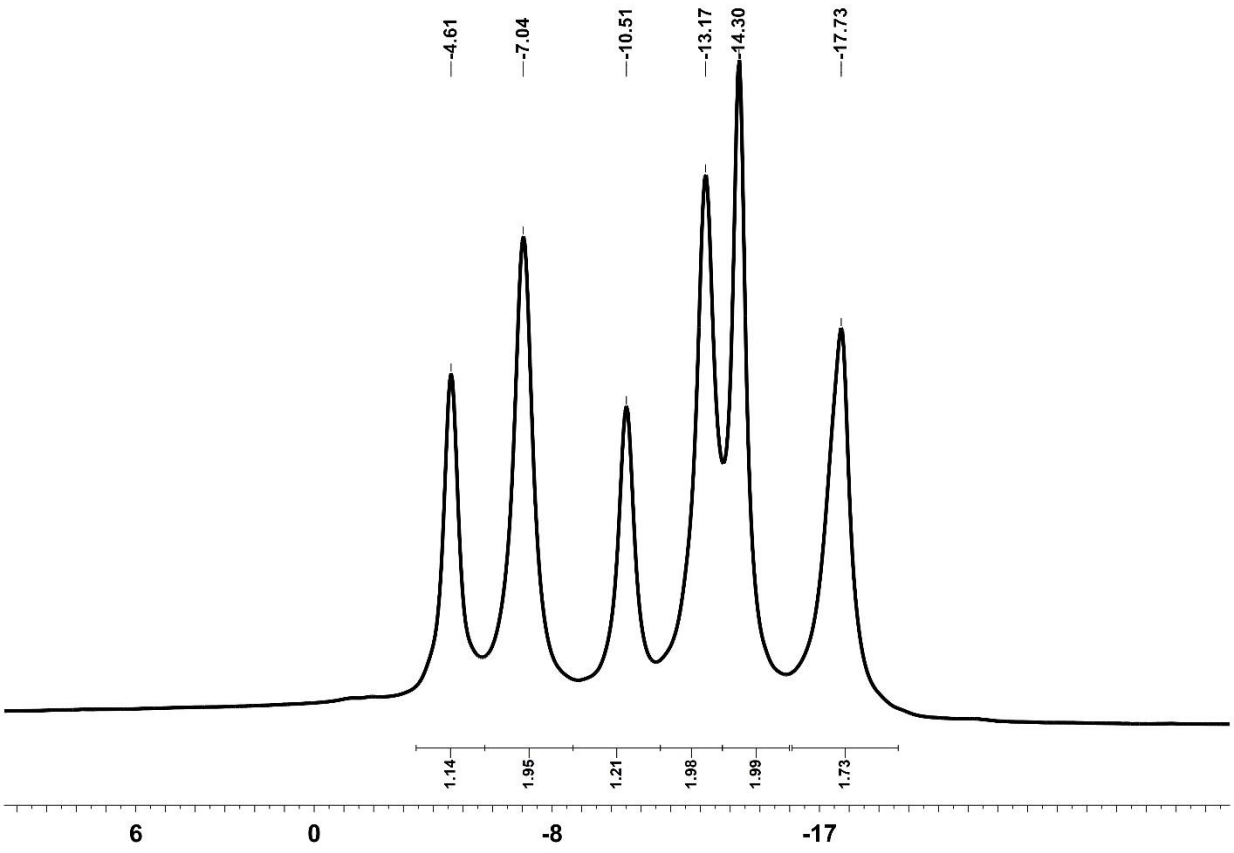

Figure 2-66. $^{11}B\{^{1}H\}$ NMR spectrum of **compound 10b** in THF-d8

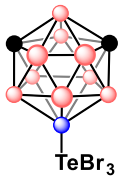

10b

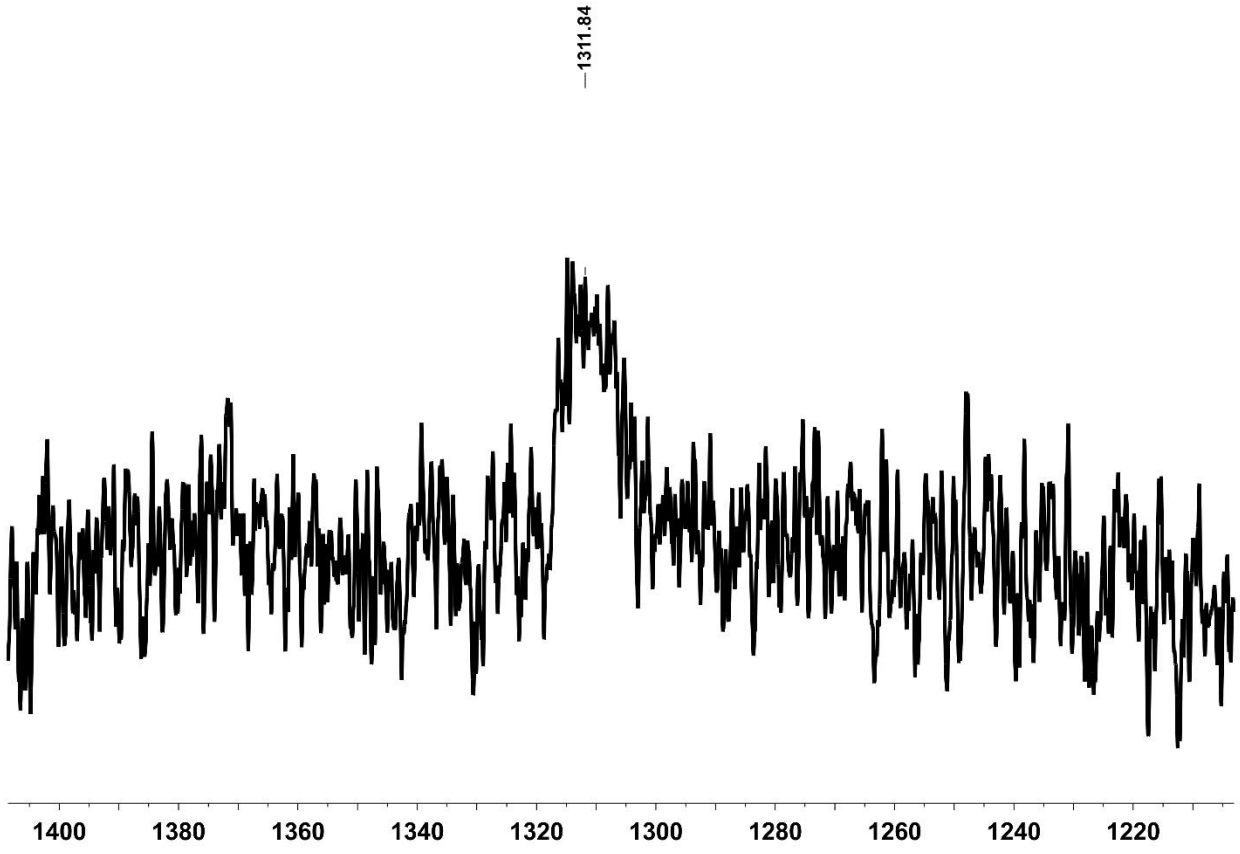

Figure 2-67. ^{125}Te NMR spectrum of **compound 10b** in THF-d8 (Apodization applied; lb = 50 Hz)

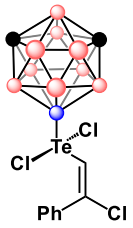

11a

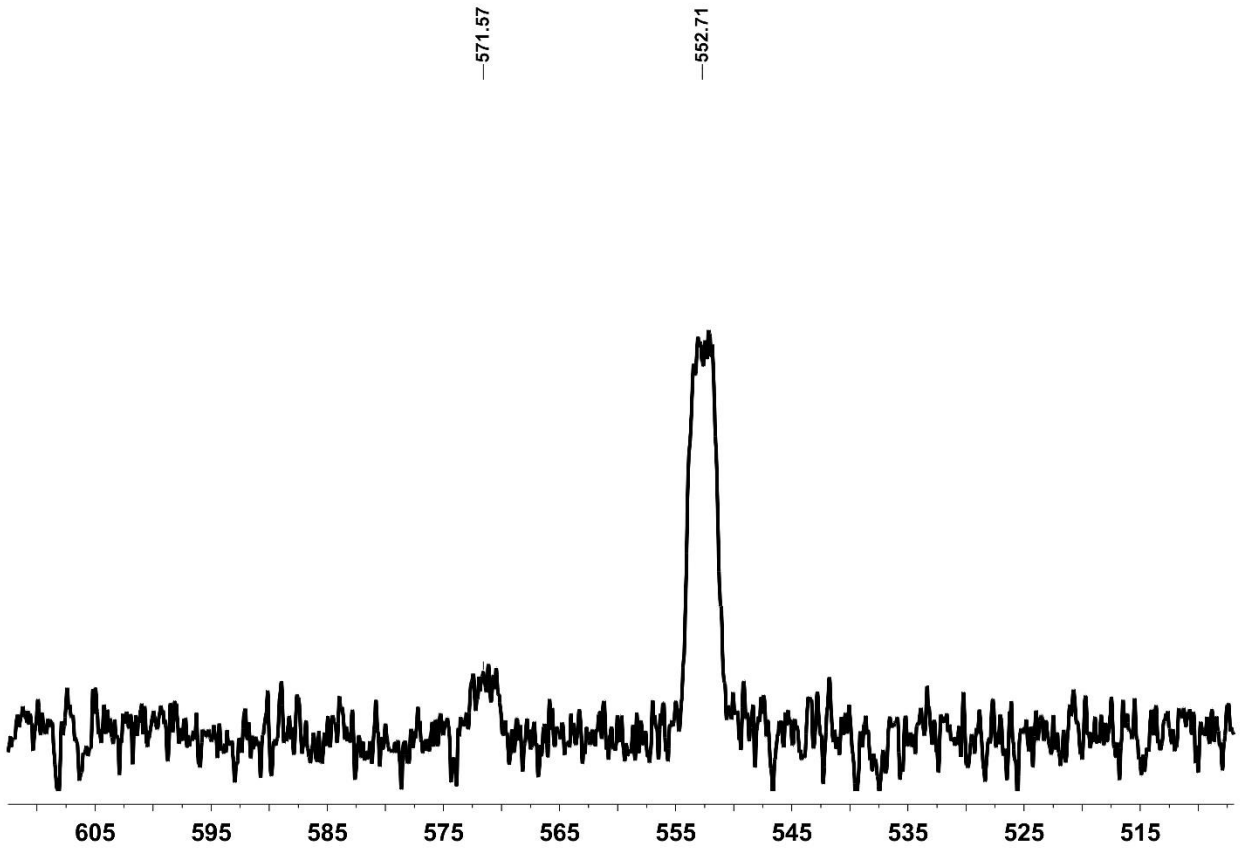

Figure 2-68. ^{125}Te NMR spectrum of **compound 11a** in $CDCl_3$ (Apodization applied; lb = 25 Hz)

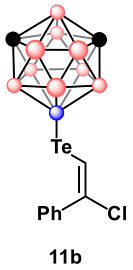

11b

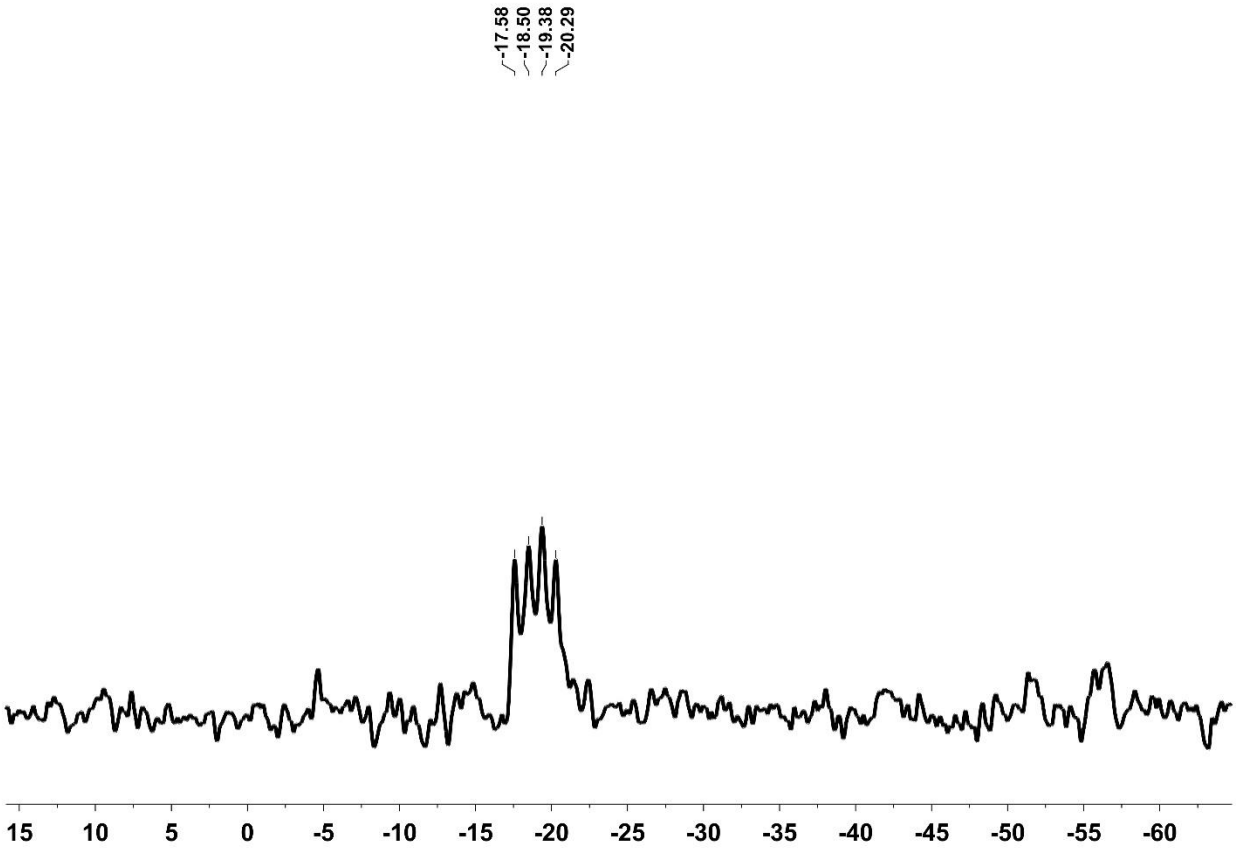

Figure 2-69. ^{125}Te NMR spectrum of **compound 11b** in $CDCl_3$ (Apodization applied; lb = 45 Hz)

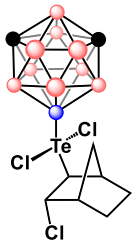

12a

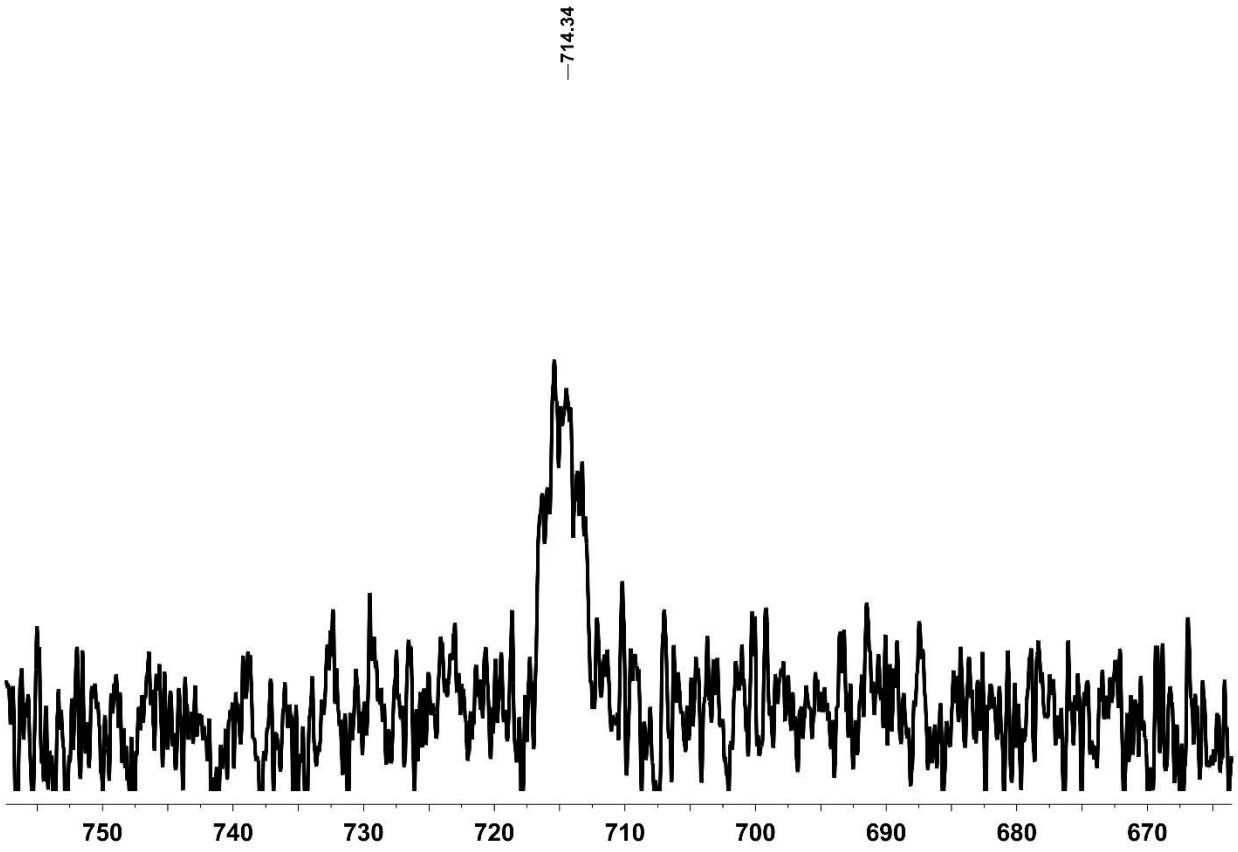

Figure 2-70. ^{125}Te NMR spectrum of **compound 12a** in $CDCl_3$ (Apodization applied; lb = 25 Hz)

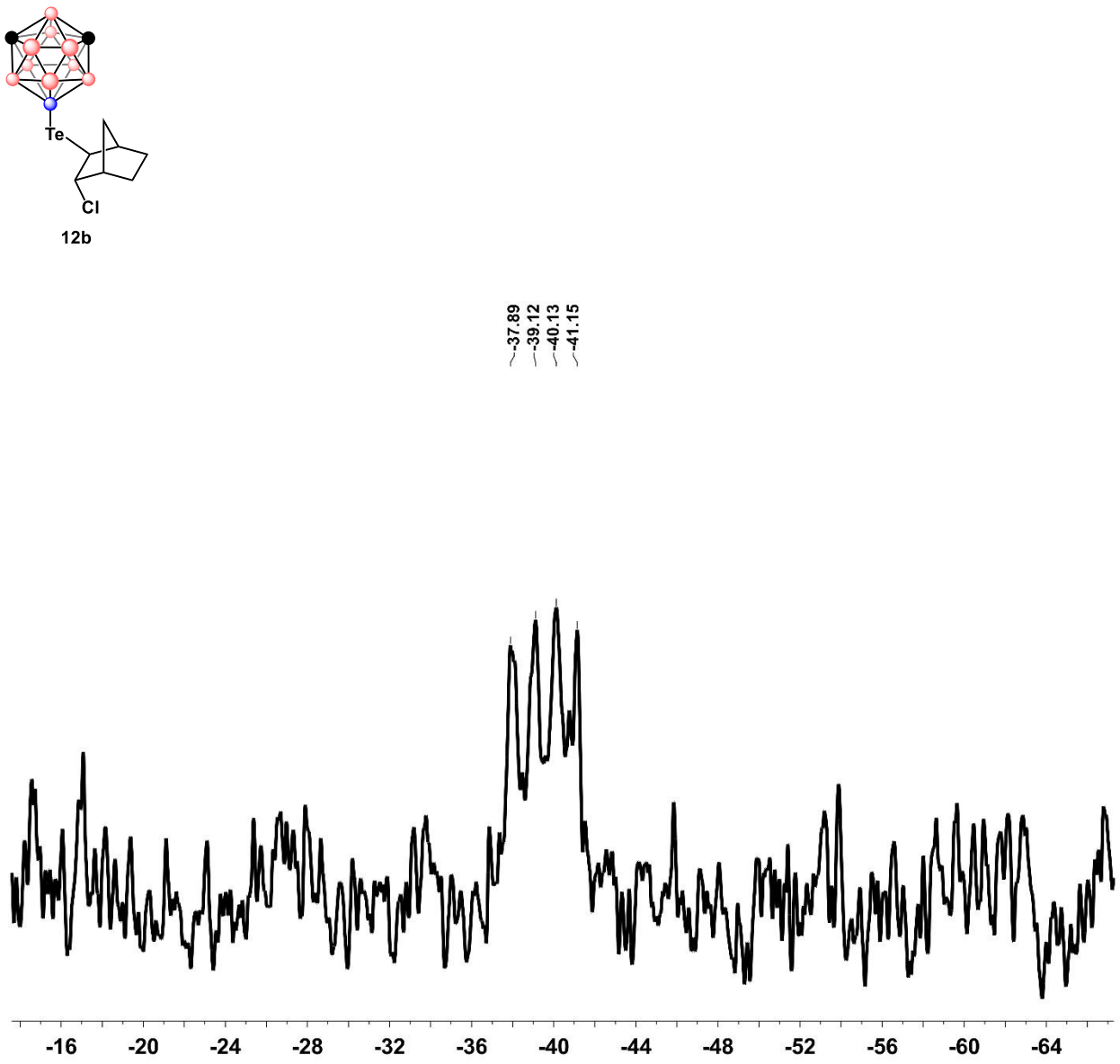

Figure 2-71. ^{125}Te NMR spectrum of **compound 12b** in $CDCl_3$ (Apodization applied; lb = 25 Hz)

2.4. Conclusion and Future Steps

In this chapter, I discussed the synthesis of various Se- and Te-functionalized carborane reagents at the B(9) position. The nucleophilic and electrophilic reactivity of these reagents was studied in a series of reactions. This work is part of a manuscript in preparation, and further work remains to be done in fully characterizing the results and expanding the scope of reactivity.

2.5. Methods

2.5.1. General Considerations

Meta- and *ortho*-$C_2B_{10}H_{12}$ (Katchem, Alfa Aesar) were used as is. Dry solvents were obtained from a Solvent Purification System (SPS). All reactions were carried out under ambient conditions (unless otherwise noted) and light was minimized when possible (fume hood light was off during all manipulations). Deuterated solvents were purchased from Cambridge Isotope Laboratories and used as is. All other reagents and solvent were purchased from commercial vendors and used as is. Plastic-backed Baker-flex Silica Gel IB2-F TLC plates were used for thin layer chromatography. SiliaFlash® G60 60-200 um (70-230 mesh) purchased from Silicycle was used for flash chromatography. TLC samples for carborane-containing compounds were stained with 1 wt. % $PdCl_2$ in 6M HCl and developed with heat.

Compounds 4a, 5a, 6a, 8a, and 9a were prepared by Harrison Mills according to modified reported procedures (see acknowledgements section) and used as is. Detailed protocols for these compounds can be found in a separate dissertation as well as a manuscript in preparation.

2.5.2. Instrumentation

^{1}H, ^{13}C, ^{11}B, and $^{11}B\{^{1}H\}$ NMR spectra were recorded on a Bruker AV400 spectrometer while ^{77}Se and ^{125}Te NMR spectra were recorded on a Bruker DRX 500 spectrometer. MestReNova software was used to process all NMR data. ^{1}H and ^{13}C spectra were referenced to residual solvent resonances in deuterated solvents and are reported relative to tetramethylsilane (δ = 0 ppm). ^{11}B and $^{11}B\{^{1}H\}$ spectra were referenced to $BF_3{\cdot}Et_2O$ as an external standard (δ = 0 ppm). ^{77}Se spectra were referenced to Ph_2Se_2 as an external standard (δ = 463.15 ppm). ^{125}Te spectra were referenced to Ph_2Te_2 in THF as an external standard (δ = 408 ppm). Gas

Chromatography Mass Spectrometry (GCMS) measurements were collected on an Agilent 6890-5975 GCMS.

2.5.3. Nucleophilic Chemistry of Selenium-Based Carboranyl Compounds

2.5.3.1. Synthesis of compound 4b

An oven-dried 50 mL Schlenk flask was charged with *ortho*-carborane (1.44 g; 10 mmol) and $AlCl_3$ (1.33 g; 10 mmol) and degassed. The solids were then dissolved in 25 mL of dry DCM, and Se_2Cl_2 (0.42 mL; 5 mmol) was slowly added to the stirring solution under steady flow of nitrogen. The reaction mixture was allowed to stir overnight, and then subsequently quenched slowly with water and extracted with DCM. The organic fractions were combined, dried with Na_2SO_4, filtered, and then dried *in vacuo*. The product was then resuspended in 30 mL of anhydrous EtOH and $NaBH_4$ (0.8 g; 21 mmol) was added under vigorous stirring for 15 minutes (until the solution turns clear and colorless). The reaction was then diluted with 100 mL of water and filtered to remove any solids. The solution was then acidified with 6M HCl until no precipitate appears (caution, the reaction mixture smells foul after this step) and the solids were collected through filtration and ran through a silica pad eluted with DCM. Finally, the selenol product was purified through sublimation at 105 ˚C to obtain 0.410 g of product (18.4% yield).

2.5.3.2. Synthesis of compound 5b

Compound 5a (67 mg; 0.15 mmol) was degassed and stirred in 1 mL of anhydrous EtOH in a 16x125 mm reaction tube equipped with a septum under a steady flow of nitrogen, while minimizing light exposure. $NaBH_4$ (50 mg; 1.35 mmol) was quickly added and the mixture was stirred for 15 minutes until it became colorless, after which propylene oxide

(42 μL; 0.6 mmol) was quickly pipetted into the reaction and the mixture was left to stir overnight under a static nitrogen atmosphere. The reaction was then diluted with 3 mL of water and 2 mL of 1M HCl was slowly added. The mixture was extracted with Et_2O and the combined organic fractions were dried with Na_2SO_4 and purified via flash column chromatography (eluted with DCM) to yield 71 mg of selenoether in 84.5% yield.

2.5.4. Electrophilic Chemistry of Selenium-Based Carboranyl Compounds

2.5.4.1. General considerations for synthesis of compounds 6b, 6c

To a stirring solution of **compound 6a** (13 mg; 0.05 mmol) in 0.75 mL of dry DCM substrate (6b: 5.84 μL, 0.05 mmol; 6c: 6.61 μL; 0.05 mmol) was added, and the reaction was left to stir overnight. The reaction mixture was then ran through a quick silica plug and analyzed by GCMS.

2.5.5. Nucleophilic Chemistry of Tellurium-Based Carboranyl Compounds

2.5.5.1. Synthesis of compound 7a

An oven-dried 100 mL Schlenk flask was charged with $TeCl_4$ (1.347 g; 5 mmol) in a glovebox, and then with 25 mL of dry DCM. *Ortho*-carborane (720 mg; 5 mmol) and $AlCl_3$ (1.33 g; 10 mmol) were degassed in a separate vial and added to the stirring reaction mixture under a steady flow of nitrogen. The mixture was stirred at 35 ˚C for 6 hours and left to cool to room temperature overnight, after which the solvent was removed *in vacuo* and the mixture was resuspended in 75 mL of anhydrous EtOH. $Na_2S{\cdot}9H_2O$ (1.2 g; 5 mmol) was added and the mixture was stirred for 4 hours. After checking the reaction for completion by TLC (1:3 DCM:Hexanes), another 600 mg of $Na_2S{\cdot}9H_2O$ were added and the reaction was stirred overnight. Then, the reaction was poured into 100 mL of water and extracted with Et_2O. The mixture was then filtered to remove any solids and the

solvent was removed from the organic fractions *in vacuo* to yield the crude product. The product was then recrystallized overnight by dissolving in around 11 mL of benzene and layered with 45 mL of hexanes in a 50 mL Erlenmeyer flask to yield 1 g of dark red powder in 74% yield.

2.5.5.2. Synthesis of compound 7b

An oven-dried 25 mL Schlenk flask was charged with **compound 7a** (270 mg; 0.5 mmol) and then degassed, after which 10 mL of anhydrous EtOH was added to dissolve the powder. To the stirring solution under a steady flow of nitrogen $NaBH_4$ (70 mg; 1.88 mmol) was added and the reaction was monitored until colorless (the mixture was overall allowed to stir for 15 minutes). MeI (90 uL; 1.45 mmol) was then quickly pipetted into the reaction, which was allowed to stir for 15 more minutes after which the reaction was poured into 10 mL of water and extracted with Et_2O. The organic fractions were combined and dried *in vacuo*. Finally, the product was purified via sublimation at 75 ˚C to yield 145 mg of product (white solid) in 51% yield. The product was initially stored in the glovebox freezer at -30 ˚C but NMR stability studies found that it is stable in solution for more than a week, thus storage in a freezer at ambient conditions should be sufficient.

2.5.5.3. Synthesis of compound 7c

An oven-dried 10 mL Schlenk flask was charged with **compound 7a** (54 mg; 0.1 mmol) and then degassed, after which 2 mL of anhydrous EtOH was added to dissolve the powder. To the stirring solution under a steady flow of nitrogen $NaBH_4$ (20 mg; 0.54 mmol) was added and the reaction was monitored until colorless (the mixture was overall allowed to stir for 15 minutes). Benzyl bromide (24.94 uL; 0.21 mmol) was then quickly

pipetted into the reaction, which was allowed to stir for 15 more minutes after which the reaction was poured into 5 mL of water and extracted with Et_2O. The organic fractions were combined and dried with Na_2SO_4, after which solvent was removed *in vacuo* to yield 50 mg of yellowish solid in 70% yield.

2.5.5.4. Synthesis of compound 7d

An oven-dried 10 mL Schlenk flask was charged with **compound 7a** (116 mg; 0.21 mmol) and then degassed, after which 1 mL of anhydrous EtOH was added to dissolve the powder. To the stirring solution under a steady flow of nitrogen $NaBH_4$ (40 mg; 1.07 mmol) was added and the reaction was monitored until colorless (the mixture was overall allowed to stir for 15 minutes). The reaction was then slowly acidified with 1 mL of 1M HCl and extracted with DCM. The combined organic layers were dried *in vacuo* and quickly transferred to a microsublimator and purified via sublimation at 65 ˚C, yielding 17 mg of white powder in 15% yield. The product was transferred to a J-Young NMR tube for characterization, but decomposition was apparent even in an inert atmosphere. Storage at -30 ˚C in the glovebox also caused decomposition, thus the tellurol must be generated and used *in situ* if needed.

2.5.5.5. Synthesis of compound 8b

The exact same procedure was used as the one for **compound 5b**, except **compound 8a** (81.3 mg; 0.15 mmol) was used instead of 5a. Yield: 74.6 mg; 75%.

2.5.6. Electrophilic Chemistry of Tellurium-Based Carboranyl Compounds

2.5.6.1. Synthesis of compound 9b

The same general procedure was used as the one for **compound 7b**, except **compound 9a** (71 mg; 0.12 mmol) was used instead of 7a and the resulting product was not purified via sublimation.

2.5.6.2. General considerations for the synthesis of compound 9c (lithiation experiments)

A 10 mL Schlenk flask was charged with either **compound 9a** (30 mg; 0.05 mmol) or **9b** (31.4 mg; 0.10 mmol) and then degassed, after which 1 mL of dry Et_2O was added to dissolve the solids. To the stirring solution cooled to 0 ˚C in an ice bath under a steady flow of nitrogen n-butyllithium (80 μL, 0.2 mmol for **compound 9a**; 40 μL, 0.1 mmol for **compound 9b**) was added and the reaction was stirred for 15 minutes, after which the crude reaction mixture was passed through a quick silica plug and characterized by GCMS.

2.5.6.3. Synthesis of compound 10a

A 16x125 mm reaction tube equipped with a septum was charged with **compound 8a** (163 mg; 0.3 mmol) and then degassed, after which 5 mL of dry DCM was added to dissolve the powder. The stirring solution was cooled to 0 ˚C in an ice bath under a steady flow of nitrogen, and then SO_2Cl_2 (121 μL; 1.5 mmol) was added and the reaction mixture was allowed to stir for 30 minutes. After 30 minutes the reaction mixture was cloudy white. It was then centrifuged and the supernatant was carefully decanted, after which the product

was washed with hexanes 3 times and dried *in vacuo* to yield 192 mg of free-flowing white powder in 85% yield.

2.5.6.4. Synthesis of compound 10b

The same procedure was used as the one for **compound 10a**, except the scale was reduced to 0.05 mmol (27 mg) with respect to **compound 8a** and Br_2 (26.4 mg; 0.165 mmol; from a stock solution in DCM) was used instead of SO_2Cl_2. The product was then characterized by NMR spectroscopy and the yield was not measured.

2.5.6.5. Synthesis of compounds 11a and 11b

A 16x125 mm reaction tube equipped with a septum was charged with **compound 10a** (40 mg; 0.1 mmol) and then degassed, after which 0.5 mL of $CDCl_3$ was added to suspend the powder. Phenylacetylene (22 μL; 0.2 mmol) was added to the stirring solution which was heated to reflux under a steady flow of nitrogen and allowed to stir overnight. After stirring overnight, the crude reaction mixture containing **compound 11a** was allowed to come to room temperature and characterized via ^{11}B, $^{11}B\{^1H\}$, and ^{125}Te NMR spectroscopy. 1 mL of a saturated aqueous solution of sodium thiosulfate was then added to the crude mixture and the biphasic mixture was vigorously stirred for 15 minutes until the organic layer looked yellowish. The organic layer was then collected and ran through a quick silica plug and then characterized via ^{11}B, $^{11}B\{^1H\}$, and ^{125}Te NMR spectroscopy.

2.5.6.6. Synthesis of compounds 12a and 12b

The same procedure was followed as the one for **compounds 11a** and **11b**, except that norbornene (18.8 mg; 0.2 mmol) was used instead of phenylacetylene.

2.6. References

1. Lenardão, E. J.; Santi, C.; Sancineto, L. *New Frontiers in Organoselenium Compounds*; Springer International Publishing: Cham, 2018. https://doi.org/10.1007/978-3-319-92405-2.
2. Krief, A.; Hevesi, L. *Organoselenium Chemistry I*; Springer Berlin Heidelberg: Berlin, Heidelberg, 1988. https://doi.org/10.1007/978-3-642-73241-6.
3. *Organoselenium Chemistry: Modern Developments in Organic Synthesis*; Wirth, T., Ed.; Topics in Current Chemistry; Springer-Verlag: Berlin Heidelberg, 2000. https://doi.org/10.1007/3-540-48171-0.
4. *Handbook of Chalcogen Chemistry: New Perspectives in Sulfur, Selenium and Tellurium, 2nd edition.*; Devillanova, F. A., Du Mont, W.-W., Eds.; RSC Publishing: Cambridge, 2013.
5. Patai, S. & Rappoport, Z. (eds) *The Chemistry of Organic Selenium and Tellurium* (John Wiley & Sons, 2013).
6. Ingolic, K. J. *Organotellurium Compounds*; Thieme Medical Publishers, Incorporated, 1990.
7. Petragnani, N. *Tellurium in Organic Synthesis*, 2nd ed.; Best synthetic methods; Academic: London, 2007.
8. Nogueira, C. W.; Zeni, G.; Rocha, J. B. T. Organoselenium and Organotellurium Compounds: Toxicology and Pharmacology. *Chem. Rev.* **2004**, 104 (12), 6255–6286. https://doi.org/10.1021/cr0406559.
9. Zakharkin, L. I.; Pisareva, I. V. Preparation of Carborane Derivatives Containing Boron-Selenium Bonds. *Izv. Akad. Nauk SSSR, Ser. Khim.* **1982**, 718–719.

10. Rys, E. G.; Balema, V. P.; Godovikov, N. N. Reaction of O- and m-Carboranes with Selenium. *Izv. Akad. Nauk SSSR, Ser. Khim.* **1987**, 2398.
11. Bregadze, V. I.; Kampel, V. Ts.; Usayatinskii, A. Ya.; Ponomareva, O. B.; Godovikov, N. N. Reaction of Selenium and Tellurium with Boromercurated and Borothallated Carboranes. *Izv. Akad. Nauk SSSR, Ser. Khim.* **1982**, 1434.
12. Zakharkin, L. I.; Pisareva, I. V.; Antonovich, V. A. Synthesis of Bis(9-o- or m-Carboranyl) Diselenides by Electrophilic Substitution of Carboranes by Selenium Chlorides in the Presence of Aluminum Chloride, and Their Reactions. *Zh. Obshch. Khim.* **1986**, 56, 2721–2728.
13. Bregadze, V. I.; Kampel, V. Ts.; Usyatinskii, A. Ya.; Ponomareva, O. B.; Godovikov, N. N. Synthesis of Carboranyl Derivatives of Selenium and Tellurium. *J. Organomet. Chem.* **1982**, 233, C33–C34. https://doi.org/10.1016/S0022-328X(00)85581-3.
14. Zakharkin, L. I.; Pisareva, I. V. Electrophilic Tellurization of O- and m-Carboranes with Tellurium(IV) Chloride in the Presence of Aluminum Chloride. *Izv. Akad. Nauk SSSR, Ser. Khim.* **1984**, 472–473.
15. Zakharkin, L. I.; Pisareva, I. V. Synthesis and Some Transformations of O- and m-Carboranes Containing a Boron-Tellurium σ-Bond. *Izv. Akad. Nauk SSSR, Ser. Khim.* **1987**, 877–880.
16. Hiiro, T.; Kambe, N.; Ogawa, A.; Miyoshi, N.; Murai, S.; Sonoda, N. Lithium-Tellurium Exchange: A New Entry to Organolithium Compounds. *Angew. Chem. Int. Ed.* **1987**, 26 (11), 1187–1188. https://doi.org/10.1002/anie.198711871.